

1993

Modeling and measurement of solid-liquid phase transformation enthalpy for fusible heat sink applications

Cheng-Kuan Wu
San Jose State University

Follow this and additional works at: https://scholarworks.sjsu.edu/etd_theses

Recommended Citation

Wu, Cheng-Kuan, "Modeling and measurement of solid-liquid phase transformation enthalpy for fusible heat sink applications" (1993). *Master's Theses*. 661.

DOI: <https://doi.org/10.31979/etd.8kys-nhdx>

https://scholarworks.sjsu.edu/etd_theses/661

This Thesis is brought to you for free and open access by the Master's Theses and Graduate Research at SJSU ScholarWorks. It has been accepted for inclusion in Master's Theses by an authorized administrator of SJSU ScholarWorks. For more information, please contact scholarworks@sjsu.edu.

INFORMATION TO USERS

This manuscript has been reproduced from the microfilm master. UMI films the text directly from the original or copy submitted. Thus, some thesis and dissertation copies are in typewriter face, while others may be from any type of computer printer.

The quality of this reproduction is dependent upon the quality of the copy submitted. Broken or indistinct print, colored or poor quality illustrations and photographs, print bleedthrough, substandard margins, and improper alignment can adversely affect reproduction.

In the unlikely event that the author did not send UMI a complete manuscript and there are missing pages, these will be noted. Also, if unauthorized copyright material had to be removed, a note will indicate the deletion.

Oversize materials (e.g., maps, drawings, charts) are reproduced by sectioning the original, beginning at the upper left-hand corner and continuing from left to right in equal sections with small overlaps. Each original is also photographed in one exposure and is included in reduced form at the back of the book.

Photographs included in the original manuscript have been reproduced xerographically in this copy. Higher quality 6" x 9" black and white photographic prints are available for any photographs or illustrations appearing in this copy for an additional charge. Contact UMI directly to order.

U·M·I

University Microfilms International
A Bell & Howell Information Company
300 North Zeeb Road, Ann Arbor, MI 48106-1346 USA
313/761-4700 800/521-0600

Order Number 1354176

**Modeling and measurement of solid-liquid phase transformation
enthalpy for fusible heat sink applications**

Wu, Cheng-Kuan, M.S.

San Jose State University, 1993

Copyright ©1993 by Wu, Cheng-Kuan. All rights reserved.

U·M·I
300 N. Zeeb Rd.
Ann Arbor, MI 48106

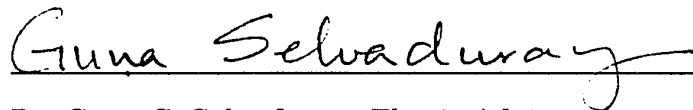
**Modeling and Measurement of Solid-Liquid
Phase Transformation Enthalpy for Fusible
Heat Sink Applications**

**A Thesis
Presented to
The Faculty of the Department of Materials Engineering
San Jose State University**

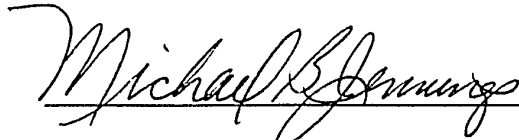
**In Partial Fulfillment
of the Requirements for the Degree
Master of Science**

**by
Cheng-Kuan Wu
August, 1993**

APPROVED FOR THE DEPARTMENT OF MATERIALS ENGINEERING



Dr. Guna S. Selvaduray, Thesis Advisor



Dr. Michael Jennings, Professor of Chemical Engineering



Dr. B. Webbon, NASA-Ames Research Center

APPROVED FOR THE UNIVERSITY



ABSTRACT

Modeling and Measurement of Solid-Liquid Phase Transformation Enthalpy for Fusible Heat Sink Applications

By Cheng-Kuan Wu

Modeling the fusion enthalpy of organic compounds and aqueous solutions was the objective of this project. From the literature, models for predicting the fusion enthalpy for both organic compounds and aqueous solutions were identified and tested against experimental data obtained from differential scanning calorimetry (DSC) measurements.

The model proposed by Chickos, for predicting the fusion enthalpy of organic compounds, was found to have an average percent deviation of 26.3%. The Rule of Mixtures and Horvath's model, for predicting the fusion enthalpy of aqueous solutions, were found to have average percent deviations of 75.9% and 142.9%, respectively.

A new model, termed the "Modified Mixture Rule," for predicting the fusion enthalpy of aqueous solutions, was developed. The average percent deviation of the Modified Mixture Rule, when tested against experimental data, was 12.5%. This modification significantly improved the accuracy of predicting the value of enthalpy of fusion from models.

ACKNOWLEDGEMENTS

The author wishes to thank his thesis adviser, Dr. Guna Selvaduray, Associate Professor, Department of Materials Engineering, for his guidance and perseverance in seeing this project through to its completion. A special note of thanks is due to Dr. Michael Jennings, Professor, Department of Chemical Engineering, for his valuable advice and for chairing the author's thesis committee.

The author is grateful to Dr. Bruce Webbon, Branch Chief, Life Sciences Division, NASA-Ames Research Center, for partial sponsorship of this project, for serving on his thesis committee, and for the valuable input that served to improve this study.

A special thank you is due to Mr. Frank Lewandowski, who so graciously consented to help edit this thesis, and gave his time so freely.

The author thanks his parents, Mr. and Mrs. Woei-Tsuen Wu, and his wife, Huei-Fang Lin, for their endearing support and patience throughout the duration of this study. To them, a very special Thank You.

TABLE OF CONTENTS

	page
ABSTRACT	iii
ACKNOWLEDGEMENT	iv
LIST OF FIGURES	ix
LIST OF TABLES	x
Chapter 1. Introduction	1
1.1 Background	1
1.2 Fusible Heat Sink	3
1.3 Cooling Capacity of a FHS Material	3
1.4 Traditional FHS Material (H ₂ O)	5
1.5 The Selection Criteria of FHS Material	5
1.6 Identification of Candidate FHS Materials	6
1.7 Discrepancies of ΔH_m between the Literature Values	9
Chapter 2. Literature Review	13
2.1 The Phenomenon of Melting	13
2.1.1 Atomic Species	14
2.1.2 Molecular Species	14
2.1.2.1 Organic Compounds	15
2.1.2.2 Aqueous Solutions	15
2.2 Models for Predicting ΔS_m and ΔH_m	18
2.2.1 ΔS_m of Atomic Species	19
2.2.2 ΔS_m of Organic Compounds	21
2.2.2.1 Semi-empirical Model by Walden	21

2.2.2.2 Semi-empirical Model by Pirsch	25
2.2.2.3 Semi-empirical Model by Procopiu	25
2.2.2.4 Quantitative Model by Chickos	26
2.2.3 ΔH_m of Aqueous Solutions	31
2.2.3.1 The Rule of Mixtures	31
2.2.3.2 Horvath's Model	31
Chapter 3. Investigation Methodology	33
3.1 Theoretical	33
3.1.1 Organic Compounds	33
3.1.2 Aqueous Solutions	35
3.2 Experimental	36
3.2.1 Materials	36
3.2.2 Equipment and Experimental Methodology	40
3.2.2.1 Experimental Setup	40
3.2.2.2 Principle of Measurement	43
3.2.2.3 Procedure for Operating the DSC	44
3.2.2.4 Appearance of DSC Curve	48
3.2.2.5 Determination of T_m , ΔH_m , $C_{p,s}$, and $C_{p,l}$	48
Chapter 4. Results and Discussion	52
4.1 Validity of the Semi-empirical Models	52
4.1.1 Procopiu's Model for ΔS_m of Atomic Species	52
4.1.2 Walden's Model for ΔS_m of Organic Compounds	58
4.1.3 Pirsch's Model for ΔS_m of Organic Compounds	58
4.1.4 Procopiu's Model for ΔS_m of Organic Compounds	61

4.2 Experimental Data	62
4.3 Evaluations of the Models for Prediction of ΔH_m	68
4.3.1 Chickos's Model for ΔH_m of Organic Compounds	68
4.3.2 The Rule of Mixtures for ΔH_m of Aqueous Solutions	70
4.3.3 Horvath's Model for ΔH_m of Aqueous Solutions	73
Chapter 5. Modified Mixture Rule	77
5.1 The Phenomenon of Hydration	78
5.2 The Equation for Predicting ΔH_m	81
5.3 Results	83
5.4 Discussion of Results	83
5.5 Identification of FHS Material by the Model	95
Chapter 6. Verification of Candidate FHS Materials	98
Chapter 7. Conclusion	101
References	103
Appendix A. Derivation of Horvath's Model	106
Appendix B. Values of ΔH_m of Solutes from Published Sources	108
Appendix C. Heating Rate v.s. Weight of Sample	109
Appendix D. Sample Calculations of Fusion Enthalpies from the DSC	111
Appendix E. Calculations of the accuracy of the DSC-4	112
Appendix F. Calculations of Fusion Enthalpy from Chickos's Model	113
Appendix G. Sample Calculations of Fusion Enthalpies from the Rule of Mixtures	118
Appendix H. Sample Calculations of Fusion Enthalpies from Horvath's Model	119
Appendix I. Hydration Numbers of Electrolytes	120
Appendix J. Hydration Numbers of Non-electrolytes	121

Appendix K. Sample Calculations of Fusion Enthalpies from the Modified Mixture Rule	127
Appendix L. Calculations of Maximum Concentrations in the Modified Mixture Rule	128
Appendix M. Calculations of Cooling Capacities	129

LIST OF FIGURES

	page
Figure 1. Components of a Space Suit	2
Figure 2. Principle of Operation of Fusible Heat Sink	4
Figure 3. Arrangement of Molecules in the Ice Crystal	17
Figure 4. View of DSC and the System-4 Microprocessor Controller	41
Figure 5. View of Accessories for the Equipment	41
Figure 6. View of an Aluminum Pan and Pan Cover Illustrating Relative Sizes	42
Figure 7. View of the Sample Chamber	42
Figure 8. Experimental Arrangement of DSC	43
Figure 9. The Process for Preparing a Sample Pan	45
Figure 10. DSC Scan Plot	49
Figure 11. Plot of ΔH_m vs. T_m for 59 Atomic Species	54
Figure 12. Plot of ΔH_m vs. T_m for 572 Organic Compounds	59
Figure 13. Dissolution of an Ionic Crystal by the Action of a Solvent	79
Figure 14. Orientations of Water Dipoles in an Electrolytic Solution	80
Figure 15. Comparison of Models for Predicting Fusion Enthalpies of 5 Electrolytic Aqueous Solutions	86
Figure 16. Comparison of Models for Predicting Fusion Enthalpies of 5 Non-electrolytic Aqueous Solutions	88
Figure 17. Bent & Stretched H-Bond Configuration in Water	92

LIST OF TABLES

	page
Table 1. Materials with Higher Fusion Enthalpies than Water	7
Table 2. Comparative values of ΔH_m in Two Literature Sources	11
Table 3. Summary of Models for Predicting ΔH_m and ΔS_m	20
Table 4. ΔS_m of 13 Atomic Species Determined by Procopiu	22
Table 5. ΔS_m of 31 Organic Materials, as Determined by Walden	23
Table 6. Carbon Group Contributions to Fusion Entropies	29
Table 7. Functional Group Contributions to Fusion Entropies	30
Table 8. Organic Materials Selected for H_m & T_m Measurements	37
Table 9. Aqueous Solutions Selected for H_m & T_m Measurements	38
Table 10. Test of Procopiu's Model for ΔS_m of Atomic Species	55
Table 11. Test of Pirsch's Model for ΔS_m of Organic Materials	60
Table 12. Test of Procopiu's Model for ΔS_m of Organic Materials	63
Table 13. Experimental Fusion Enthalpy, Melting Point, and Heat Capacity	64
Table 14. Test of Chickos's Model for ΔH_m of Organic Materials	69
Table 15. Test of the Rule of Mixtures for ΔH_m of Aqueous Solutions	71
Table 16. Test of Horvath's Model for ΔH_m of Aqueous Solutions	74
Table 17. Test of the Modified Mixture Rule for ΔH_m of Aqueous Solutions	84
Table 18. The Maximum Allowable Concentration of the Solutions in the Application of the Modified Mixture Rule	94
Table 19. Solutes with a Fusion Enthalpy Higher than Water	96
Table 20. Verification of Candidate FHS Materials	99

CHAPTER 1

INTRODUCTION

Fusible Heat Sink (FHS) materials are a possible source for thermal regulation of space suited astronauts. The fusion enthalpy values of the FHS material is one of the major factors used to determine the duration of Extra Vehicular Activity (EVA). Modeling the fusion enthalpy of FHS materials is therefore the objective of this project. This chapter describes the applications, specifications, and identification of FHS materials.

1.1 Background

A space suit is a special suit designed for a human being in space. During Extra Vehicular Activity (EVA), a space suit provides the environment necessary to protect the human body from the atmospheric and temperature conditions that exist in space. The Portable Life Support System (PLSS), an integral part of the space suit, supplies astronauts with breathing air and removes metabolic heat. The components of a space suit are shown in Figure 1.⁽¹⁾ Inside the space suit during activity periods, the body gives off approximately 2900 calories per minute, which is equivalent to a 100 watt light bulb.⁽²⁾ In daily life, one may not notice the metabolic heat generated because it will be exhausted to the environment through the clothing that is worn. When one wears a thermally insulated space suit, the excess metabolic heat cannot be exhausted to the outside. The space suit, therefore, must be capable of managing the metabolic heat generated during the EVA.

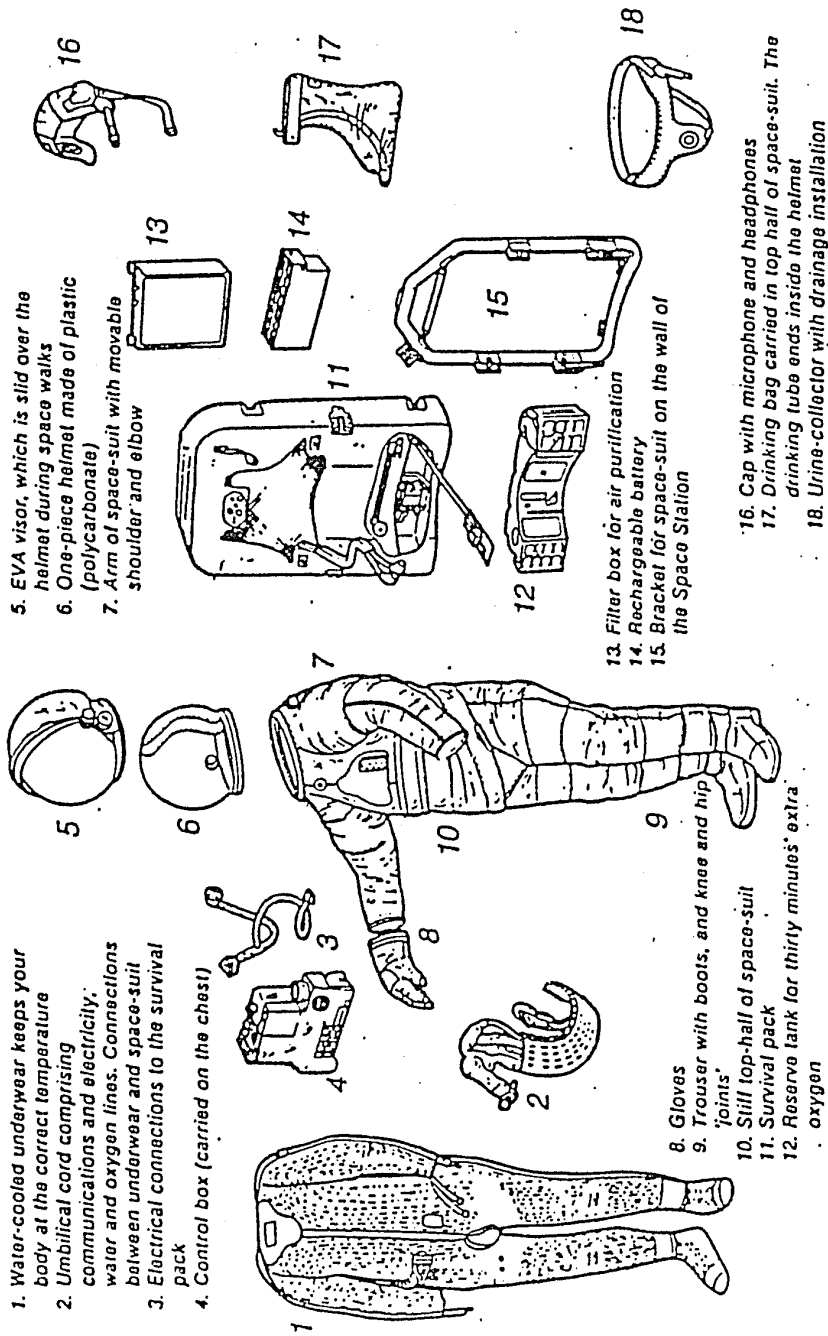


Figure 1. Components of a Space Suit (after Ref. 1)

1.2 Fusible Heat Sink

Due to the requirement that the space suit both isolate and insulate its occupant from the environment, exhaustion of the metabolic heat to the outside is not easily achievable. If the metabolic heat cannot be exhausted, then it must be stored. One possible method of "storage" is in a fusible heat sink (FHS), which is a reservoir that contains a material that is initially solid and is transformed to a liquid during operation, as shown in Figure 2. The excess heat generated during the EVA will be absorbed by this material which goes through a solid-liquid phase transformation in the process, thus continually providing cooling capacity.⁽³⁾ The ability to store this heat will be one of the factors that determines the length of the Extra Vehicular Activity. The fusible heat sink is built inside the Portable Life Support System, or survival pack, which is also shown in Figure 1.

1.3 Cooling Capacity of a FHS Material

The amount of heat that a FHS is able to absorb during operation is defined as its cooling capacity, ΔH_{tot} , and is given by Equation 1.

$$\Delta H_{tot} = \int_{T_{s,i}}^{T_m} c_{p,s} dT + \Delta H_m + \int_{T_m}^{T_{l,f}} c_{p,l} dT \quad [1]$$

where $T_{s,i}$ is the initial solid temperature,

$T_{l,f}$ is the final liquid temperature,

T_m is the melting point of the material,

$C_{p,l}$ is the heat capacity of the liquid phase,

$C_{p,s}$ is the heat capacity of the solid phase, and

ΔH_m is the latent heat of fusion at the melting point.

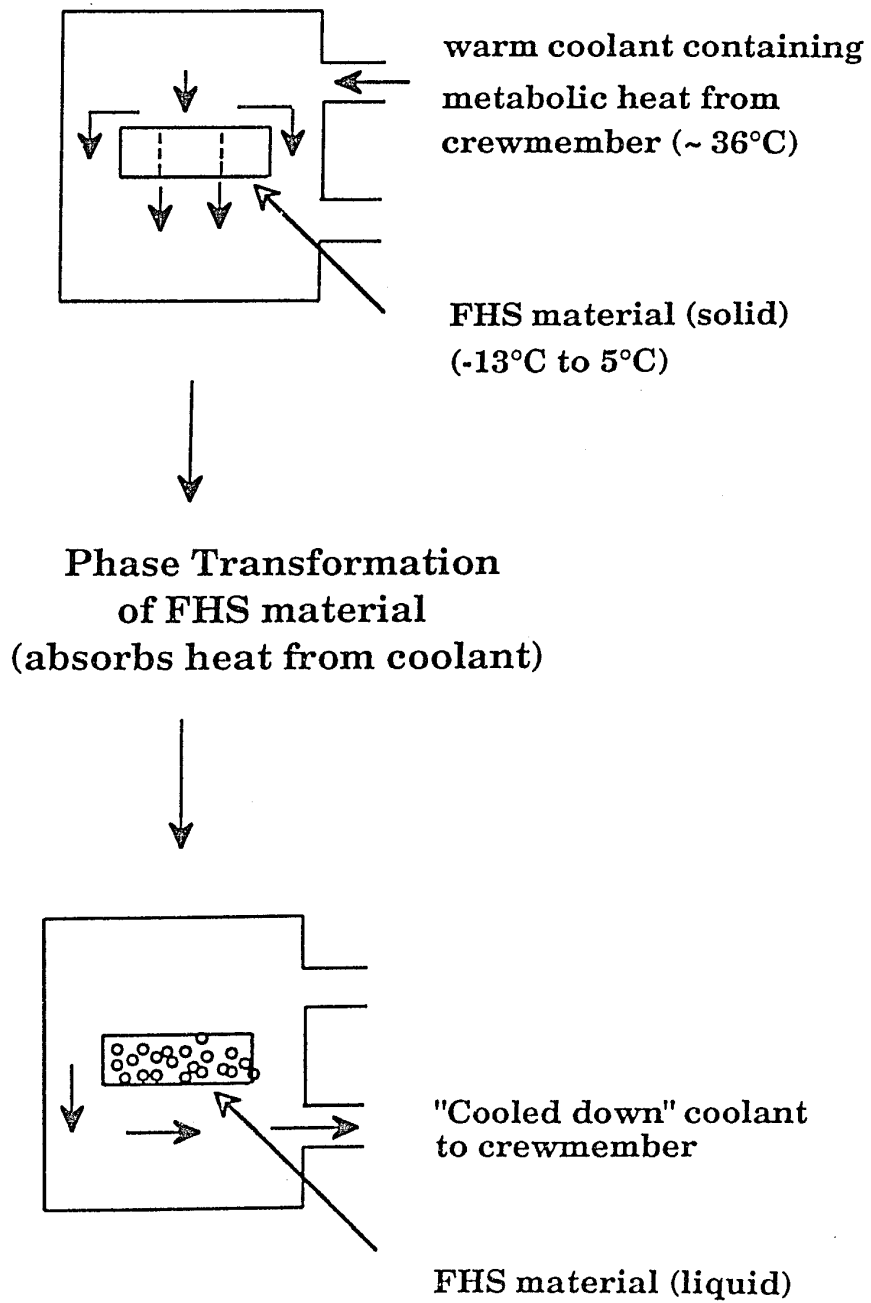


Figure 2. Principle of Operation of Fusible Heat Sink

ΔH_m plays a significant role in determining the cooling capacity because it contributes between 80% to 90% of the total cooling capacity⁽³⁾ and therefore, is the parameter chosen for modeling in this project.

1.4 Traditional FHS Material (H₂O)

In the conventional design, the reservoir of the FHS initially contains ice. During the EVA, the ice will absorb the metabolic heat and melt into water. Therefore the latent heat of fusion for water, and the amount of ice, determines the maximum duration of the EVA. Water has been the traditional choice as a FHS material because it is non-toxic, non-flammable and inexpensive.⁽³⁾

1.5 Selection Criteria for FHS Material

The primary selection criterion for a FHS material is the requirement that the material have a solid-liquid phase transformation within the temperature range of -13°C (0°F) to 5°C (40°F). This temperature range bounds the practical limits. A temperature lower than -13°C could pose a hazard to living cells, while a temperature higher than 5°C could require excessive heat transfer. The second criterion is the requirement that the cooling capacity of the material be greater than that of water, which is 90.97 cal/g⁽³⁾. As stated earlier, a material with a high enthalpy of solid to liquid phase transformation, within the -13°C to 5°C temperature range, could enable both an extension of time between recharging and/or a reduction in size and/or mass of the Portable Life Support System (PLSS). Therefore, promising alternatives should have a higher cooling capacity than water.

Besides the previous two criteria, several other criteria must be taken into account. The material identified should not pose any significant health risks to the astronaut, not be degraded during thermal cycling, not expand or contract excessively during the phase change, and be compatible with existing EVA PLSS.

1.6 Identification of Candidate FHS Materials

Selvaduray and Lomax⁽³⁾ conducted initial studies for NASA to determine the availability of candidate FHS materials that would be viable alternatives to water. The initial effort to identify suitable materials was restricted to employing the first two criteria listed above, namely that the solid-liquid transition temperature be within the -13°C to 5°C temperature range, and that the total cooling capacity, ΔH_{tot} , be greater than that for water. Based on data available in the literature, Selvaduray and Lomax identified a total of 49 candidate materials that appeared to be promising alternatives to water. The results of their study is shown in Table 1.⁽³⁾

The values of ΔH_{tot} in the third column of Table 1 were calculated according to Equation 1, with an initial temperature of -13°C and a final temperature of 5°C. The data necessary for computing ΔH_{tot} are the values of ΔH_m , $C_{p,s}$, and $C_{p,l}$. The authors were not able to find $C_{p,s}$ and $C_{p,l}$ for all of the compounds identified. Compounds containing the remark " ΔH_m data only" in Table 1 means that ΔH_{tot} was computed based solely on ΔH_m . They justified including compounds for which $C_{p,s}$ and $C_{p,l}$ data were not available because inclusion of the heat capacity contribution would only increase the value of ΔH_{tot} . Initial estimates of the cooling capacity, ΔH_{tot} , in Table 1

Table 1. Materials with Higher Fusion Enthalpies than Water (after Ref. 3)

Compound Name	Melting Point (°C)	ΔH_{tot} (cal/g)	Remarks
Glycerol triacetate	-7.8	1457.84	ΔH_{m} data only
Triethylene glycol	-7.2	1289.28	
Benzene, hexafluoro	5	1280.07	
Heptanoic acid	-9	1119.59	ΔH_{m} data only
2-Methyl-2-butanol	-8.4	1028.93	ΔH_{m} data only
2,3-Butanedione	-2	1016.74	ΔH_{m} data only
Benzoic acid,2-fluoro	1	969.07	ΔH_{m} data only
Cyclohexanol,2-methyl(trans,dl)	-4	897.73	
Cyclohexanol,4-methyl(cis)	-9	874.47	
Cyclohexanol,3-methyl(trans,l)	-1	835.06	
Tert-Butyl hydroperoxide	-8	778.96	ΔH_{m} data only
Benzene,1,4-difluoro	-13	717.29	ΔH_{m} data only
Cyclohexanone,2-methyl(dl)	-13	613.34	ΔH_{m} data only
Cinnamitrile	-4	593.5	
4-Methoxybenzaldehyde	0	469.34	ΔH_{m} data only
Coniine	-2	453.34	ΔH_{m} data only
Arsinic trichloride	-8.5	405.61	
Benzyl alcohol	-1.5	366.42	
Indene	-1.8	234.64	
Benzene,1,2,3,4-tetramethyl	-6	202.64	
Methyldiphenolamine	-7.6	164.17	
Cyclohexane1,2-dibromo(trans,dl)	-4	160.35	ΔH_{m} data only
Benzene	5	159.26	
Biphenyl,2-methyl	0	153.35	ΔH_{m} data only
1,2-Dihydronaphthalene	-8 to -7	138.26	ΔH_{m} data only
Biphenyl,3-methyl	4	121.25	ΔH_{m} data only
Piperidene	-7	97.99	

Table 1. Materials with Higher Fusion Enthalpies than Water (after Ref. 3)
(continued)

Compound Name	Melting Point (°C)	ΔH_{tot} (cal/g)	Remarks
Sodium chloride	-4.378	94.30557	Conc. 7.0%
Potassium chloride	-4.3	93.5291	Conc. 9.0%
Sodium bromide	-4.206	93.08707	Conc. 11.0%
Lithium chloride	-3.727	92.94917	Conc. 4.0%
Potassium chromate	-4.05	92.8657	Conc. 18.0%
Potassium bromide	-4.122	92.73127	Conc. 13.0%
Formic acid	-4.267	92.64415	Conc. 10.0%
Glycerol	-4.094	92.5118	Conc. 16.0%
Sodium nitrate	-3.841	92.50245	Conc. 10.0%
Potassium iodide	-3.869	92.46738	Conc. 16.0%
Cesium chloride	-4.224	92.42732	Conc. 19.0%
Sodium hydroxide	-4.074	92.33973	Conc. 4.5%
Acetic acid	-4.259	92.23876	Conc. 13.0%
Ethylene glycol	-4.16	92.1678	Conc. 12.0%
Silver nitrate	-2.862	91.90444	Conc. 16.0%
Potassium nitrate	-2.754	91.8233	Conc. 10.0%
Potassium sulfate	-2.754	91.8233	Conc. 5.0%
Ethanol	-4.21	91.34832	Conc. 9.5%
Potassium hydroxide	-4.144	91.27768	Conc. 6.0%
Potassium dichromate	-0.435	91.26456	Conc. 2.5%
Methanol	-4.41	91.18045	Conc. 7.0%
Alinine	-6	91.1	ΔH_{m} data only
Water	0	90.97	

were therefore on the conservative side.

For the case of aqueous solutions contained in Table 1, thermodynamic data was available only for the individual components, but not the solutions. ΔH_m , $C_{p,s}$, and $C_{p,l}$ were therefore calculated according to the Rule of Mixtures, and these values in turn, were used to calculate ΔH_{tot} .

Selvaduray and Lomax subsequently undertook a modest effort to confirm their results experimentally. During the course of experimental confirmation, and also during critical evaluation of the data contained in the literature, they discovered several discrepancies.

1.7 Discrepancies of ΔH_m between the Literature Values

As can be seen from Table 1, triethylene glycol was found to be very attractive compared to water. Therefore an attempt to measure the melting point of triethylene glycol was made. Experiments showed that triethylene glycol would not freeze at temperatures as low as -40°C . The Material Safety Data Sheet from the manufacturer of triethylene glycol also stated that its melting point was -7°C . The manufacturer was contacted, and they were not able to obtain a melting/freezing temperature despite lowering the temperature to -40°C .

The reported values for ΔH_m of triethylene glycol also varied widely. One value of 1278 cal/g was reported by Moureu et al.⁽⁴⁾ in 1937, and another value of 29 cal/g was reported by Pickard et al.⁽⁵⁾ in 1911.

Discrepancies also occur in the recently published literature. The values of fusion enthalpies of some materials reported in the CRC Handbook of Chemistry and Physics⁽⁶⁾ are somewhat different from those reported in

Lange's Handbook of Chemistry.⁽⁷⁾ Comparative values of fusion enthalpies from these two sources are tabulated in Table 2.

Uncertainties in existing literature values made it necessary to conduct an experimental program to measure the thermodynamic properties of candidate FHS materials. Selvaduray and Lomax had identified 1215 compounds that had a solid-liquid transition within the temperature range of -13°C to 5°C. This represents an extremely large number and an experimental program involving the measurement of thermodynamic properties of all these 1215 compounds would be impractical. Therefore it was decided to model the enthalpy of fusion first, and then verify the reliability of the model by experimentation. The most reliable models for predicting fusion enthalpy may identify suitable FHS materials for space suit applications and therefore evaluating these models is one of the primary objectives of this project.

Chapter 2 is a review of the literature to locate existing models that have been proposed for determining the enthalpy of fusion. Chapter 3 describes the methodology for investigating the values of fusion enthalpy. Both a theoretical and an experimental approach were taken to obtain the values of fusion enthalpy. Models reviewed from the literature for predicting fusion enthalpy were employed to calculate the theoretical ΔH_m and experiments were subsequently conducted to test the reliability of the findings from the theoretical models. Chapter 4 evaluates the current models for predicting the values of fusion enthalpy. Chapter 5 introduces modifications of the current models for predicting the fusion enthalpy of

Table 2. Comparative Values of ΔH_m in Two Literature Sources
(after Ref. 6 and 7)

Material	ΔH_m (cal/mole) from CRC handbook ⁽⁶⁾	ΔH_m (cal/mole) from Lange's handbook ⁽⁷⁾
MgCl ₂	8100	10300
NaF	7000	7970
KCl	6410	6282
LiBr	2900	4220
LiCl	3200	4740
CaCl ₂	6100	6800
NaCl	7220	6730
KBr	5000	6100
NaNO ₃	3760	3490
KI	4100	5740
CsCl	3600	3800
NaOH	2000	1580
KNO ₃	2840	2300
K ₂ SO ₄	8100	8480

aqueous solutions. These modifications were the result of this study and its reliability and possible application are discussed. Chapter 6 presents the results of experimental verification of candidate FHS materials. Chapter 7 contains the summary of this study and the recommendations for future study.

CHAPTER 2

LITERATURE REVIEW

This chapter contains two main topics: an examination of the solid-liquid phase change mechanism and a summary of thermodynamic models for that process. The phenomenon of melting, in terms of atomic species and molecular species, is introduced in Section 2.1 since this is essential for understanding the meaning of fusion or melting. Considering the value of fusion enthalpy as the most significant determining factor for choosing a FHS material, the purpose of the literature review was to locate existing models for determining the enthalpy of fusion, ΔH_m . Models for computing the entropy of fusion, ΔS_m , have also been reviewed since ΔH_m can be computed by the product of ΔS_m and the melting point, T_m . These models are reviewed in Section 2.2.

2.1 The Phenomenon of Melting

For quasi-equilibrium conditions during melting, the free energy of the solid state is equal to that of the liquid state and therefore both phases coexist. From the viewpoint of chemical bonding of materials there is a difference between the solid and liquid states and this difference accounts for the enthalpy of fusion. All materials can be grouped as either atomic or molecular species and the phenomenon of melting in each case is different. They are therefore described individually.

2.1.1 Atomic Species

This class of materials, typically elemental species such as Cu, Al, Pb, etc., have a specific crystal structure in their solid state. Each atom is surrounded by a certain number of nearest neighbor atoms, which is referred to as the coordination number. Most models assume that the force that binds these atoms together is the inter-atomic bond, such as Cu-Cu, Al-Al or Pb-Pb bonds. The higher the coordination number, the more tightly the atoms are bound, and therefore the lower the energy level. During melting, the thermal energy becomes high enough to break some of the inter-atomic bonds, and therefore the coordination number decreases. For example, the coordination number of Al decreases from 12, in the solid phase, to 10.6 in the liquid phase.⁽⁸⁾ The structure of liquid Al corresponds to a close-packed solid, but with a coordination number of 10.6 instead of 12, i.e., each Al atom in the liquid state has on the average 10.6 atoms and 1.4 holes as the nearest neighbors. The phenomenon of melting for this type of material involves the rupture of inter-atomic bonds.

2.1.2 Molecular Species

Materials that are molecular in nature can be divided into organic and aqueous species. The phenomenon of melting in organic compounds and aqueous solutions are also different from each other, and are described separately.

2.1.2.1 Organic Compounds

Unlike atomic species, inter-molecular bonding dominates the liquid-solid phase transformation in the case of organic compounds. Most models assume that van der Waal's bonding and dipole-dipole interactions are the two types of inter-molecular bonds that bind neighboring organic molecules. Van der Waal's bonding is caused by the instantaneous location of a few more electrons on one side of the nucleus than on the other, thus providing a weak fluctuating dipole moment to attract the neighboring molecules. Dipole-dipole interactions result from the charge asymmetry of the molecule, thus contributing the dipole moment to attract the neighboring molecules. For those molecules which are symmetric (e.g., CH_4 , CCl_4), the inter-molecular bonds consist of van der Waal's bonding only, while for those molecules which are asymmetric (e.g., CO , CHN), the inter-molecular bonds consist of both van der Waal's bonding and dipole-dipole interactions. During melting, the thermal energy is high enough to break some of the van der Waal's bonds and dipole-dipole bonds. The amount of these inter-molecular bonds which are broken will account for the value of the enthalpy of fusion. The thermal energy gained from melting is insufficient to break the inter-atomic primary bonds such as C-H, C-Cl, C-O, or C-N, contained within the organic molecule.

2.1.2.2 Aqueous Solutions

Hydrogen bonding is the major bond type in the case of aqueous solutions and water. It is caused by the hydrogen atom in a H_2O molecule being attracted to a highly electronegative oxygen atom in the neighboring H_2O molecule, thus providing a dipolar interaction to bind the nearby

aqueous species or H₂O molecules. Besides aqueous solutions and water, hydrogen bonding also exists in other compounds such as HF, NH₃, HCl, etc., due to the high value of the electronegativity of F, N, and Cl atoms. However, only the bonding characteristics of aqueous solutions is introduced here.

Considering that the major component (solvent) in aqueous solutions is water, an understanding of the model for melting of water is helpful in understanding the melting phenomenon of aqueous solutions. Figure 3 shows the structure of H₂O in its solid state.⁽⁹⁾ As seen from Figure 3, the ice crystals are arranged in a hexagonal configuration. The dashed line in Figure 3 represents the hydrogen bonding which binds the neighboring H₂O molecules, and therefore constitutes the lattice energy in H₂O. During melting some hydrogen bonds are broken by the thermal energy which is added. In other words, the lattice energy will be exceeded by other energy forms. The ratio of the values of the fusion enthalpy to the lattice energy is therefore a measure of the percentage of hydrogen bonds being broken during melting. The values of the fusion enthalpy and the lattice energy of H₂O were reported in the literature to be 1.436 kcal/mol^(6,7) and 13.4 kcal/mol⁽¹⁰⁾ respectively. The ratio of the fusion enthalpy (1.436 kcal/mol) to the lattice energy (13.4 kcal/mol) was calculated to be approximately 11%. This means that only 11% (1.436/13.4) of the hydrogen bonds are broken during the melting of ice. However, the inter-atomic O-H primary bonds are not broken during melting.

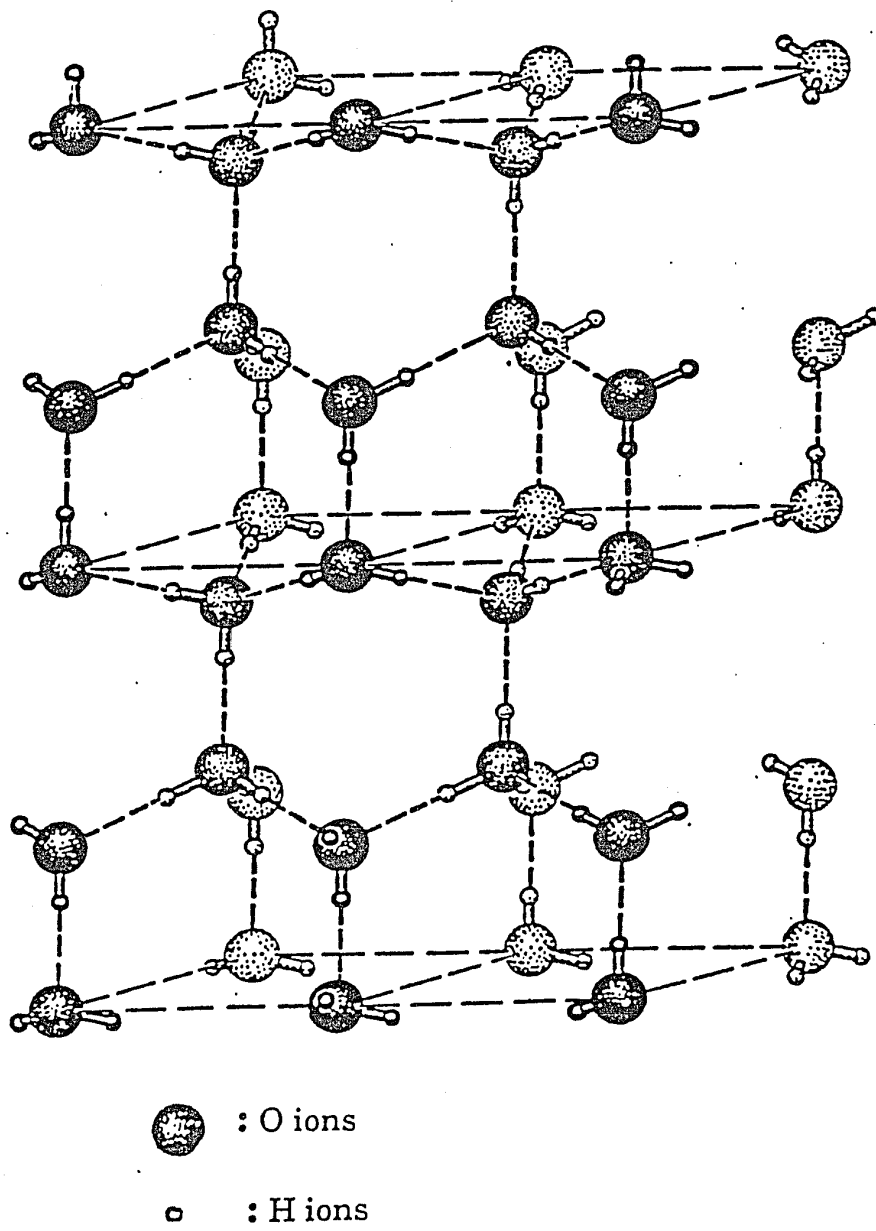


Figure 3 . Arrangement of Molecules in the Ice Crystal
(after Ref. 9)

2.2 Models for Predicting ΔS_m and ΔH_m

The purpose of the literature review was to locate models for predicting the enthalpy of fusion, ΔH_m . The models for predicting the entropy of fusion, ΔS_m , were also reviewed since the value of the fusion entropy (ΔS_m) is equal to the ratio of the fusion enthalpy (ΔH_m) to the melting point (T_m), based on thermodynamics as explained below.

For quasi-equilibrium conditions during melting, the Gibbs free energy of a pure specie in the solid state (G^s) is equal to that in the liquid state (G^l). The terms G^s and G^l are defined in Equations 2 and 3 respectively.

$$G^s = H^s - TS^s \quad [2]$$

where H^s is the enthalpy of a substance in the solid state, T is the temperature, and S^s is the entropy of a substance in the solid state.

$$G^l = H^l - TS^l \quad [3]$$

where H^l is the enthalpy of a substance in the liquid state, T is the temperature, and S^l is the entropy of a substance in the liquid state. Since the value of G^s is equal to G^l at the melting point, T_m , combining Equations 2 and 3 yields Equation 4.

$$H^l - H^s = T_m (S^l - S^s) \quad [4]$$

The term " $H^l - H^s$ " is the difference of the enthalpy between the solid state and the liquid state, which is the enthalpy of fusion, ΔH_m . The term " $S^l - S^s$ " is the difference of the entropy between the solid state and the liquid state, which is the entropy of fusion, ΔS_m . Equation 4 can be rewritten to yield Equation 5.

$$\Delta S_m = \Delta H_m / T_m \quad [5]$$

A number of models for predicting the fusion enthalpy or fusion entropy for different types of materials have been proposed. They were either derived

semi-empirically or quantitatively. These models are reviewed in this section and are summarized in Table 3. Separate columns are provided in Table 3 for the property of material modeled, the method of modeling, and the types of materials modeled. These models are reviewed in the following three subsections. One model for predicting ΔS_m of atomic species is described in Section 2.2.1, four models for predicting ΔS_m of organic compounds are described in Section 2.2.2, and two models for predicting ΔH_m of aqueous solutions are described in Section 2.2.3.

2.2.1 ΔS_m of Atomic Species

Perhaps the simplest model for predicting the fusion entropy of atomic species was proposed by Procopiu.⁽¹¹⁾ He investigated the fusion entropy of 13 metals by computing the ratio of the molar fusion enthalpy to the melting point. The ratio was found to be approximately equal to the gas constant, 1.986 entropy units (e.u. or cal/mol $^\circ$ K), which represents the energy of translation for one degree of freedom of the atoms. The equation that Procopiu used to determine the values of the fusion entropy is shown as Equation 6.

$$\Delta S_m \text{ (e.u.)} = [\Delta H_m \text{ (cal/g)} * M \text{ (g/mole)}] / T(^{\circ}\text{K}) \quad [6]$$

where ΔS_m is the fusion entropy in entropy units (e.u.),
 ΔH_m is the fusion enthalpy in calories per gram (cal/g),
 M is the atomic weight (g/mole), and
 T_m is the melting point ($^{\circ}$ K).

Table 3. Summary of Models for Predicting ΔS_m and ΔH_m

Proposed by	Property	Methodology	Type of Materials
Procopiu (1948)	ΔS_m	Semi-empirical	Atomic Species
Walden (1908)	ΔS_m	Semi-empirical	Organic
Pirsch (1937)	ΔS_m	Semi-empirical	Organic
Procopiu (1948)	ΔS_m	Semi-empirical	Organic
Chickos (1991)	ΔS_m	Quantitative	Organic
Rule of Mixtures*	ΔH_m	Quantitative	Aqueous Solution
Horvath (1985)	ΔH_m	Quantitative	Aqueous Solution

* It was not possible to determine who first proposed the Rule of Mixtures.

The term " $\Delta H_m \cdot M$ " is the molar fusion enthalpy. The results obtained by Procopiu are shown in Table 4.⁽¹¹⁾ The values of ΔH_m and T_m used by Procopiu were from the published literature.

According to this model, the enthalpy of fusion is dependent only on the melting point of the particular specie.

2.2.2 ΔS_m of Organic Compounds

Four models, either based on semi-empirical investigations or quantitative treatment, for predicting the ΔS_m of organic compounds have been proposed. These are described below.

2.2.2.1 Semi-empirical Model by Walden

Walden⁽¹²⁾ investigated a number of organic materials in order to find the relationship between the molar fusion enthalpy and the melting point. By computing the ratio of the molar fusion enthalpy to the melting point, he found that the fusion entropy ranges from 12.5 e.u. to 14.8 e.u., with an average of 13.5 e.u.. Table 5 shows the values of fusion entropy that were determined by Walden.⁽¹²⁾ The reported values of the fusion enthalpy in units of "cal/g" are contained in the fourth column of Table 5. The values of the molar fusion enthalpy were calculated by the product of the molecular weight (second column) and the fusion enthalpy in units of "cal/g" (fourth column), and are listed in the fifth column. The sixth column shows the calculated values of the fusion entropy in e.u..

Table 4. ΔS_m of 13 Atomic Species Determined by Procopiu (after Ref. 11)

Metal	Atomic wt. M (g/mol)	Melting Point T_m (K)	ΔH_m		ΔS_m (e.u.)
			cal/g	cal/mol	
Na	23.0	370	31.7	729.1	1.97
K	39.1	335	15.7	613.9	1.83
Cu	63.6	1356	41.6	2645.8	1.95
Ag	107.9	1234	21.07	2273.5	1.84
Cd	112.4	594	10.8	1213.9	2.04
Pb	207.2	600	5.86	1214.2	2.02
Al	27.0	931	76.8	2073.6	2.23
Fe	55.8	1535	59.0	3292.2	2.14
Au	197.2	1337	15.8	3115.8	2.33
Hg	200.6	234	2.77	555.7	2.37
Ni	58.7	1708	73.8	4332.1	2.54
Zn	65.4	692.5	28.3	1850.1	2.67
Pt	195.2	2028	27.2	5309.4	2.62

Table 5. ΔS_m of 31 Organic Materials, as Determined by Walden
(after Ref. 12)

Material	Mol. wt. (g/mol)	Melting Point (K)	ΔH_m		ΔS_m (e.u.)
			(cal/g)	(cal/mol)	
$C_{10}H_4Br_2$	236	358	20.6	4862	13.6
$C_6H_4Cl_2$	147	325.5	29.9	4395	13.5
C_6H_4ClBr	191.5	340	25.1	4807	14.1
$C_6H_4ClNH_2$	127.5	342	37.2	4743	13.9
$C_{10}H_7NO_2$	173	329	25.3	4377	13.3
$C_{10}H_7Br$	207	332	17.8	3685	12.7
C_7H_7Cl	126.5	280	28.0	3542	12.7
C_7H_7Br	171	299.9	21.9	3745	12.5
C_7H_7J	216	307	18.8	4061	13.2
$(C_6H_5)_2NH$	169	326	26.3	4445	13.6
$C_7H_7NH_2$	107	311.9	39.0	4173	13.4
$C_6H_5NH_2$	93	266	39.9	3711	13.9
$C_6H_4(CH_3)_2$	106	289	38.8	4113	14.2
$C_{10}H_8$	128	353	35.7	4570	12.9
$(C_6H_5)_2$	154	343.2	29.4	4528	13.2
$(C_6H_5)_2CH_2$	168	299.3	25.2	4234	14.1
$(C_6H_5)_3CH$	244	366	21.5	5246	14.3
$C_6H_4(NO_2)_2$	168	363	29.0	4872	13.4
$C_6H_5NO_2$	123	278.3	30.1	3702	13.3
$C_6H_4(C_3H_5)(OCH_3)$	148	295.5	27.3	4040	13.7
$C_6H_5COCH_3$	122	292.5	30.3	3697	12.6
$(C_6H_5)_2CO$	182	321	23.7	4313	13.4
C_7H_7COOH	136	350	32.0	4352	12.5
$C_6H_4(OH)COOC_{10}H_7$	264	366	18.0	4752	13.0

Table 5. ΔS_m of 31 Organic Materials, as Determined by Walden
(after Ref. 12) (continued)

Material	Mol. wt. (g/mol)	Melting Point (K)	ΔH_m		ΔS_m (e.u.)
			(cal/g)	(cal/mol)	
$C_6H_4(OCH_3)_2$	138	295.5	27.3	3767	12.8
$CH_3C_6H_2(NO_2)_3$	227	352	21.5	4881	13.9
$CH_3C_6H_3(NO_2)_3$	182	343	26.4	4805	14.0
$C_{14}H_{10}$	178	486	40.5	7209	14.8
$C_6H_5NHC_7H_7$	183	309	21.9	4008	13.0
$(C_6H_4)_2NH$	167	509	42.1	7031	13.8
N_2O_4	92	262.05	37.2	3422	13.1

2.2.2.2 Semi-empirical Model by Pirsch

Pirsch considered the value of fusion entropy to be related to the structure of the molecule, particularly the symmetry of the molecule.⁽¹³⁾ Therefore he classified the organic molecules into 3 groups: spherical molecules, ring-shaped molecules, and irregular molecules, in order of decreasing symmetry. He found the fusion entropy to be about 3 e.u. for spherical molecules (e.g., CH₄, CCl₄, (CH₃)₆C₂, Cl₃CCO₂H, (CH₃)₃COH), 13 e.u. for ring-shaped molecules (e.g., C₆H₆, cyclic compounds), and greater than 20 e.u. for irregular-shaped molecules or chains (e.g., alkanes).⁽¹⁴⁾

There may be two reasons to account for the smaller value of the fusion entropy, namely 3 e.u. for spherical molecules. First, the ratio of the surface area to the volume of the molecule is the smallest in the case of spherical molecules, and this results in the lowest free energy or inter-molecular interaction. Second, the spherical molecules are symmetric and therefore do not possess the dipole moments to enhance the inter-molecular interaction.

2.2.2.3 Semi-empirical Model by Procopiu

Procopiu found that for a number of organic materials the value of the fusion entropy was approximately equal to the number of atoms in the molecule. This represents the energy for 1 degree of freedom of kinetic energy for each atom.⁽¹⁵⁾

He formulated Equation 7 to predict the fusion entropy of organic compounds.

$$\Delta S_m = n * (1/2 * R) = n * (1/2 * 1.986) = n \quad [7]$$

where R is the gas constant (1.986 e.u.), and n is the number of atoms in the molecules. The term "1/2 *R" is related to one degree of freedom contributed from each atom. For organic materials containing n atoms, the entropy is therefore " n* (1/2*R) ".

2.2.2.4 Quantitative Model by Chickos

James S. Chickos⁽¹⁶⁾ used the group additivity theory for estimating the fusion entropies of organic compounds, namely hydrocarbons and hydrocarbon derivatives. This includes both monofunctional and multifunctional groups. The group additivity theory is based upon the assumption that the fusion entropy is a group property and can be estimated from the additivity of the contributions of each constituent part, provided that the structural environment of each group is taken into account. Fusion entropies are then summed from both carbon group contributions and functional group contributions.

The equations proposed by Chickos for predicting the fusion entropies of different categories of hydrocarbons are as follows:

(1) For acyclic and aromatic hydrocarbons,

$$\Delta S_m = \sum (n_i) (C_i) (G_i) \quad [8]$$

where n_i refers to the number of identical groups in the molecule, and C_i and G_i are group coefficients and group values respectively.

(2) For cyclic hydrocarbons,

$$\Delta S_m = [8.41 + 1.025 (n-3)] + \sum (n_i) (C_i) (G_i) \quad [9]$$

where n is the size of the ring.

(3) For polycyclic hydrocarbons,

$$\Delta S_m = [8.41 N + 1.025 (R-3N)] + \sum (n_i) (C_i) (G_i) \quad [10]$$

where N is the number of rings, and R is the total number of ring atoms.

The equations for predicting fusion entropies for hydrocarbon derivatives bearing functional groups were proposed as follows:

(1) For acyclic and aromatic hydrocarbon derivatives,

$$\Delta S_m = \sum (n_i) (C_i) (G_i) + \sum (n_j) (C_j) (G_j) + \sum (n_k) (C_k) (G_k) \quad [11]$$

where n_i is the number of carbon atoms without a functional group,
 n_j is the number of carbon atoms attached to the functional group,
 n_k is the number of functional groups,
 G_i and G_j are group values from carbon group contributions,
 G_k are group values from functional group contributions, and
 C_i/C_j and C_k are group coefficients for carbon groups and
functional groups respectively.

(2) For cyclic hydrocarbon derivatives,

$$\Delta S_m = [8.41 + 1.025 (n-3)] + \sum (n_i) (C_i) (G_i) + \sum (n_j) (C_j) (G_j) \\ + \sum (n_k) (C_k)(G_k) \quad [12]$$

where n is the size of the ring.

(3) For polycyclic hydrocarbons,

$$\Delta S_m = [8.41 N + 1.025 (R-3N)] + \sum (n_i) (C_i) (G_i) + \sum (n_j) (C_j) (G_j) + \sum (n_k) (C_k) (G_k) \quad [13]$$

where N is the number of rings, and R is the total number of ring atoms.

Table 6 is a list of entropy contributions from the carbon groups.⁽¹⁶⁾ Each carbon group, in terms of different structural environments (primary, secondary, etc.) and hybridizations (sp^2 , sp^3 , etc.), as listed in the first column, contributes a different amount towards the fusion entropy as listed in the third column (G_i). The group coefficients (C_j), as shown in the fifth column, are used as correction factors for those carbons bearing functional groups.

Table 7 is a listing of the entropy contribution from functional groups.⁽¹⁶⁾ Each functional group will also contribute a certain amount towards the fusion entropy, as listed in the second column (G_k). The group coefficients (C_k), as shown from the fourth to sixth columns, are used as correction factors when more than one functional group appears.

A total of 649 organic compounds were used by Chickos to evaluate the group values (G_i, G_k) and group coefficients (C_i, C_j, C_k) shown in Tables 6 and 7. This was done by regression analysis. The fusion entropies of these 649 materials had been compiled from 29 different sources. The model proposed by Chickos gave a quantitative treatment of fusion entropy and has been the most extensive means for analyzing the value of ΔS_m of organic materials thus far. The absolute average percent deviation of this model for predicting ΔS_m of hydrocarbons from the experimentally measured values was reported to be 12.1% by Chickos⁽¹⁷⁾ and this accounts for the reliability of the group additivity theory for the predictions of ΔS_m .

Table 6 : Carbon Group Contributions to Fusion Entropies (after Ref. 16)

	acyclic hydrocarbon groups	group value G_i	group coefficients ^b	
			C_i	C_j
primary sp^3 carbon atom	$CH_3[C]$	4.38	1.0	1.0
secondary sp^3 carbon atom	$CH_2[C_1]$	2.25	1.0	1.0
tertiary sp^3 carbon atom	$CH[C_1]$	-3.87	1.0	0.69
quaternary sp^3 carbon atom	$C[C_1]$	-9.25	1.0	0.67
secondary sp^2 carbon	Acyclic Olefinic and Acetylenic Groups			
tertiary sp^2 carbon	$C_nH_2[C_{sp}]^a$	3.48	1.0	1.0
quaternary sp^2 carbon	$C_nH[C_2C_{sp}]^a, C_nH[C_{sp}C_{sp}]^a$	1.16	1.0	3.23
tertiary sp carbon	$C_n[C_{sp}^2C_1]$	-2.72	1.0	1.0
quaternary sp carbon	$C_nH[C_{sp}]$	2.6	[1.0]	[1.0]
	$C_n[C_{sp}^2], C_n[C_{sp}C]$	0.52	[1.0]	[1.0]
tertiary sp^3 carbon	Aromatic Hydrocarbon Groups			
quaternary sp^2 carbon adjacent to an sp^3 carbon	$C_nH[C_n]$	1.54	1.0	1.0
peripheral quaternary sp^2 carbon adjacent to sp^3 carbon	$C_n[C_{2n}C_{sp}]^a$	-2.47	1.0	1.0
internal quaternary sp^2 carbon adjacent to sp^3 carbon	$C_n[C_{2n}C_{sp}]^a$	-1.02	1.0	1.0
quaternary sp^2 carbon adjacent to sp carbon	$C_n[C_{2n}]$	0.1	[1.0]	[1.0]
	$C_n[C_{2n}C_{sp}]$	-0.6	[1.0]	[1.0]
contribution of the ring: $(C_nH_2)_n$	Cyclic Molecules			
ring size: n atoms;	$[C_n]$			
cyclic tertiary sp^3 carbon	$\Delta S = 8.41 + 1.025(n - 3)$			
cyclic quaternary sp^3 carbon	$C_nH[C_2C]$, $C_nH[C_{2n}]$	-3.82	1.0	0.76
cyclic tertiary sp^2 carbon	$C_n[C_{2n}C_1]$, $C_n[C_2C]$, $C_n[C_{4n}]$	-7.88	[1.0]	1.0
cyclic quaternary sp^2 carbon	$C_nH[C_{2n}]$	-1.04	1.0	0.62
cyclic tertiary sp carbon	$C_n[C_1]$	-2.8	1.0	0.86
cyclic quaternary sp carbon	$C_n[C_{2n}]$	-1.28	[1.0]	[1.0]
total number of ring atoms: R	Polycyclic Molecules			
number of rings: N ;	$\Delta S = [8.41]N + 1.025[R - 3M]$			

a, aromatic; p, peripheral; i, internal; c, cyclic; u, unsaturated. ^b Values in brackets are tentative assignments.

Table 7. Functional Group Contributions to Fusion Entropies (after Ref. 16)

functional group (k)	group value G_k	group coefficient (C_k)			
		C_1	C_2	C_3	C_4
Type I					
aldehyde	4.70	1.0			
bromine	4.29	1.0	1.0	1.0	0.82
carboxylic acid	3.56	1.0	1.83	1.88	1.72
chlorine	2.0	1.0	2.0	2.0	1.93
fluorine on					
sp^2 carbon	3.11	1.0	1.0	1.0	1.0
sp^3 carbon	3.52	1.0	1.0	1.0	1.0
ring carbon	3.80	1.0	1.0	1.0	1.0
hydroxyl group					
alcohol	0.27	1.0	12.6	18.9	26.4
phenol	3.96	1.0	1.0	[1.0]	[1.0]
iodine	4.05	[1.0]	[1.0]		
nitrile	2.30	1.0	1.4		
nitro group	4.15	1.0	1.0	1.0	
primary amide	6.26	1.0	1.0		
primary amine					
aromatic	3.70	[1.0]	1.0		
aliphatic	3.88	1.0	1.82		
thiols	4.30	1.0	[1.0]		
urea, monoalkyl	6.16	1.0			
Aromatic Type II					
aromatic heterocyclic nitrogen	1.75	1.0	[1.0]	[1.0]	
Acyclic Type II					
secondary amides					
amines	-0.1	1.0	1.0		
secondary	-0.52	[1.0]	[1.0]		
tertiary	-3.8	[1.0]			
carbamate	-0.14	[1.0]			
carbonate	-3.38	[1.0]			
disulfide	1.26	[1.0]			
ester	0.88	1.0	1.0	1.0	1.0
ether	0.26	1.0	[1.0]	1.0	[1.0]
ketone	0.75	1.0	1.0		
sulfide	1.72	1.0			[0.36]
sulfone	0.78	[1.0]			
Cyclic Type II					
cyclic amine					
secondary	0.44	[1.0]			
tertiary	-4.08	[1.0]	[1.0]		
tertiary sp^2	0.40	[1.0]	[1.0]		
cyclic ether	0.32	[1.0]	[1.0]	[1.0]	[1.0]
cyclic ketone	-0.45	[1.0]	1.0		
cyclic sulfide	0.52	1.0	[1.0]		
lactone	-0.55	1.0	[1.0]		

2.2.3 Fusion Enthalpy of Aqueous Solutions

Two models for predicting the fusion enthalpy of aqueous solutions were identified, namely, the Rule of Mixtures and Horvath's model which is a model for dilute solutions.

2.2.3.1 The Rule of Mixtures

The Rule of Mixtures is commonly used to determine the enthalpy of fusion of a binary system which shows ideal behavior. The equation for predicting fusion enthalpies of ideal solutions is as follows:

$$\Delta H_m (\text{ideal solution}) = X_a \Delta H_a + X_b \Delta H_b \quad [14]$$

where ΔH_a and ΔH_b are the fusion enthalpies for components a and b respectively, and X_a and X_b are the respective molar fractions of components a and b.

For predicting fusion enthalpies of aqueous solutions, Equation 14 can be rewritten as follows :

$$\Delta H_m (\text{aqueous solutions}) = X_a \Delta H_a + X_{H_2O} \Delta H_{H_2O} \quad [15]$$

where X_a and X_{H_2O} are the molar fraction of solute "a" and water respectively, and ΔH_a and ΔH_{H_2O} are the fusion enthalpy of solute "a" and water respectively.

2.2.3.2 Horvath's Model

A.L.Horvath⁽¹⁸⁾ proposed the following equation for computing the melting point of a dilute solution:

$$T_m = (T_m^0) / (1 + RT_m^0 * N_2 \div \Delta H_m + N_1) \quad [16]$$

where T_m is the melting point (K) of the solution,
 T_m^0 is the melting point (K) of the pure solvent,
 ΔH_m is the molar enthalpy of fusion (cal/mole) of the solution, and
 N_1 and N_2 are the number of moles of solvent and solute
respectively.

The results and the origin of this equation were not addressed by the author. Therefore this equation was rederived from a thermodynamic viewpoint, and is shown in Appendix A.

For the purpose of predicting the fusion enthalpies of aqueous solutions Equation 16 can be rewritten as follows:

$$\Delta H_m = R * T_m^0 * (N_2 / N_1) * [T_m / (T_m^0 - T_m)] \quad [17]$$

where T_m^0 is the melting point of pure water, 273K, and T_m is the melting point of the aqueous solution. Thus, by measuring the melting point of an aqueous solution, it would be possible to compute the ΔH_m for that particular solution.

All the seven models described in this chapter were tested for their accuracy. The four semi-empirical models were tested using data available from the published literatures. The three quantitative models, namely Chickos's model, the Rule of Mixtures, and Horvath's model, were tested against experimental data. The experimental methodology employed in this investigation is described in Chapter 3.

CHAPTER 3

INVESTIGATION METHODOLOGY

This chapter presents the methodology for investigating the value of the enthalpy of fusion. Both a theoretical and an experimental approach were taken in this research. A theoretical investigation of the ΔH_m from the models is needed in order to make future experimental work easier. The existing models, as described in Chapter 2, were employed to calculate the theoretical ΔH_m . These models included Chickos's model applied to organic compounds, and both the Rule of Mixtures and Horvath's model applied to aqueous solutions. An experimental investigation of ΔH_m was also needed, considering the fact that literature values of ΔH_m are occasionally unreliable for organic compounds, and frequently unavailable for aqueous solutions. Experiments were conducted to test the validity of the findings from the theoretical models. The experimental methodology employed in this study is described in Section 3.2.

3.1 Theoretical

The candidate FHS materials are either organic compounds or aqueous solutions, as shown in Table 1. Therefore the fusion enthalpies of organic compounds and aqueous solutions were modeled in this project.

3.1.1 Organic Compounds

A total of 4 models, namely Walden's model, Pirsch's model, Procopiu's model, and Chickos's model, for predicting ΔS_m of organic compounds were

found from the literature. Based on a limited number of organic materials, Walden found the ΔS_m to have a constant value of 13.5 e.u.. However, due to the lack of sound theoretical reasoning, it is doubtful that this statement will hold true for all the thousands of organic materials that exist today. Pirsch categorized the organic compounds into three groups and considered each material in the same group to have the same value of fusion entropy. This characterization is also too broad to quantify the fusion entropies of all organic compounds. Procopiu considered the value of ΔS_m to be approximately equal to the number of atoms. According to this, any two molecules with the same number of atoms are expected to have the same value of fusion entropy, which would be unlikely. These three models are all too general and are unlikely to accurately predict fusion entropy of organic materials. In this investigation, they were tested against data available from the literature⁽¹⁹⁾ to determine their validity, but were not employed for modeling purposes due to the lack of sound theoretical reasoning.

Chickos used the group additivity theory and regression analysis to characterize organic materials into different structural environments, hybridizations, and functional groups. The absolute average percentage deviation between the calculated fusion entropy and experimental values was reported by Chickos to be 12.1% for hydrocarbons.⁽¹⁷⁾ Based on his reported accuracy, the group additivity theory for predicting ΔS_m of organic materials appears to be reliable. As can be seen from Tables 6 and 7, Chickos's model is a very specific and quantitative model, compared to the other three models. Therefore this model was chosen for modeling and testing against the experimental data.

To predict ΔH_m of organic materials from Chickos's model, the following equation was used:

$$\Delta H_m = T_m * \Delta S_m \quad [5]$$

where T_m is the melting point which was determined experimentally, and ΔS_m is the fusion entropy which was determined from Equations 8 through 13, according to the applicable category. The values of the entropy contribution from both carbon groups and functional groups were obtained from Tables 6 and 7.

3.1.2 Aqueous Solutions

Two models for predicting ΔH_m of aqueous solutions were found from the literature, the Rule of Mixtures and Horvath's model. The validity of these two models had not been investigated previously due to the fact that experimental values of ΔH_m for aqueous solutions have been unavailable.

Based on the Rule of Mixtures, the ΔH_m of aqueous solutions is given by Equation 15:

$$\Delta H_m (\text{aqueous solutions}) = X_a \Delta H_a + X_{H_2O} \Delta H_{H_2O} \quad [15]$$

where ΔH_a and ΔH_{H_2O} are the fusion enthalpies of solute "a" and water respectively, and X_a and X_{H_2O} are molar fractions of solute "a" and water respectively. The values of X_a and X_{H_2O} are determined from the original compositions. The values of ΔH_a and ΔH_{H_2O} were obtained from the published literature.^(6,19) These are listed in Appendix B.

Based on Horvath's model, the ΔH_m of aqueous solutions is given by Equation 17.

$$\Delta H_m = R * T_m^0 * (N_2 / N_1) * [T_m / (T_m^0 - T_m)] \quad [17]$$

where T_m is the melting point (K) of the solution which was determined experimentally, T_m^0 is the melting point (K) of pure water 273°K, and N_1 and N_2 are the number of moles of water and the dissociated solute ions, respectively, determined from the original compositions.

3.2 Experimental

Experimental values of fusion enthalpy are needed as a standard to test the reliability of the models, as proposed in Section 3.1, for predicting the values of fusion enthalpy. The materials for which the values of ΔH_m and T_m were measured are presented in Section 3.2.1. The experimental methodology for obtaining the values of fusion enthalpies is described in Section 3.2.2.

3.2.1 Materials

The materials that were chosen for experimental verification of ΔH_m and T_m are listed in Tables 8 and 9. Those listed in Table 8 constitute the organic compounds, and those listed in Table 9 constitute the aqueous solutions. Those materials identified by an " * " in Tables 8 and 9, are candidate FHS materials identified by Selvaduray and Lomax. The cooling capacity was determined only for candidate FHS materials that yielded an experimental T_m between -13°C to 5°C. All materials were purchased from Aldrich Chemical Company and all aqueous solutions were prepared using de-ionized water.

Table 8. Organic Compounds Selected for ΔH_m and T_m Measurements

Material	Purity
Glycerol triacetate*	100%
Triethylene glycol*	99%
Benzene,hexafluoro*	100%
Heptanoic acid*	99%
2-methyl-2-butanol*	99%
2,3-Butanedione*	99%
Benzoic acid,2-fluoro*	97%
Cyclohexanol,2-methyl(trans)*	99%
Cyclohexanol,4-methyl(cis)*	98%
Tert-Butyl hydroperoxide*	100%
Benzene,1,4-difluoro*	99%
Cyclohexanone,2-methyl*	99%
Cinnamonnitrile*	97%
Cyclooctatetraene*	98%
4-Methoxybenzaldehyde*	98%
Benzyl alcohol*	99%
Indene*	99%
Cyclohexane,1,2-dibromo*	99%
Benzene*	98%
Biphenyl,2-methyl*	99%
Naphthalene,1-iodo*	99%
1,2-dihydronaphthalene*	98%
Biphenyl,3-methyl*	95%
Piperidene*	99%

* Candidate FHS materials identified by Selvaduray and Lomax

Table 9. Aqueous Solutions Selected for ΔH_m and T_m Measurements

Materials	Concentration	Purity
Magnesium chloride	1.0%	98%
	5.0%	98%
	10.0%	98%
	15.0%	98%
Lithium bromide	1.0%	99%
	5.0%	99%
	10.0%	99%
	15.0%	99%
Lithium chloride	1.0%	99%
	4.0%*	99%
	12.0%	99%
Calcium chloride	8.0%	97%
	12.0%	97%
	15.0%	97%
Sodium chloride	7.0%*	98%
	15.0%	98%
Potassium chloride	9.0%*	99%
Sodium bromide	11.0%*	99%
Potassium chromate	18.0%*	98%
Potassium bromide	13.0%*	99%
Sodium nitrate	10.0%*	98%
Potassium iodide	16.0%*	99%
Cesium chloride	19.0%*	99%
Sodium hydroxide	4.5%*	97%
Silver nitrate	16.0%*	99%
Potassium nitrate	10.0%*	100%

* Candidate FHS materials identified by Selvaduray and Lomax

Table 9. Aqueous Solutions Selected for ΔH_m and T_m Measurements (continued)

Materials	Concentration	Purity
Potassium sulfate	5.0%*	99%
Potassium hydroxide	6.0%*	99%
Potassium dichromate	2.5%*	99%
Formic acid	2.0%	96%
	10.0%*	96%
	32.0%	96%
Acetic acid	2.0%	99.8%
	13.0%*	99.8%
	20.0%	99.8%
Ethylene glycol	2.0%	99%
	12.0%*	99%
	28.0%	99%
Ethanol	9.5%*	100%
	24.0%	100%
Glycerol	16.0%*	99.5%
	40.0%	99.5%

* Candidate FHS materials identified by Selvaduray and Lomax

3.2.2 Equipment and Experimental Methodology

A Perkin-Elmer Differential Scanning Calorimeter, Model DSC-4, was used to determine the fusion enthalpies, melting temperatures, and heat capacities. The experimental setup, the principle of measurement, the operating procedures, and the interpretations of the curve from the DSC scans are described below.

3.2.2.1 Experimental Setup

The Differential Scanning Calorimeter and the System 4 Microprocessor Controller, both made by Perkin-Elmer Corporation, were used in this study and are shown in Figure 4. The accessories for the equipment are the sample sealer, the sample pan holder, and a box of aluminum pans and pan covers. These are shown in Figure 5 from left to right, respectively. Figure 6 is a photograph of both the aluminum pan and pan cover, illustrating relative sizes. The sample holder and the reference holder, which are located inside the Differential Scanning Calorimeter, were also photographed in order to show where the material investigated was located, and are shown in Figure 7. During experiments, the material under investigation is placed into the sample holder while an empty pan as a reference is placed into the reference holder.

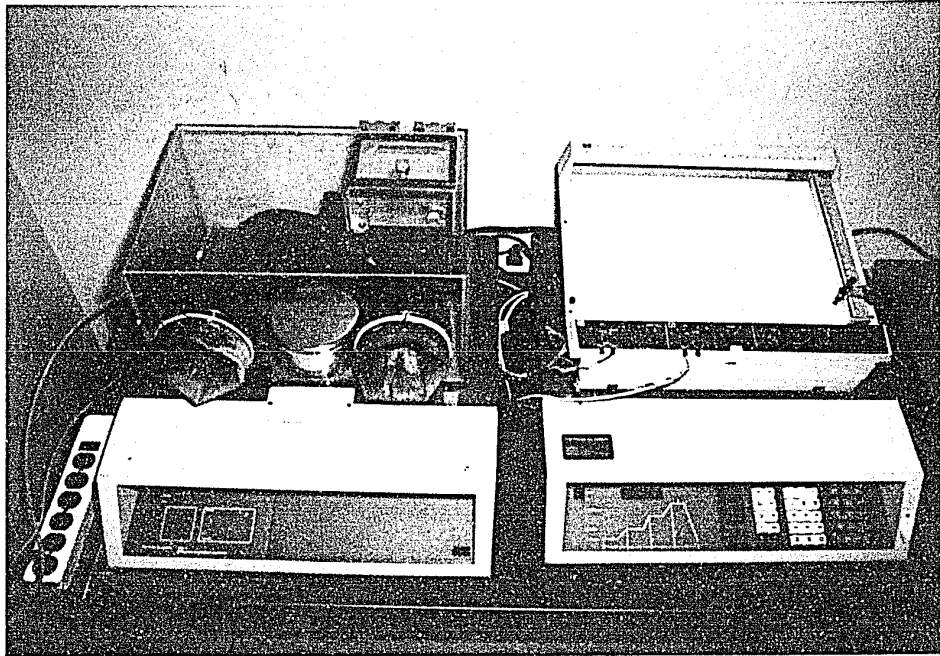


Figure 4 . View of the DSC and the System 4 Microprocessor Controller

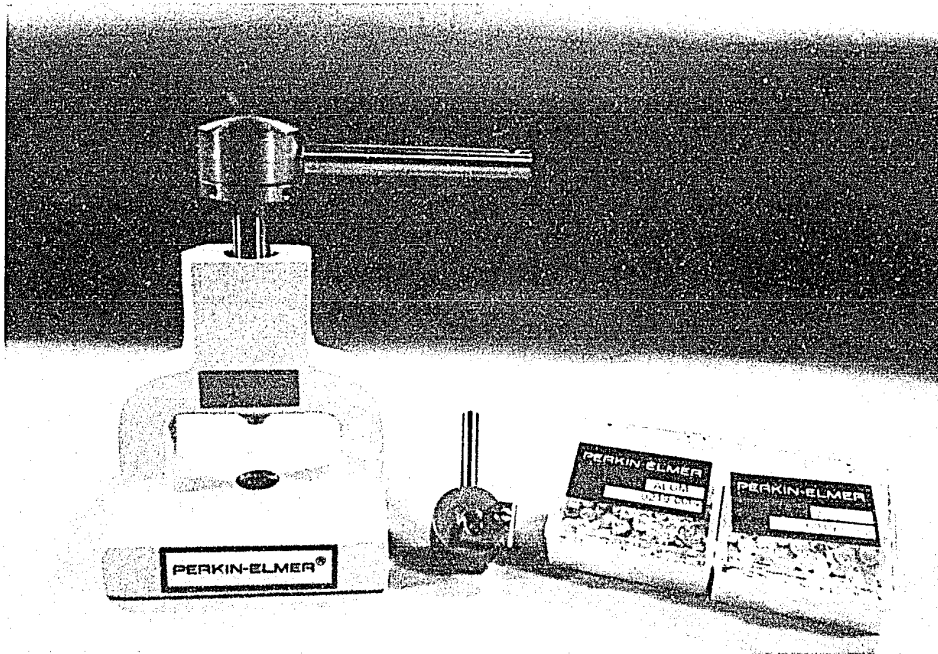


Figure 5 . View of the Accessories for the Equipment

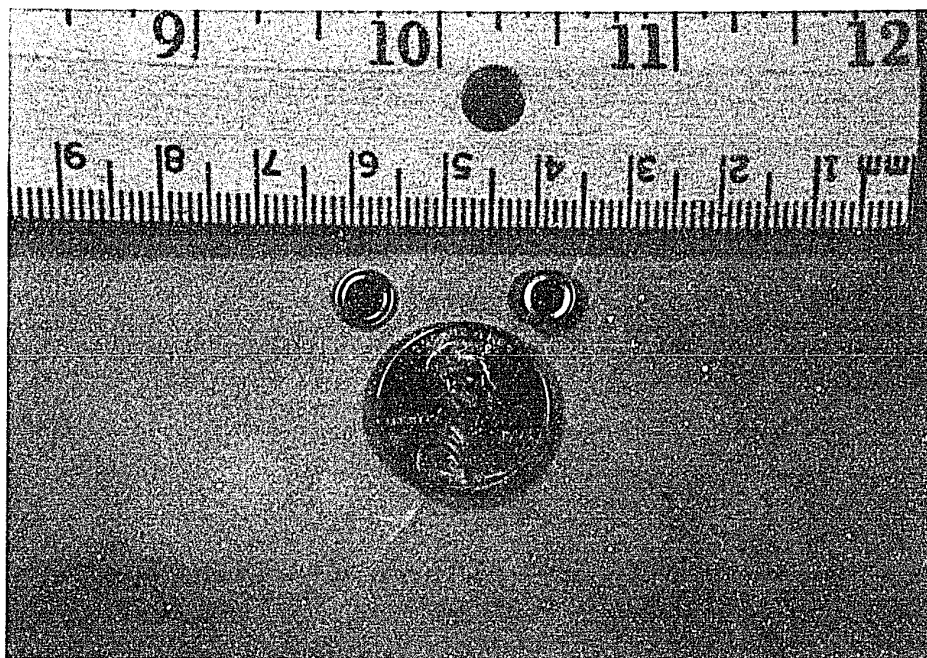


Figure 6 . View of an Aluminum Pan and Pan Cover Illustrating Relative Sizes

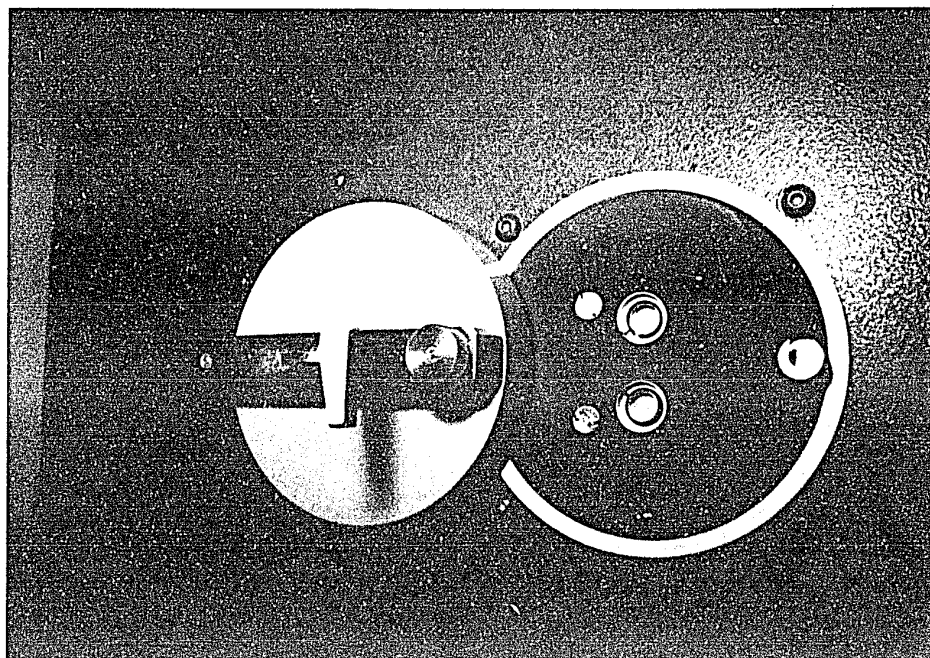


Figure 7 . View of the Sample Chamber Including the Sample Holder (Circle in the Bottom) and the Reference Holder (Circle in the Top)

3.2.2.2 Principles of Measurement

The arrangement of the DSC in Figure 8 is presented to explain the functioning of a Differential Scanning Calorimeter. The sample material and reference material (an empty pan) are placed in identical environments. Resistance thermometers are used to detect the temperature in both holders. During experiments, the material investigated is placed in the sample holder while the reference holder contains only an empty pan. The temperatures of the two holders are maintained at the same level by two heaters, one for each holder. The difference in energy required to maintain the two holders at identical temperatures is a measure of the thermal property of the material being investigated.

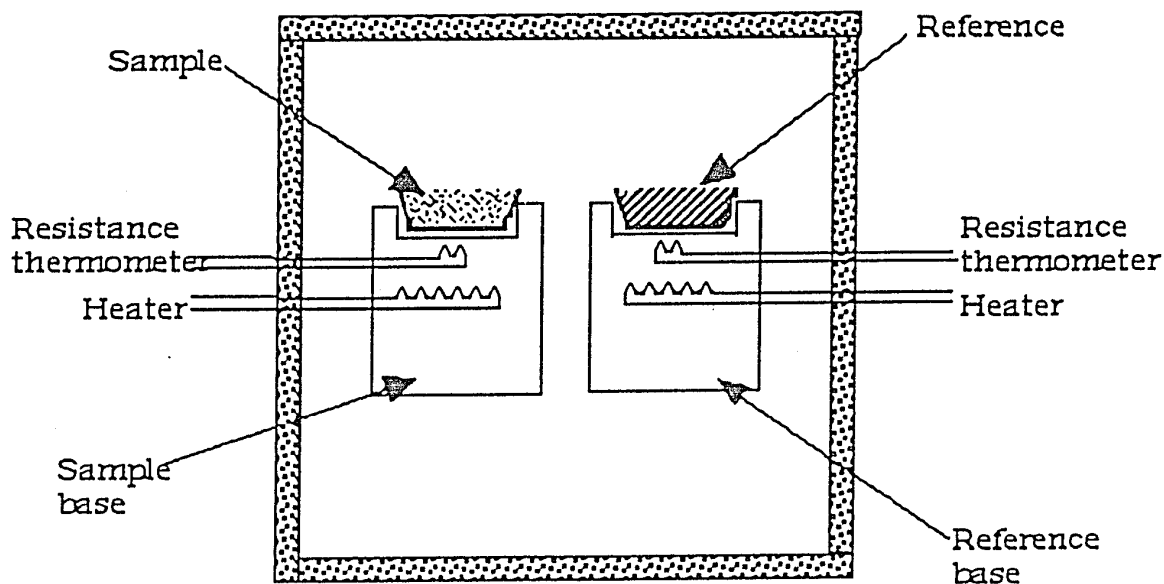


Figure 8 . Experimental Arrangement of DSC

3.2.2.3 Procedure for Operating the DSC

In order to verify accurate functioning of the DSC, calibration runs were first done with de-ionized water and indium. To prepare a de-ionized water sample pan for calibrating the DSC, four stages should be followed. These four stages are illustrated by means of the four photographs shown in Figures 9a, 9b, 9c, and 9d. Figure 9a shows the pan being placed on top of the sample pan holder. Figure 9b shows how de-ionized water was dropped into the pan. Figure 9c shows a pan cover being placed on the pan. Figure 9d shows the use of a sample sealer to seal the pan and pan cover. After the initial calibration of the instrument is finished, the procedure for operating the DSC are as follows.

The first step is to purge the sample chamber with nitrogen gas to remove the moisture inside the chamber. Moisture becomes a condensate during cooling and affects the accuracy of the results from the experiment.

The second step is to calibrate the ordinate (energy). This is to make certain that the Y-axis displacement in the chart recorder (heat flow rate), coincides with the preset programmed value of energy supply rate. As suggested by the operation manual, the calibration was performed at 50°C.

The third step is to cool the instrument down to -50°C. Dry ice, which sublimates at -78.6 °C,⁽²⁰⁾ was used as a coolant.

The fourth step is to optimize the flatness of the baseline. The baseline ought to be horizontal if the environment of the two holders is identical. However, the slope of the baseline may become positive or negative due to slight differences between the construction of the sample holder cover and the reference holder cover. The purpose of baseline optimization is to retain a

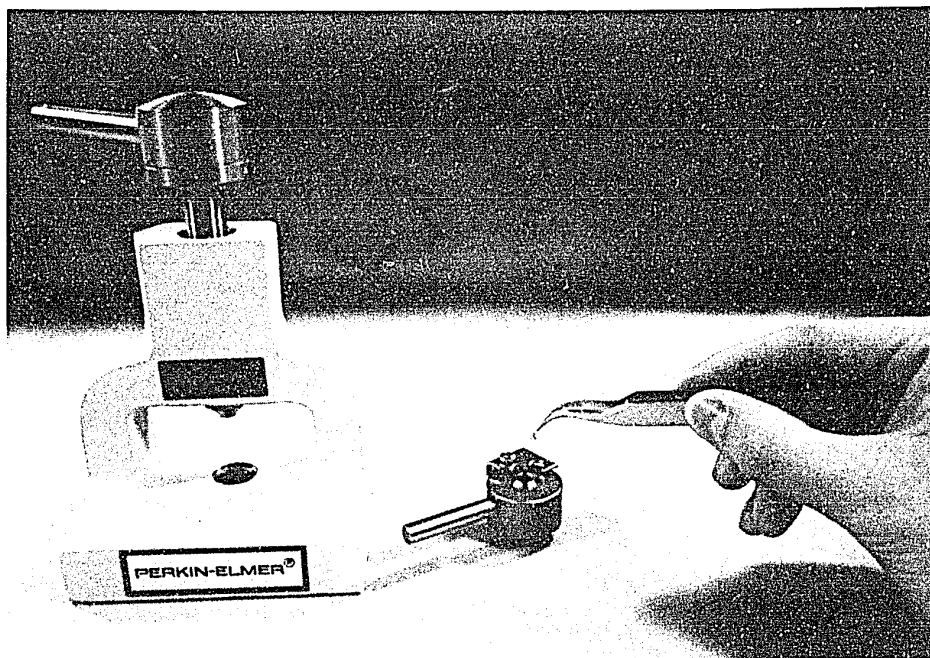


Figure 9a . The Process for Preparing a Sample Pan (Stage one)

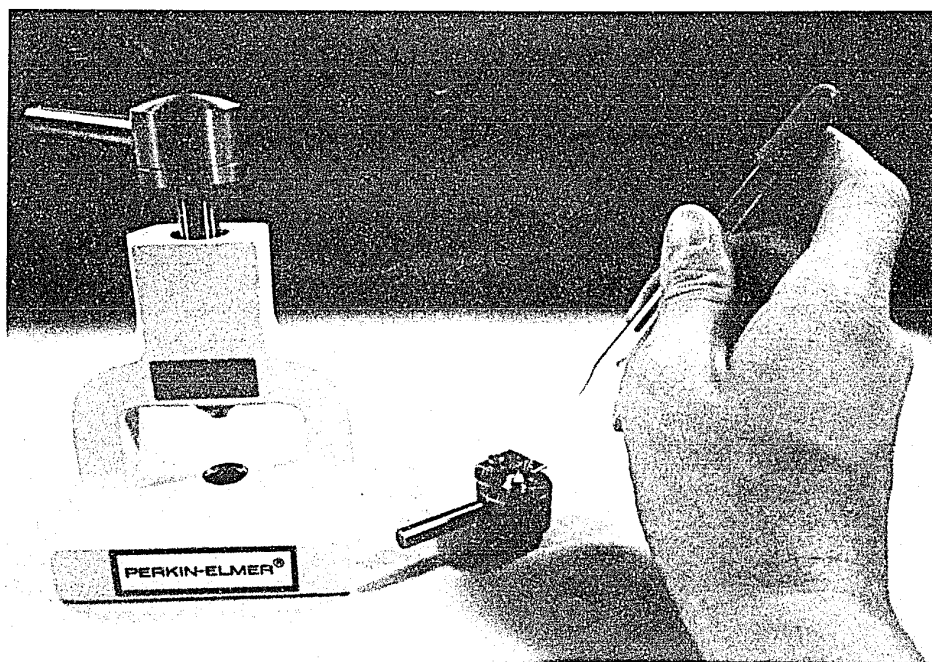


Figure 9b . The Process of Preparing a Sample Pan (Stage two)

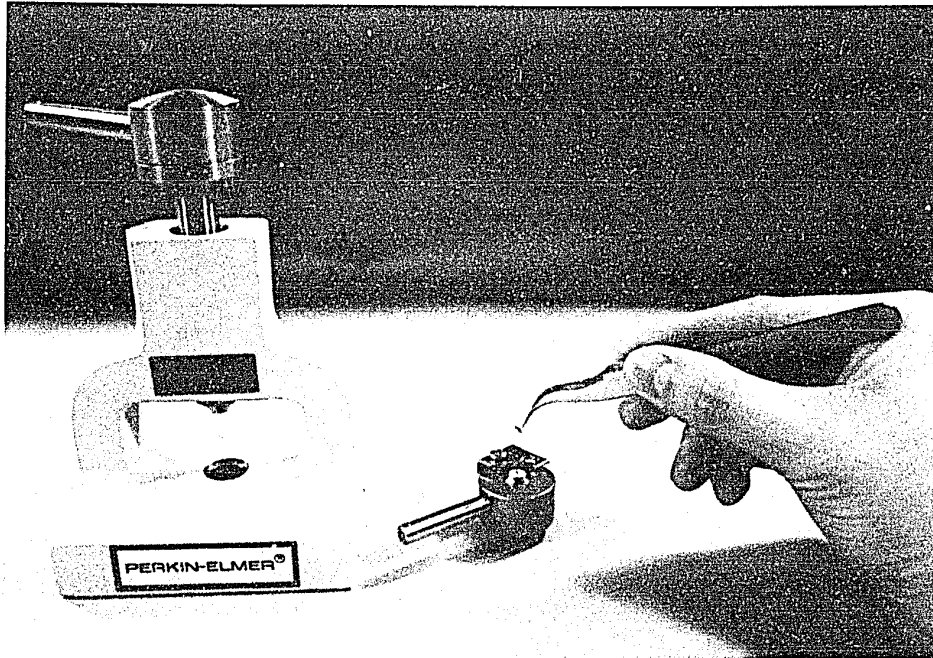


Figure 9c . The Process for Preparing a Sample Pan (Stage three)

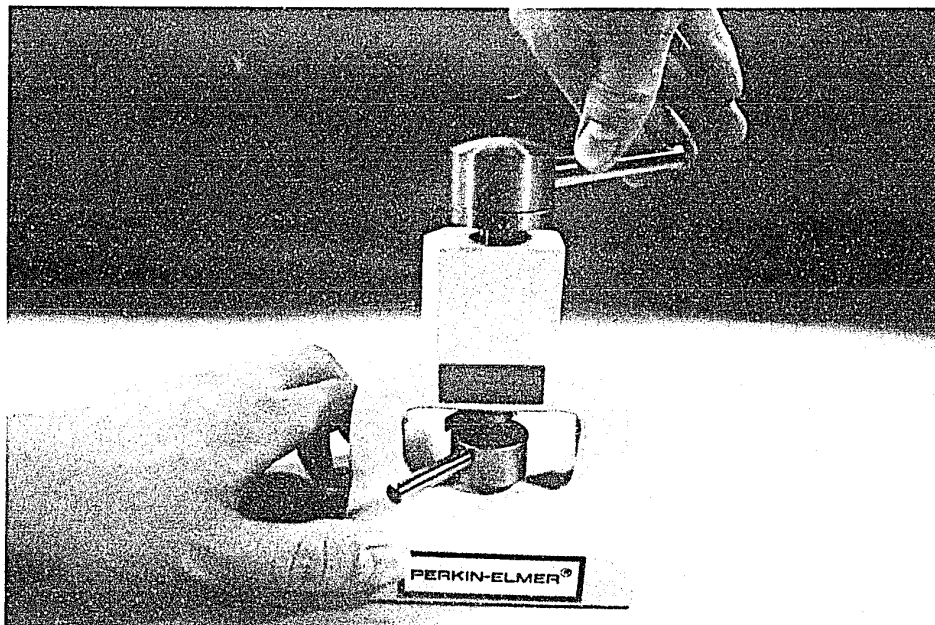


Figure 9d . The Process for Preparing a Sample Pan (Stage four)

horizontal baseline by adjusting the heat flow rate. This step is performed over a temperature range of -50°C to 30°C , with both holders empty.

The fifth step is to prepare the sample materials for investigation. First a pan and pan cover are weighed using a microbalance accurate to 0.0001 grams. Both the pan and pan cover are made of aluminum. A pan cover should be used to avoid the loss of weight of volatile material, due to evaporation during scanning. The material investigated, with an approximate weight of several milligrams, is then dropped into the pan and covered with the pan cover. The pan cover and sample pan are then sealed together in the sample sealer to ensure the air-tightness between them and then weighed. The process of preparing a sample pan was illustrated by means of the four photographs in Figures 9a through 9d. After weighing, this sample pan is placed into the sample holder shown in Figure 7. The same weighing and sealing procedure is followed to prepare an empty pan for the reference holder.

The sixth step is to set up the parameters of scanning, including heating rate, initial temperature, and final temperature. The materials investigated were scanned from -50°C to 30°C at a heating rate of $2^{\circ}\text{C}/\text{min}$. The maximum allowable heating rate is a function of the weight of the material. Heavier materials require a slower heating rate to complete the phase transition. The relationship between maximum allowable heating rate and the weight of material was investigated. The data for water is shown in Appendix C. From these measurements it was determined that a heating rate of $2^{\circ}\text{C}/\text{min}$ would be slow enough to be insensitive to the sample weight. After scanning, the sample pan is weighed to determine if any evaporation had occurred. If the

evaporation is greater than 2%, then a new sample should be made up, and the measurement repeated.

The last step is to scan an empty pan in order to determine the heat capacity of the material being measured. This is done by placing an empty pan in both holders and using the same procedure as that for the scanning of the material investigated.

3.2.2.4 Appearance of DSC Curve

Figure 10 shows a typical DSC scan. The X axis is the temperature scale and the Y axis is the heat flow rate. The curve from the DSC scan appears to be "peak-like." This is explained in the following paragraph.

In the case of a solid-liquid transition, the heat flow rate is expected to reach a maximum which corresponds to the absorption of the latent heat of melting. Therefore, the graph obtained should theoretically be "delta-shaped" or "pulse-shaped," meaning that the phase transition happens at a specific temperature (melting point). However, owing to the delay in heat transfer from the bottom layer of the material (inside the sample pan) to the top, the curve is "peak-like" instead of "pulse-shaped."

3.2.2.5 Determination of T_m , ΔH_m , $C_{p,s}$ and $C_{p,l}$

Figure 10 illustrates how data concerning T_m , ΔH_m , $C_{p,s}$, and $C_{p,l}$ is obtained from a Differential Scanning Calorimeter scan. The tangent line AA' of the sample curve intersects the sample solid baseline BB' and the sample liquid baseline CC' at points M and N. The melting temperature, T_m ,

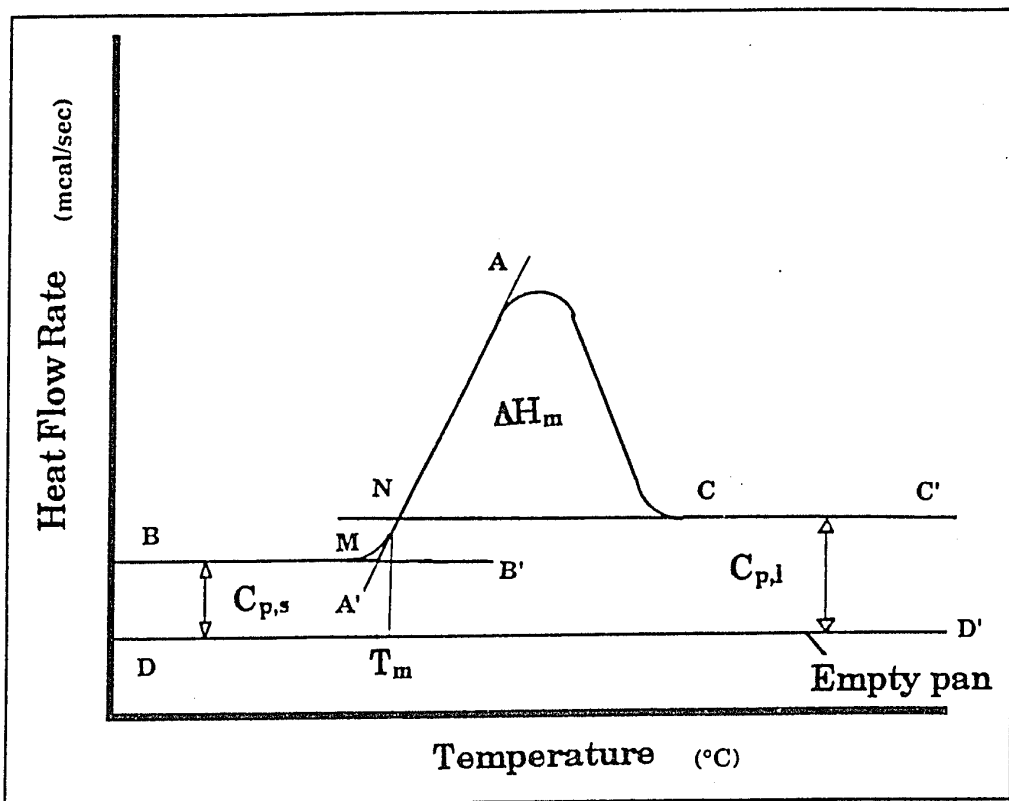


Fig 10 . DSC Scan Plot

is determined by locating the mid-point of the segment MN, as shown in Figure 10.

The fusion enthalpy, ΔH_m is determined using Equation 18.

$$\Delta H_m = [(R * A) / (W * S)] * K' \quad [18]$$

where ΔH_m is the fusion enthalpy of the material in calories per gram,
 R is the range sensitivity in mcal/sec-inch,
 A is the area of the peak (ΔNAC) in square inches,
 W is the weight of the material in milligrams,
 S is the recorder chart speed in inch/sec, and
 K' is the instrument constant.

The value of K' is obtained from the calibration of indium (In) and is determined using Equation 19.

$$K' = (\Delta H_{m (ref)}) / [(R * A) / (W * S)] \quad [19]$$

where $\Delta H_{m (ref)}$ is the enthalpy of fusion of indium from the reference (Perkin-Elmer Catalogue). R, A, W, and S are the same parameters as those described in Equation 18. A detailed sample calculation for determining ΔH_m of water is shown in Appendix D.

The $C_{p,s}$ and $C_{p,l}$ data is obtained by comparison with experiments conducted with empty pans. The value of $C_{p,s}$ is determined by Equation 20.

$$C_{p,s} = (dH/dt) / [(dT/dt) (W)] \quad [20]$$

where dH/dt is the heat flow rate, determined by measuring the distance between the empty baseline (DD') and the sample's baseline in the solid state (BB'), dT/dt is the heating rate, and W is the weight of the sample.

The value of $C_{p,l}$ is determined by Equation 21.

$$C_{p,l} = (dH/dt) / (dT/dt) (W) \quad [21]$$

where dH/dt is the heat flow rate, determined by measuring the distance between the empty baseline (DD') and the sample's baseline in the liquid state (CC'), dT/dt is the heating rate, and W is the weight of the sample.

The experimental values of fusion enthalpy determined according to the procedure documented in this chapter were used to evaluate the three quantitative models: Chickos's model, the Rule of Mixtures, and Horvath's model. These results are presented in Chapter 4.

CHAPTER 4

RESULTS AND DISCUSSION

This chapter presents the results of the evaluation of the seven existing models described in Chapter 2. The four semi-empirical models for predicting fusion entropy, as described in Section 2.2, were tested using available published literature data. The results are presented, along with a discussion of their validity, in Section 4.1. The experimental data including the values of melting point, enthalpy of fusion, and heat capacity is presented in Section 4.2. The three quantitative models for predicting fusion enthalpy, as described in Section 3.1, were tested against the experimental data. The results are presented, along with a discussion of their validity, in Section 4.3.

4.1 Validity of the Semi-empirical Models

Four semi-empirical models for predicting ΔS_m were tested. The entropy of fusion was calculated based on the models presented in Chapter 2. The results of these calculations are summarized in this section. For ease of understanding, the results for each model are presented separately. The calculated values were compared with the published literature values and the percentage deviation determined.

4.1.1 Procopiu's Model for ΔS_m of Atomic Species

Procopiu found that the value of fusion entropy was approximately equal to the gas constant, 1.986 e.u. (cal/mol^oK), for 13 selected atomic species. To determine if this model is applicable for a wider range of atomic species, a

total of 59 atomic species were investigated. The results are shown in Figure 11. The X axis is the melting point and the Y axis is the fusion enthalpy. The line OZ corresponds to the constant value of fusion entropy, 1.986 e.u., as predicted by Procopiu. As can be seen from Figure 11, Procopiu's model is reliable for most atomic species.

To further determine the accuracy of this model in applications to different groups, these 59 atomic species were arranged according to the Periodic Table and tested individually. The results are shown in Table 10. The third column contains the ΔS_m determined by Procopiu's model. The ΔS_m values in the fourth column were obtained by dividing the ΔH_m values reported in the literature⁽⁶⁾ by the melting point. The fifth column contains the absolute percent value of the deviation between the calculated values and the values determined from the literature.

As can be seen from Table 10, Procopiu's model has an accuracy within 35% for most atomic species except Ga, Si, Ge, Sn, As, Sb, Bi, Ne, Ar, Xe, La, Pr, Nd, and Pm. The elements Si, Ge, Sn belong to the IVA group. The elements As, Sb, Bi belong to the VA group. The elements Ne, Ar, Xe belong to the VIIIA group. The elements La, Pr, Nd, Pm belong to the Lanthanides. Procopiu's model seems quite reliable when applied to materials in the IA, IIA, IB, IIB, IIIB, IVB, VB, VIB, VIIB, and VIII groups. Within the constraints of this project it was not possible to pursue the reasons that might explain this behavior.

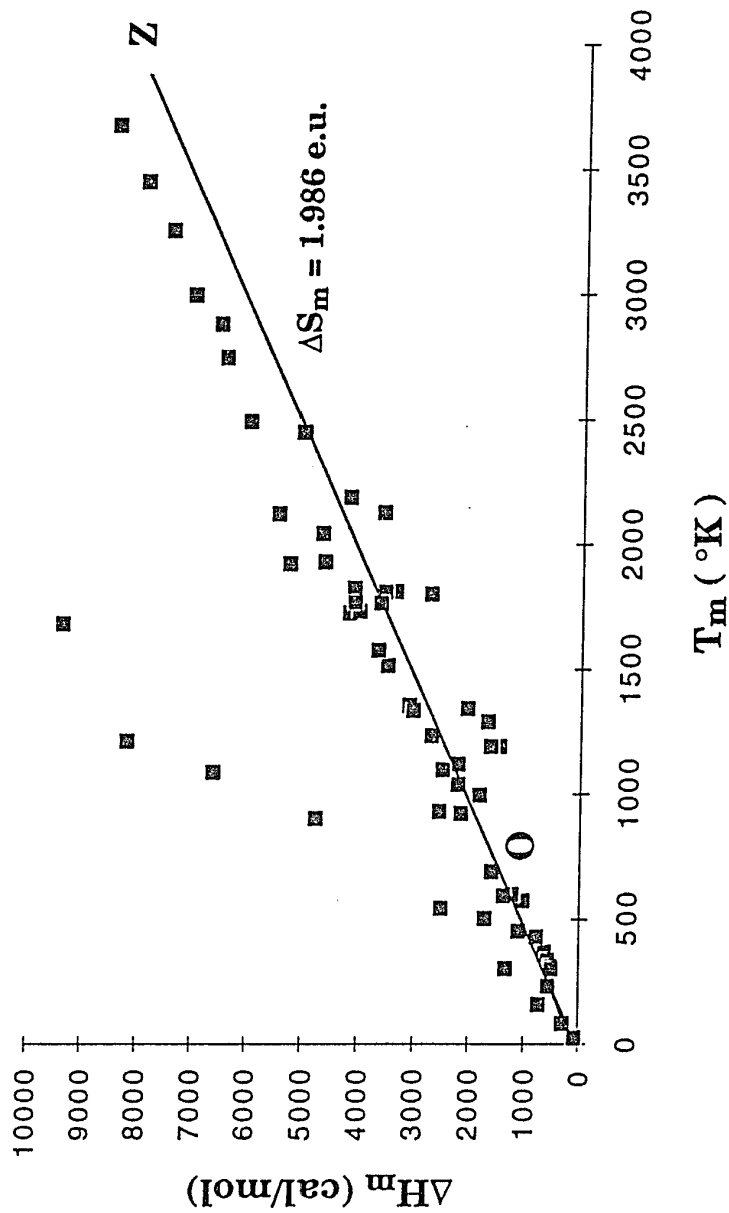


Figure 11 . Plot of ΔH_m vs. T_m for 59 Atomic Species
 (ΔH_m and T_m data from Ref. 6)

Table 10. Test of Procopiu's Model for ΔS_m of Atomic Species

Atomic Species	Periodic Table Group	ΔS_m (e.u.) (by Procopiu)	ΔS_m (e.u.) (from literature ⁽⁶⁾)	% deviation
Li	IA	1.986	2.43	18%
Na	IA	1.986	1.70	17%
K	IA	1.986	1.71	16%
Rb	IA	1.986	1.68	18%
Cs	IA	1.986	1.66	20%
Mg	IIA	1.986	2.34	15%
Ca	IIA	1.986	1.98	0%
Sr	IIA	1.986	2.13	7%
Ba	IIA	1.986	1.83	9%
B	IIIA	1.986	2.06	4%
Al	IIIA	1.986	2.74	28%
Ga	IIIA	1.986	4.41	55%
In	IIIA	1.986	1.82	9%
Tl	IIIA	1.986	1.79	11%
Si	IVA	1.986	5.57	64%
Ge	IVA	1.986	6.74	71%
Sn	IVA	1.986	3.40	42%
Pb	IVA	1.986	2.04	3%
As	VA	1.986	6.07	67%
Sb	VA	1.986	5.28	62%
Bi	VA	1.986	4.60	57%
Ne	VIIIA	1.986	3.17	37%
Ar	VIIIA	1.986	3.50	43%
Xe	VIIIA	1.986	4.58	57%
Cu	IB	1.986	2.29	13%
Ag	IB	1.986	2.19	9%
Au	IB	1.986	2.27	13%

Table 10. Test of Procopiu's Model for ΔS_m of Atomic Species (continued)

Atomic Species	Periodic Table Group	ΔS_m (e.u.) (by Procopiu)	ΔS_m (e.u.) (from literature ⁽⁶⁾)	% deviation
Zn	IIB	1.986	2.30	14%
Cd	IIB	1.986	2.33	15%
Hg	IIB	1.986	2.38	17%
Sc	IIIB	1.986	1.86	7%
Y	IIIB	1.986	1.52	31%
Ti	IVB	1.986	2.41	18%
Zr	IVB	1.986	2.58	23%
Hf	IVB	1.986	2.41	18%
V	VB	1.986	1.92	3%
Nb	VB	1.986	2.35	15%
Ta	VB	1.986	2.29	13%
Cr	VIB	1.986	1.69	18%
Mo	VIB	1.986	2.28	13%
W	VIB	1.986	2.30	14%
Mn	VIIB	1.986	2.31	14%
Re	VIIB	1.986	2.30	14%
Fe	VIII	1.986	1.97	1%
Co	VIII	1.986	2.06	4%
Ni	VIII	1.986	2.43	18%
Pd	VIII	1.986	2.25	12%
Pt	VIII	1.986	2.30	14%
Os	VIII	1.986	2.35	15%
La	Lanthanides	1.986	1.24	60%
Pr	Lanthanides	1.986	1.37	45%
Nd	Lanthanides	1.986	1.31	52%
Pm	Lanthanides	1.986	1.37	45%

Table 10. Test of Procopiu's Model for ΔS_m of Atomic Species (continued)

Atomic Species	Periodic Table Group	ΔS_m (e.u.) (by Procopiu)	ΔS_m (e.u.) (from literature ⁽⁶⁾)	% deviation
Sm	Lanthanides	1.986	1.53	30%
Eu	Lanthanides	1.986	2.27	13%
Gd	Lanthanides	1.986	2.33	15%
Ho	Lanthanides	1.986	2.32	14%
Er	Lanthanides	1.986	2.32	14%
Lu	Lanthanides	1.986	2.74	28%

4.1.2 Walden's Model for ΔS_m of Organic Compounds

Walden found the value of ΔS_m to be approximately constant at 13.5 e.u., based on data for 31 organic materials. To determine if this model is applicable for a wider range of organic materials, a total of 572 organic materials were investigated. The values of melting point and fusion enthalpy of these 572 materials had been compiled by William E. Acree, Jr.⁽¹⁹⁾ The graph of their fusion enthalpies versus melting points is shown in Figure 12. To test the reliability of Walden's model, the lines OM, OA, and OB were drawn in Figure 12. These lines correspond to the constant values of fusion entropy 13.5 e.u., 13.5 - 20% e.u., and 13.5 + 20% e.u., respectively. According to Walden's model, each organic material should lie on OM, or at least lie between OA and OB, considering a $\pm 20\%$ deviation of this model. However, a large number of organic materials lie outside this region, as can be seen from Figure 12. Walden's model is therefore not reliable in predicting the fusion entropy of organic materials.

4.1.3 Pirsch's Model for ΔS_m of Organic Compounds

Pirsch considered the value of ΔS_m to be 3 e.u. for spherical molecules, 13 e.u. for ring-shaped molecules, and greater than 20 e.u. for irregular shaped molecules. According to this, materials which belong to the same category and also possess the same chemical formula ought to have the same values of ΔS_m . A total of fifteen materials, including those with the same chemical formula, from these three categories were selected to test Pirsch's statement. This is shown in Table 11. The second column contains the structural category of the materials. The third column is the fusion entropy

OB : $\Delta S_m = 13.5 + 20\% \text{ e.u.}$
 OM : $\Delta S_m = 13.5 \text{ e.u.}$
 OA : $\Delta S_m = 13.5 - 20\% \text{ e.u.}$

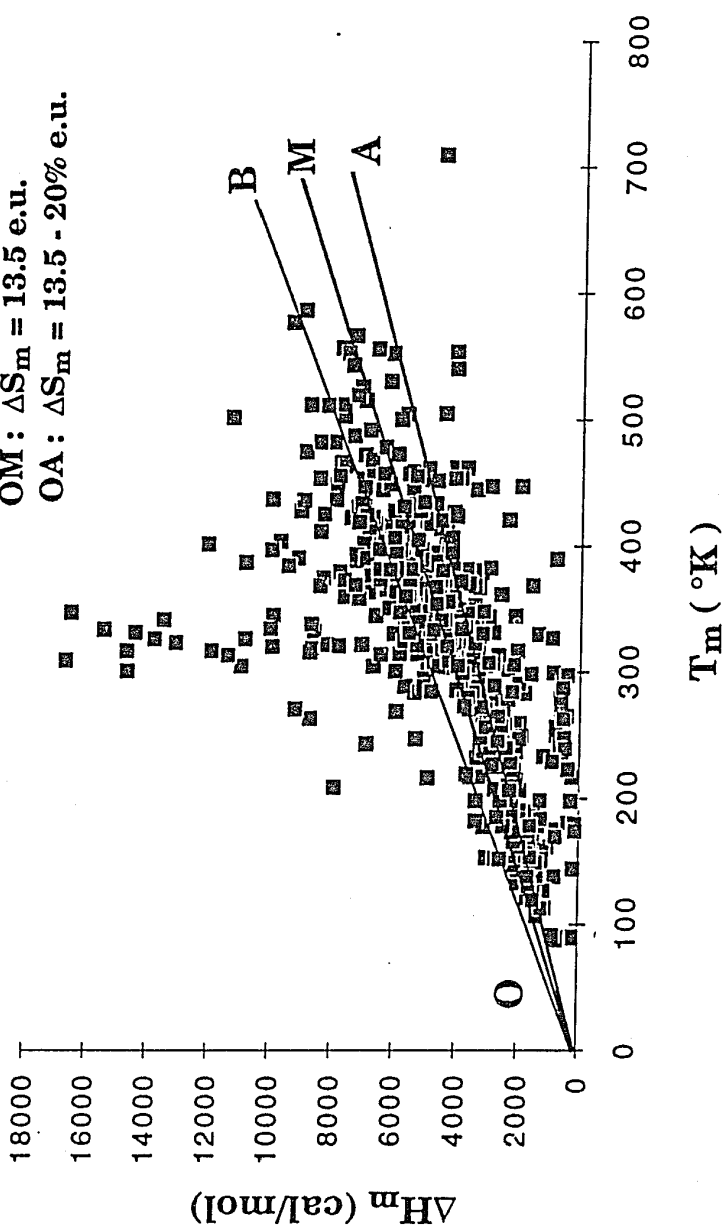


Figure 12 . Plot of ΔH_m vs. T_m for 572 Organic Materials
 (ΔH_m and T_m data from Ref. 19)

Table 11. Test of Pirsch's Model for ΔS_m of Organic Materials

Materials	Category	ΔS_m (e.u.) (by Pirsch)	ΔS_m (e.u.) (literature ⁽¹⁹⁾)	% deviation
CH ₄	Spherical	3	2.47	21%
CD ₄	Spherical	3	2.40	25%
CCl ₄	Spherical	3	3.13	4%
CCl ₃ COOH	Spherical	3	4.25	29%
(CH ₃) ₃ COH	Spherical	3	5.44	45%
C ₆ H ₆	Ring-shaped	13	8.54	52%
C ₆ Cl ₆	Ring-shaped	13	11.29	15%
C ₆ H ₁₂ (cyclohexane)	Ring-shaped	13	2.25	478%
C ₆ H ₁₂ (methyl-cyclopentane)	Ring-shaped	13	12.69	2%
C ₇ H ₁₄ (cycloheptane)	Ring-shaped	13	1.70	665%
C ₇ H ₁₄ (methyl-cyclohexane)	Ring-shaped	13	11.02	18%
C ₈ H ₁₆ (cyclooctane)	Ring-shaped	13	2.0	550%
C ₈ H ₁₆ (ethyl-cyclohexane)	Ring-shaped	13	12.31	6%
C ₁₃ H ₈ Cl ₂ O	Irregular	>20	17.15	
C ₁₄ H ₈ O ₂	Irregular	>20	13.99	

predicted by Pirsch. The fourth column is the fusion entropy obtained from the available literature⁽¹⁹⁾. The absolute percent deviation of Pirsch's model was then calculated, and is listed in the fifth column.

As seen from Table 11, materials in the same category, even with the same chemical formula, do not have the same ΔS_m values as predicted by this model. For example, cyclooctane (C_8H_{16}) and ethyl-cyclohexane (C_8H_{16}) are not only in the same category (ring-shaped) but also have the same chemical formula and therefore should have the same value for ΔS_m , namely 13 e.u.. Actual ΔS_m values for these two compounds are extremely different: 2 e.u. for cyclooctane and 12.3 e.u. for ethyl-cyclohexane. This is contrary to Pirsch's model and may be due to differences in intermolecular force caused by different dipole moments. Cyclooctane has a symmetrical structure and therefore does not have a dipole moment. However, ethyl-cyclohexane is not symmetric and possesses dipole moments which enhance the intermolecular force. The same was found with C_6H_{12} and C_7H_{14} compounds. This model resulted in huge deviations of 550%, 665%, and 478% for predicting the fusion entropy of cyclooctane, cycloheptane, and cyclohexane, respectively. The results suggest that Pirsch's model is too general and cannot be used to predict the fusion entropy of organic materials accurately.

4.1.4 Procopiu's Model for ΔS_m of Organic Compounds

Procopiu concluded that the fusion entropy of a molecule was equal to the number of atoms in the molecule. From this model, any two molecules with the same number of atoms are expected to have the same value for fusion entropy. Therefore, some materials with the same chemical formula

were selected for investigation to determine if they have the same values of ΔS_m , as this model suggests. Ten materials were selected to test Procopiu's model and the results are shown in Table 12. The second column in Table 12 contains the fusion entropy predicted by Procopiu. The third column is the fusion entropy obtained from the compiled source⁽¹⁹⁾ and the fourth column contains the absolute percentage value of the deviation between the calculated values and the values determined from the literature.

As seen from Table 12, materials with the same number of atoms do not have the same fusion entropies as expected from this model. There were huge deviations of 1100%, 1135%, 700% for predicting the fusion entropy of cyclooctane, cycloheptane, and cyclohexane, respectively. Discrepancies of 459% and 1268% were also found in the case of 2,2-dimethylpropane and 2,2,3,3-tetramethylpentane. It is thus found that this model does not apply to symmetric molecules or branched molecules. Procopiu's model considers the value of ΔS_m to be dependent solely on the number of atoms, which obviously ignores the effect of any intermolecular forces that exist.

4.2 Experimental Data

The melting points, T_m , and fusion enthalpies, ΔH_m , of materials in Tables 8 and 9 were measured by the Differential Scanning Calorimeter (DSC) and are presented in Table 13. In order to verify the candidate FHS materials identified by Selvaduray and Lomax, the solid heat capacity, $C_{p(\text{solid})}$, and liquid heat capacity, $C_{p(\text{liquid})}$, were also measured. Only materials that proved to have melting points within -13°C to 5°C were selected for experimental measurement of ΔH_m , $C_{p(\text{solid})}$, and $C_{p(\text{liquid})}$.

Table 12. Test of Procopiu's Model for ΔS_m of Organic Compounds

Materials	ΔS_m (e.u.) by Procopiu (=number of atoms)	ΔS_m (e.u.) from literature ⁽¹⁹⁾	% deviation
C ₅ H ₁₂ (n-Pentane)	17	14.04	21%
C ₅ H ₁₂ (2,2-Dimethylpropane)	17	3.04	459%
C ₉ H ₂₀ (n-Nonane)	29	16.84	72%
C ₉ H ₂₀ (2,2,3,3-Tetramethylpentane)	29	2.12	1268%
C ₆ H ₁₂ (cyclohexane)	18	2.25	700%
C ₆ H ₁₂ (methyl-cyclopentane)	18	12.69	42%
C ₇ H ₁₄ (cycloheptane)	21	1.70	1135%
C ₇ H ₁₄ (methyl-cyclohexane)	21	11.02	91%
C ₈ H ₁₆ (cyclooctane)	24	2.0	1100%
C ₈ H ₁₆ (ethyl-cyclohexane)	24	12.31	95%

Table 13. Experimental Fusion Enthalpy, Melting Point, and Heat Capacity

Materials	T_m (°C)	ΔH_m (cal/mol)	$C_{p(\text{solid})}$ (cal/mol°C)	$C_{p(\text{liquid})}$ (cal/mol°C)
Water*	0.087	1451	9.4	19.1
Indium	156.0	789	-	-
Glycerol triacetate*	x	nm	-	-
Triethylene glycol*	x	nm	-	-
Benzene, hexafluoro*	5.34	2893	-	-
Heptanoic acid*	-10.14	3679	75.6	49.5
2-methyl-2-butanol*	x	nm	-	-
2,3-Butanedione*	x	nm	-	-
Cyclohexanol, 2-methyl (trans)*	x	nm	-	-
Cyclohexanol, 4-methyl (cis)*	-3.96	2143	34.3	52.5
Tert-Butyl hydroperoxide*	x	nm	-	-
Benzene,1,4-difluoro*	-22.79	2671	-	-
Cyclohexanone,2-methyl*	-14.14	3696	-	-
Cinnamonnitrile*	5.08	2891	-	-
Cyclooctatetraene*	-8.21	2425	32.3	38.5
4-Methoxybenzaldehyde*	-1.89	3782	46.9	50.3
Benzyl alcohol*	x	nm	-	-
Indene*	-6.15	1754	41.8	52.3
Cyclohexane,1,2-dibromo*	-4.98	2896	39.7	48.4
Benzene*	x	nm	-	-
Biphenyl,2-methyl*	-0.48	2865	42.1	69.0
Naphthalene,1-iodo*	x	nm	-	-
1,2-dihydronaphthalene*	-10.05	2450	41.0	48.2
Biphenyl,3-methyl*	x	nm	-	-
Piperidene*	-18.46	2619	-	-

* Candidate FHS materials identified by Selvaduray and Lomax

x No transformation was detected from -50°C to 30°C

nm Not measured

Table 13. Experimental Fusion Enthalpy, Melting Point, and Heat Capacity (continued)

Materials	Percent	T_m (°C)	ΔH_m (cal/mol)	$C_{p(\text{solid})}$ (cal/mol°C)	$C_{p(\text{liquid})}$ (cal/mol°C)
Magnesium chloride	1%	-0.13	1316	-	-
	5%	-6.53	975	-	-
	10%	-14.43	565	-	-
	15%	-24.94	309	-	-
Lithium bromide	1%	-0.217	1438	-	-
	5%	-5.61	1043	-	-
	10%	-9.58	764	-	-
	15%	-16.78	609	-	-
Lithium chloride	1%	-1.63	1264	-	-
	4% *	-7.96	925	12.0	16.8
	12%	-24.84	331	-	-
Calcium chloride	8%	-4.75	1108	-	-
	12%	-6.24	1018	-	-
	15%	-8.22	910	-	-
Sodium chloride	7% *	-20.6 ($T_{tr,1}$)	1282	-	-
		-10.2 ($T_{tr,2}$)			
	15%	-20.5	1231	-	-
Potassium chloride	9% *	-8.55	1373	8.3	14.7
Sodium bromide	11% *	-29.94 ($T_{tr,1}$)	1418	-	-
		-9.68 ($T_{tr,2}$)			
Potassium chromate	18% *	-10.96 ($T_{tr,1}$)	1511	6.7	18.3
		-8.7 ($T_{tr,2}$)			
Potassium bromide	13% *	-12.15 ($T_{tr,1}$)	1361	7.9	18.2
		-11.04 ($T_{tr,2}$)			

* Candidate FHS materials identified by Selvaduray and Lomax

$T_{tr,1}$ Eutectic temperature

$T_{tr,2}$ Liquidus temperature

Table 13. Experimental Fusion Enthalpy, Melting Point, and Heat Capacity (continued)

Materials	Percent	T _m (°C)	ΔH _m (cal/mol)	C _{p(solid)} (cal/mol°C)	C _{p(liquid)} (cal/mol°C)
Sodium nitrate	10.0% *	-16.35 (T _{tr,1}) -8.5 (T _{tr,2})	1443	-	-
Potassium iodide	16.0% *	-20.82 (T _{tr,1}) -8.95 (T _{tr,2})	1479	-	-
Cesium chloride	19.0% *	-22.66 (T _{tr,1}) -10.75 (T _{tr,2})	1424	-	-
Sodium hydroxide	4.5% *	-7.27	737	11.1	15.7
Silver nitrate	16.0% *	-8.68 (T _{tr,1}) -7.72 (T _{tr,2})	1471	7.1	18.3
Potassium nitrate	10.0% *	-2.41	1583	6.5	17.1
Potassium sulfate	5.0% *	-0.81	1492	7.5	17.1
Potassium hydroxide	6.0% *	-7.26	921	13.1	10.5
Potassium dichromate	2.5% *	-0.02	1547	7.4	20.3
Formic acid	2.0%	-1.15	1259	-	-
	10.0% *	-7.53	1084	11.1	15.9
	32.0%	-25.07	480	-	-
Acetic acid	2.0%	-1.21	1387	-	-
	13.0% *	-8.54	1111	11.9	19.8
	20.0%	-10.65	939	-	-
Ethylene glycol	2.0%	-0.06	1386	-	-
	12.0% *	-5.52	1120	14.6	23.6
	28.0%	-21.64	470	-	-

* Candidate FHS materials identified by Selvaduray and Lomax

T_{tr,1} Eutectic temperature

T_{tr,2} Liquidus temperature

Table 13. Experimental Fusion Enthalpy, Melting Point, and Heat Capacity (continued)

Materials	Percent	T_m (°C)	ΔH_m (cal/mol)	$C_{p(\text{solid})}$ (cal/mol°C)	$C_{p(\text{liquid})}$ (cal/mol°C)
Ethanol	9.5% *	-6.72	954	14.9	19.1
	24.0%	-17.6	417	-	-
Glycerol	16.0% *	-7.95	947	13.0	19.0
	40.0%	-24.78	406	-	-

* Candidate FHS materials identified by Selvaduray and Lomax

The accuracy of the apparatus (DSC-4) was determined to be within 2%, based on calibration runs with water and indium. The data used to arrive at this conclusion is shown in Appendix E. Ten organic compounds, as identified with an "x" in the second column of Table 13, did not have solid-liquid transitions during the heating process from -50°C to 30°C. It is probable that their melting points are below -50°C.

4.3 Evaluations of the Models for Predictions of ΔH_m

This section contains the results obtained in evaluation of the quantitative models. Evaluation of Chickos's model for predicting fusion enthalpies of organic compounds is presented in Section 4.3.1. The Rule of Mixtures is evaluated in Section 4.3.2, and Horvath's model is evaluated in Section 4.3.3. For ease of understanding, the results for each model are presented separately. The calculated values were compared with the experimental measurements and the percentage deviation determined.

4.3.1 Chickos's Model for ΔH_m of Organic Materials

The fusion enthalpies of organic compounds predicted from Chickos's model were compared to those determined from differential scanning calorimetry. The results are shown in Table 14. The second column in Table 14 is the ΔH_m calculated according to Chickos's model. The detailed calculations are contained in Appendix F. The ΔH_m values in the third column were determined by DSC. The fourth column contains the absolute percent deviation between the calculated values and the values determined experimentally.

Table 14. Test of Chickos's Model for ΔH_m of Organic Materials

Materials (Organic compounds)	ΔH_m (cal/mol) (by Chickos's model)	ΔH_m (cal/mol) (from DSC)	%deviation
Benzene,hexafluoro	3490	2893	21%
Heptanoic acid	5044	3679	37%
Cyclohexanol,4-methyl(cis)	2532	2143	18%
Benzene,1.4-difluoro	2587	2671	3%
Cyclohexanone,2-methyl	2378	3696	36%
Cinnamotrile	3862	2891	34%
Cyclooctatetraene	1381	2425	43%
4-methoxybenzaldehyde	3649	3782	4%
Indene	2386	1754	36%
Cyclohexane,1.2-dibromo	3822	2896	32%
Biphenyl,2-methyl	3742	2865	31%
1,2-dihydronaphthalene	3175	2450	30%
Piperidene	3035	2619	16%
average deviation = 26.3%			

As can be seen from Table 14, the average deviation between the calculated values and measured values was found to be 26.3%.

4.3.2 The Rule of Mixtures for ΔH_m of Aqueous Solutions

The fusion enthalpies of aqueous solutions, as predicted from the Rule of Mixtures, are compared to those determined from experiments. The results are shown in Table 15. The second column in Table 15 is the ΔH_m predicted by the Rule of Mixtures. The ΔH_m values in the third column were determined from differential scanning calorimetry. The fourth column is the absolute percent of the deviation between the calculated values and the values determined experimentally. A sample calculation for determining the ΔH_m of $MgCl_2$, according to the Rule of Mixtures, is contained in Appendix G.

The Rule of Mixtures for predicting ΔH_m of aqueous solutions was tested and the absolute average deviation was calculated to be 75.9%. However, the values ranged from a high of 434.3% to a low of 0.1%. As seen from Table 15, the Rule of Mixtures gives accurate predictions of fusion enthalpies for dilute solutions. However, this model appears to become inaccurate when the concentration of the solute is increased. The Rule of Mixtures assumes that the solution is a mixture of pure components and does not take into account the nature of interaction between the constituents. In dilute solutions, this interaction might not be great enough to affect the fusion enthalpies of the solutions. In concentrated solutions, because more solute and solvent (water) molecules are involved, the interactions of constituents become important and play a significant role in determining the fusion enthalpies of solutions. Due to this, a factor concerning the interaction of solute and water will be

Table 15. Test of the Rule of Mixtures for ΔH_m of Aqueous Solutions

Materials (Aqueous Solution)		ΔH_m (cal/mol) (by Rule of Mixtures)	ΔH_m (cal/mol) (from DSC)	%deviation
Magnesium chloride	1%	1449	1316	10.1%
	5%	1502	975	54.1%
	10%	1573	565	178.4%
	15%	1651	309	434.3%
Lithium bromide	1%	1439	1438	0.1%
	5%	1452	1043	39.2%
	10%	1469	764	92.3%
	15%	1488	609	144.3%
Lithium chloride	1%	1443	1264	14.2%
	4%	1466	925	58.5%
	12%	1532	331	362.8%
Calcium chloride	8%	1501	1108	35.5%
	12%	1537	1018	51.0%
	15%	1566	910	72.1%
Sodium chloride	7%	1567	1282	22.2%
	15%	1734	1231	40.9%
Potassium chloride	9%	1552	1373	13.0%
Sodium bromide	11%	1535	1418	8.3%
Potassium chromate	18%	1545	1511	2.3%
Potassium bromide	13%	1515	1361	11.3%
Sodium nitrate	10%	1490	1443	3.3%

Table 15. Test of the Rule of Mixtures for ΔH_m of Aqueous Solutions
(continued)

Materials (Aqueous Solution)		ΔH_m (cal/mol) (by Rule of Mixtures)	ΔH_m (cal/mol) (from DSC)	%deviation
Potassium iodide	16.0%	1490	1479	0.7%
Cesium chloride	19.0%	1489	1424	4.6%
Sodium hydroxide	4.5%	1448	737	96.4%
Silver nitrate	16.0%	1462	1472	0.6%
Potassium nitrate	10.0%	1463	1583	7.6%
Potassium sulfate	5.0%	1472	1492	1.3%
Potassium hydroxide	6.0%	1447	921	57.1%
Potassium dichromate	2.5%	1448	1547	6.4%
Formic acid	2.0%	1448	1259	15.0%
	10.0%	1503	1084	38.7%
	32.0%	1685	480	251.0%
Acetic acid	2.0%	1444	1387	4.1%
	13.0%	1493	1111	34.4%
	20.0%	1528	939	62.7%
Ethylene glycol	2.0%	1443	1386	4.1%
	12.0%	1484	1120	32.5%
	28.0%	1563	470	232.5%
Ethanol	9.5%	1427	954	49.6%
	24.0%	1410	417	238.1%
Glycerol	16.0%	1543	947	62.9%
	40.0%	1780	406	338.4%
average deviation = 75.9%				

introduced in the following chapter, to improve the Rule of Mixtures in predicting the fusion enthalpy. The validity of the Rule of Mixtures for predicting fusion enthalpies of aqueous solutions appears to be limited to dilute solutions.

4.3.3 Horvath's Model for ΔH_m of Aqueous Solutions

The fusion enthalpies of aqueous solutions, as predicted from Horvath's model, were compared to those determined experimentally. The results are shown in Table 16. The second column in Table 16 contains the ΔH_m predicted by Horvath's model. The ΔH_m values in the third column were determined from the DSC. The fourth column contains the absolute percent deviation between the calculated values and the values determined experimentally. A sample calculation for determining the ΔH_m of $MgCl_2$, according to Horvath's model, is contained in Appendix H.

Horvath's model for predicting ΔH_m of aqueous solutions was found to have an average deviation of 142.9%. The results show that wide discrepancies occur in the case of some dilute solutions. These dilute solutions are magnesium chloride (1%), ethylene glycol (2%), and potassium dichromate (2.5%). This might be explained by the following.

Horvath gave Equation 17 below for predicting the fusion enthalpies of dilute solutions.

$$\Delta H_m = R \cdot T_m^0 \cdot (N_2 / N_1) \cdot [T_m / (T_m^0 - T_m)] \quad [17]$$

As seen from this equation, the term " ΔH_m " is very sensitive to the term " $T_m^0 - T_m$ " especially when " $T_m^0 - T_m$ " is very small. For the case of ethylene glycol (2%), the value of " $T_m^0 - T_m$ " was measured to be 0.06°K and therefore

Table 16. Test of Horvath's Model for ΔH_m of Aqueous Solutions

Materials (Aqueous Solution)		ΔH_m (cal/mol) (by Horvath's model)	ΔH_m (cal/mol) (from DSC)	%deviation
Magnesium chloride	1.0%	6524	1316	395.7%
	5.0%	661	975	32.2%
	10.0%	613	565	8.5%
	15.0%	540	309	74.7%
Lithium bromide	1.0%	2854	1438	98.5%
	5.0%	564	1043	45.9%
	10.0%	687	764	10.1%
	15.0%	606	609	0.4%
Lithium chloride	1.0%	774	1264	38.8%
	4.0%	639	925	30.9%
	12.0%	627	331	89.4%
Calcium chloride	8.0%	1296	1108	17.0%
	12.0%	1538	1018	51.1%
	15.0%	1500	910	64.8%
Sodium chloride	15.0%	726	1231	41.0%
Potassium chloride	9.0%	801	1373	41.7%
Sodium hydroxide	4.5%	837	737	13.6%
Potassium nitrate	10.0%	2412	1583	52.4%
Potassium sulfate	5.0%	2974	1492	99.3%
Potassium hydroxide	6.0%	814	921	11.6%
Potassium dichromate	2.5%	34853	1547	2153.0%
Formic acid	2.0%	1023	1259	18.7%
	10.0%	831	1084	23.3%
	32.0%	987	480	105.6%

Table 16. Test of Horvath's Model for ΔH_m of Aqueous Solutions (continued)

Materials (Aqueous Solution)		ΔH_m (cal/mol) (by Horvath's model)	ΔH_m (cal/mol) (from DSC)	!%deviation!
Acetic acid	2.0%	746	1387	46.2%
	13.0%	752	1111	32.3%
	20.0%	1001	939	6.6%
Ethylene glycol	2.0%	14604	1386	953.7%
	12.0%	1039	1120	7.2%
	28.0%	711	470	51.3%
Ethanol	9.5%	881	954	7.7%
	24.0%	971	417	132.9%
Glycerol	16.0%	673	947	28.9%
	40.0%	708	406	74.4%
average deviation =				142.9%

the value of " ΔH_m " is predicted to be 14604 cal/mol from Equation 17. If the value of " $T_m^0 - T_m$ " is measured to be 0.26°K, then the value of " ΔH_m " will be predicted to be 3359 cal/mol, which is much closer to the experimental ΔH_m , 1386 cal/mol. Evaluation of this model would be difficult especially for a very dilute solution due to inevitable experimental errors.

Another limitation of Horvath's model is that it cannot predict fusion enthalpies of solutions that show multiple transitions during solid-liquid transformation, a typical example being those systems that exhibit eutectic behavior.

The two present models, namely the Rule of Mixtures and Horvath's model, for predicting the fusion enthalpy of aqueous solutions appear to be quite unreliable. Based on the data obtained during the course of this investigation, a modified model resulting from this study for predicting the ΔH_m of aqueous solutions has been developed and is presented in Chapter 5.

CHAPTER 5

MODIFIED MIXTURE RULE

This chapter describes a newly developed model, resulting from this study, for predicting the fusion enthalpy of aqueous solutions. The reliability and applicability of this model are also discussed.

As seen from Chapter 4, the models for predicting fusion enthalpies of aqueous solutions are not reliable. The Rule of Mixtures closely predicts the values of fusion enthalpy for dilute aqueous solutions; however, it becomes inapplicable when the concentration of solute increases. This is due to the lack of information of the interaction between the solute and the water which exists in an aqueous solution. One major interaction of the solute and water results from hydration. The phenomenon of hydration is, therefore, explained here to describe the interaction of solute and water molecule, in an effort to improve the Rule of Mixtures and make it applicable to higher concentrations. This newly developed model has been termed "The Modified Mixture Rule," to distinguish it from the original Rule of Mixtures.

The phenomenon of hydration is described in Section 5.1 since this is necessary for an understanding of the new model. An equation for predicting fusion enthalpies of aqueous solutions is developed in Section 5.2. An evaluation of this model, based on results determined experimentally, is contained in Section 5.3 and the results are discussed in Section 5.4. An application of this model for identifying FHS materials is described in Section 5.5.

5.1 The Phenomenon of Hydration

For most aqueous solutions that display eutectic behavior, addition of the solute to water results in a stronger solute-water bond than either solute-solute or water-water bonds. This is called "hydration," meaning a bond between the water and the solute. When an ionic solute (electrolyte) is dissolved in water, it dissociates into cations and anions. Each cation and anion will be bonded to a number of water molecules. For each mole of solute, the total number of moles of water bonded to this solute is referred to as its hydration number. Figure 13 shows the phenomenon of hydration when NaCl is dissolved in water.⁽²¹⁾ Because of hydration, the hydrogen bonding of water molecules in the neighborhood of the solute must be broken during solution. The energy for breaking the hydrogen bonds, the hydration energy, is a possible factor to account for the inaccuracy of the Rule of Mixtures when determining the fusion enthalpy of solutions.

Two types of aqueous solutions were identified in Table 1. They were electrolytic aqueous solutions (e.g., LiCl or NaCl in H₂O) and non-electrolytic aqueous solutions (e.g., formic acid in H₂O). Each type of aqueous solution displays a different hydration phenomenon.

Bockris stated that for electrolytic aqueous solutions, hydration can be divided into two parts, called "primary" (close) hydration and "secondary" (distant) hydration.⁽²²⁾ Figure 14 shows the orientations of water dipoles in the presence of an electrolyte.⁽²³⁾ As seen from Figure 14, water dipoles can be divided into 3 regions, corresponding to their different orientations. Primary hydration happens in the inner region where all the water molecules are oriented axially. Secondary hydration happens in the in-between region

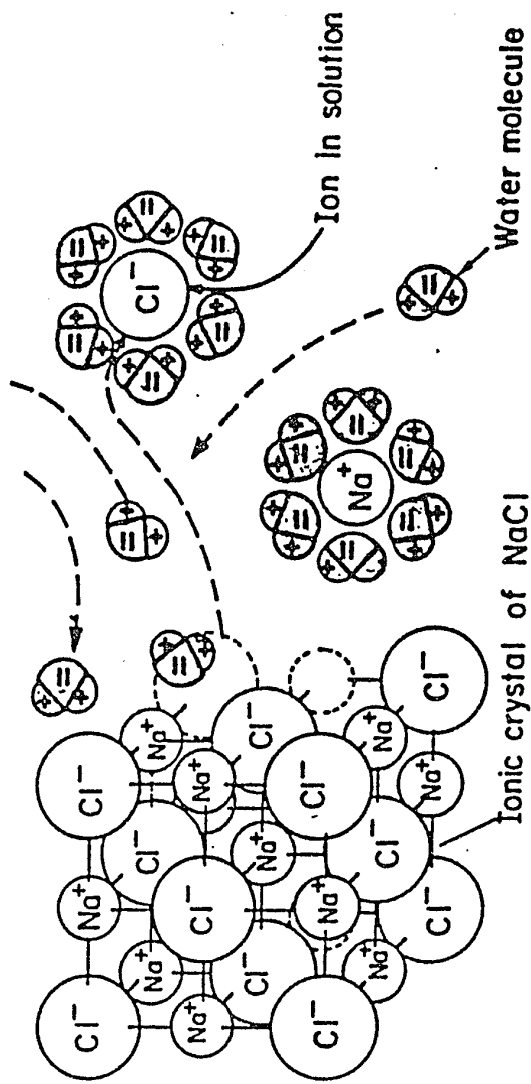


Figure 13 . Dissolution of an Ionic Crystal by the Action of a Solvent

(after Ref. 21)

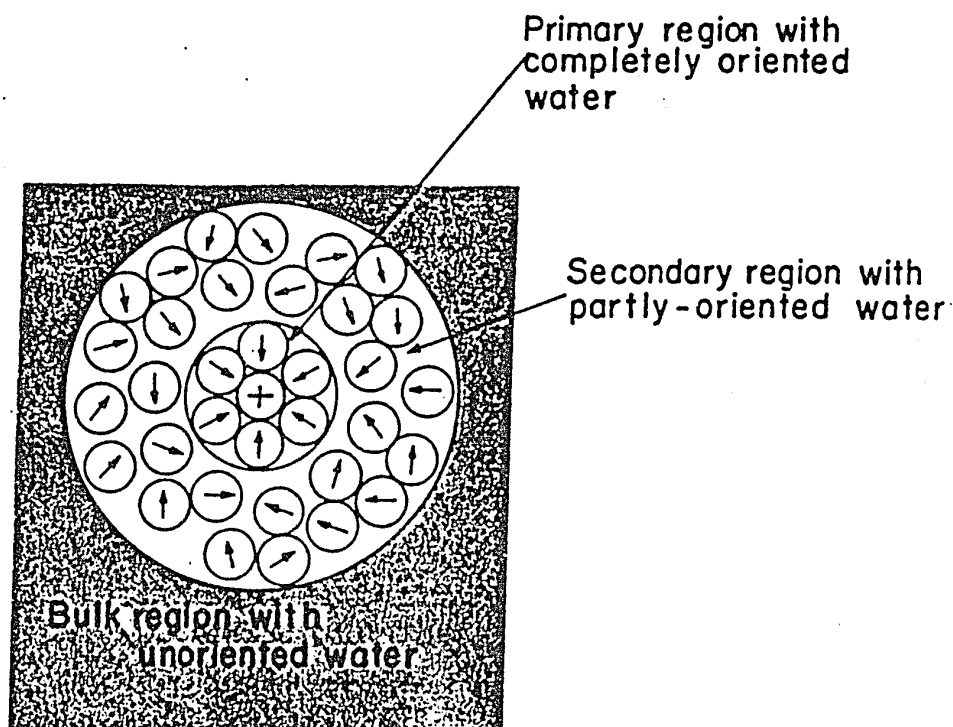


Figure 14 . Orientation of Water Dipoles in a Electrolytic Solution
(after Ref. 23)

where the water molecules are partly oriented. Water molecules in the bulk region are not reoriented in the presence of the solute.

Primary hydration consists of the stable combination of the "neighboring" water molecules with the solute ions. Secondary hydration signifies the electrostatic interaction of the solute ions and the water molecule dipoles which are not in the vicinity of the solute. Although the interaction energy of an ion with a single water molecule which is not in its immediate vicinity is very small, the total energy obtained by summation over many molecules reaches a large value, and forms a considerable part of the hydration energy of ions.⁽²⁴⁾ For electrolytic aqueous solutions, both primary and secondary hydration phenomena should be considered.

Although non-electrolytic solutes do not dissociate into ions when added to water, this type of solution contains polar molecules and possesses local dipole charges to interact with the "neighboring" water molecules and therefore participate in primary hydration. However this type of solution does not display secondary hydration due to the very weak electrostatic interaction of the dipoles of solutes and the distant water molecules as compared to the stronger ion-dipole interaction in the electrolytic aqueous solutions.

5.2 The Equation for Predicting Fusion Enthalpy

The Rule of Mixtures, as given by Equation 15, predicts the fusion enthalpy inaccurately due to lack of information on the interaction between the solute and the water that exist in an aqueous solution. One major interaction between the solute and the water arises from the hydration

behavior of the components. Due to hydration, additional hydrogen bonds must be broken. The energy for breaking the hydrogen bonds, the hydration energy, needs to be considered as a negative term to account for the value of fusion enthalpy. By introducing the factor of hydration energy, Equation 15 was modified to produce Equation 22 in order to improve the accuracy of the Rule of Mixtures in predicting fusion enthalpy of aqueous solutions.

$$\begin{aligned}\Delta H_{m(aq)} &= [X_a\Delta H_a + X_{H_2O}\Delta H_{H_2O}] - [M] \\ &= [X_a\Delta H_a + X_{H_2O}\Delta H_{H_2O}] - (X_a) * (h) * (E_H)\end{aligned}\quad [22]$$

where X_a is the molar fraction of solute "a",

X_{H_2O} is the molar fraction of water,

ΔH_a is the fusion enthalpy of solute "a",

ΔH_{H_2O} is the fusion enthalpy of water,

M is the hydration energy,

h is the hydration numbers, and

E_H is the energy of hydrogen bonds per mole water.

The term "M," the hydration energy, is equivalent to the product of the number of moles of hydrated water ($X_a * h$) and the hydrogen bond energy per mole water (E_H). In the case of electrolytic solutions, the term "h" corresponds to the total hydration number (considering both primary and secondary hydration). The values of "h" were available from Robinson⁽²⁵⁾ and are listed in Appendix I. In the case of non-electrolytic solutions, the term "h" corresponds to the primary hydration number. The values of "h" were available from CRC Handbook of Chemistry and Physics⁽²⁶⁾ and are listed in Appendix J. The hydrogen bond energy per mole of water is 3.0 kcal/mol,

according to Nemethy and Scheraga.⁽²⁷⁾ The values of ΔH_a and ΔH_{H_2O} were from the published literature^(6,19) and are listed in Appendix B.

5.3 Results

The fusion enthalpies of aqueous solutions, as predicted by the Modified Mixture Rule, were compared to those obtained experimentally. The percent deviation between the calculated ΔH_m and those obtained experimentally were determined and are shown in Table 17. The average deviation was found to be 12.5%, with the values ranging from a high of 58.1% to a low of 0.3%. A sample calculation for the case of determining ΔH_m for $MgCl_2$, according to the Modified Mixture Rule, is presented in Appendix K.

5.4 Discussion of Results

The Modified Mixture Rule is a modification of the Rule of Mixtures. To determine if the Modified Mixture Rule is more reliable than the Rule of Mixtures, results from these two models are compared by means of the graphs in Figures 15 and 16. The experimental data of the fusion enthalpy obtained from the DSC were used as the standard for comparison.

Comparisons of the reliability of the two models in predicting the fusion enthalpies of 5 electrolytic solutions, namely, $MgCl_2$, LiBr, LiCl, $CaCl_2$, and NaCl, are shown in Figures 15a through 15e respectively.

Comparisons of the reliability of the two models in predicting the fusion enthalpies of 5 non-electrolytic solutions, namely, formic acid, acetic acid, ethylene glycol, ethanol, and glycerol, are shown in Figures 16a through 16e respectively.

Table 17. Test of the Modified Mixture Rule for ΔH_m of Aqueous Solutions

Materials		ΔH_m (cal/mol) by Modified Mixture Rule	ΔH_m (cal/mol) from DSC	%deviation
Magnesium chloride	1.0%	1370	1316	4.1%
	5.0%	1097	975	12.5%
	10.0%	727	565	28.7%
	15.0%	324	309	4.9%
Lithium bromide	1.0%	1391	1438	3.3%
	5.0%	1206	1043	15.6%
	10.0%	956	764	25.1%
	15.0%	683	609	12.2%
Lithium chloride	1.0%	1353	1264	7.0%
	4.0%	1096	925	18.5%
	12.0%	367	331	10.9%
Calcium chloride	8.0%	1000	1108	9.7%
	12.0%	758	1018	25.5%
	15.0%	564	910	38.0%
Sodium chloride	7.0%	1329	1282	3.7%
	15.0%	1193	1231	3.1%
Potassium chloride	9.0%	1419	1373	3.4%
Sodium bromide	11.0%	1269	1418	10.5%
Potassium bromide	13.0%	1376	1361	1.1%
Potassium iodide	16.0%	1338	1479	9.5%
Formic acid	2.0%	1402	1259	11.3%
	10.0%	1259	1084	16.1%
	32.0%	759	480	58.1%
Acetic acid	2.0%	1392	1387	0.3%
	13.0%	1122	1111	0.9%
	20.0%	922	939	1.8%

Table 17. Test of the Modified Mixture Rule for ΔH_m of Aqueous Solutions (continued)

Materials		ΔH_m (cal/mol) by Modified Mixture Rule	ΔH_m (cal/mol) from DSC	%deviation
Ethylene glycol	2.0%	1390	1386	0.3%
	12.0%	1139	1120	1.7%
	28.0%	648	470	37.9%
Ethanol	9.5%	1074	954	12.6%
	24.0%	440	417	5.5%
Glycerol	16.0%	1118	947	18.1%
	40.0%	415	406	2.2%
				average deviation = 12.5%

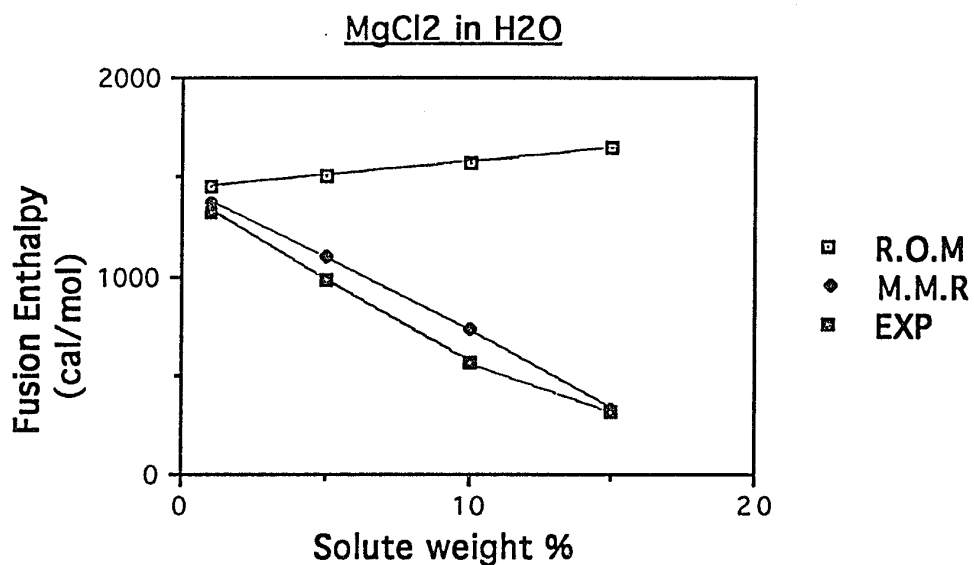


Figure 15a . Comparison of the Rule of Mixtures (R.O.M) and the Modified Mixture Rule (M.M.R) in Predicting ΔH_m of MgCl₂ Electrolyte Aqueous Solution

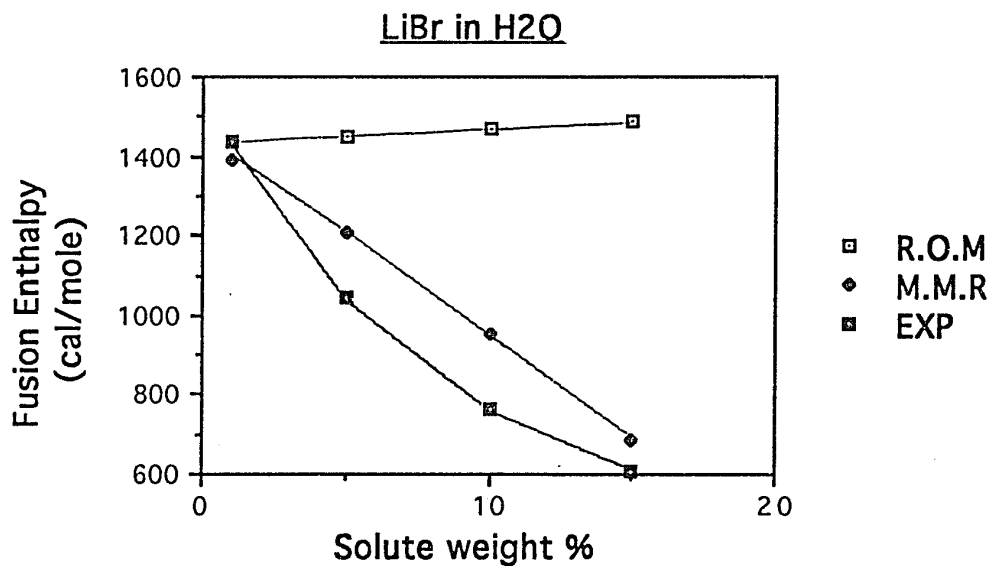


Figure 15b . Comparison of the Rule of Mixtures (R.O.M) and the Modified Mixture Rule (M.M.R) in Predicting ΔH_m of LiBr Electrolyte Aqueous Solution

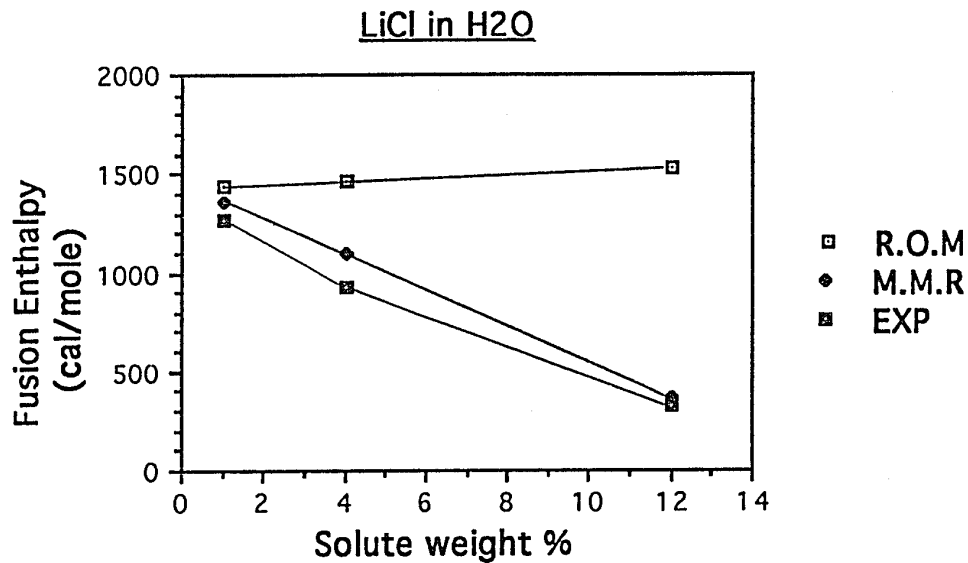


Figure 15c. Comparison of the Rule of Mixtures (R.O.M) and the Modified Mixture Rule (M.M.R) in Predicting ΔH_m of LiCl Electrolyte Aqueous Solution

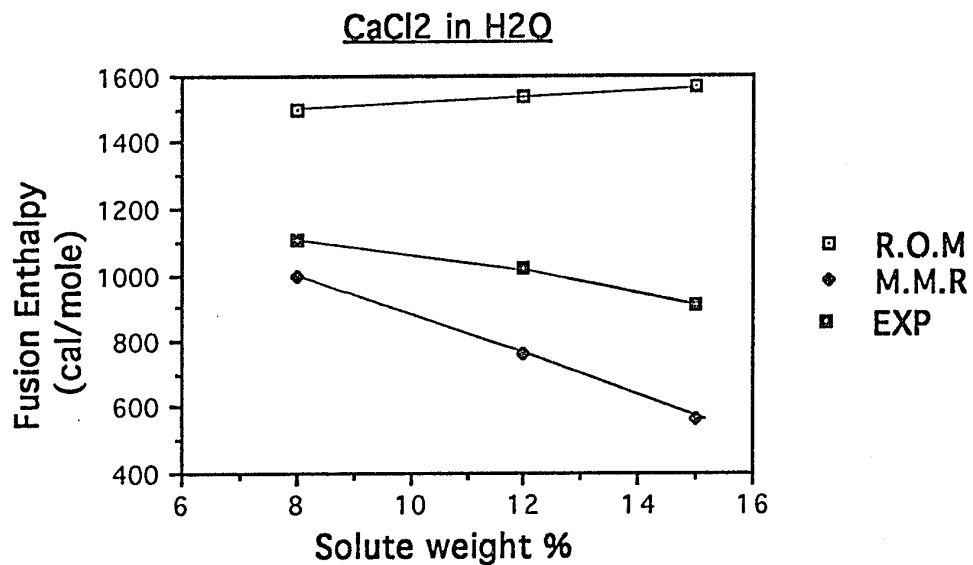


Figure 15d . Comparison of the Rule of Mixtures (R.O.M) and the Modified Mixture Rule (M.M.R) in Predicting ΔH_m of CaCl₂ Electrolyte Aqueous Solution

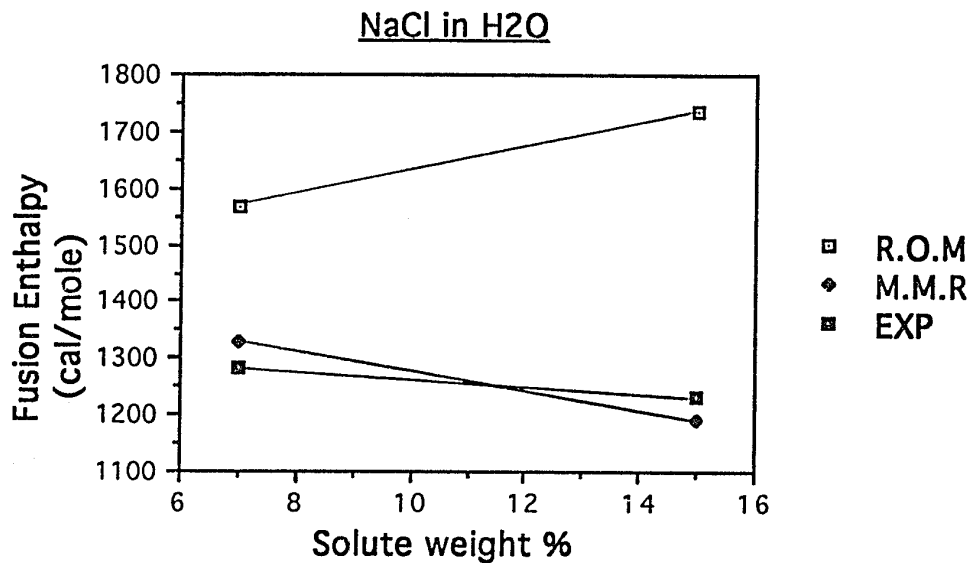


Figure 15e . Comparison of the Rule of Mixtures (R.O.M) and the Modified Mixture Rule (M.M.R) in Predicting ΔH_m of NaCl Electrolyte Aqueous Solution

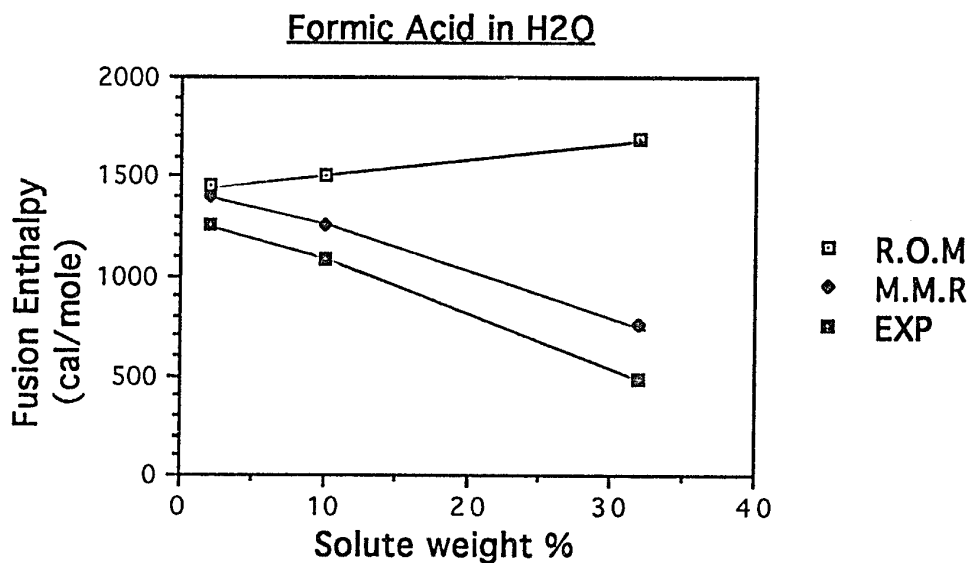


Figure 16a . Comparison of the Rule of Mixtures (R.O.M) and the Modified Mixture Rule (M.M.R) in Predicting ΔH_m of Formic Acid Non- electrolyte Aqueous Solution

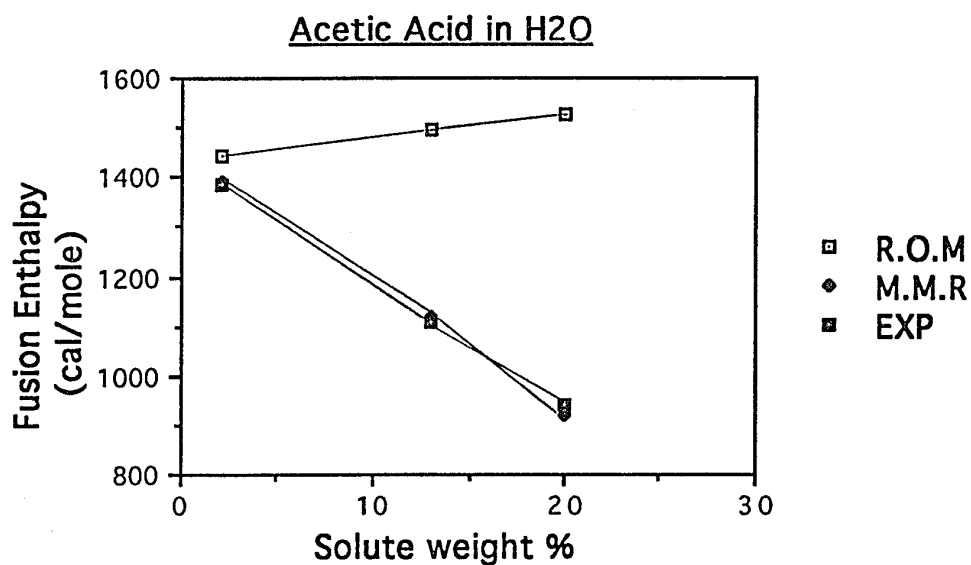


Figure 16b . Comparison of the Rule of Mixtures (R.O.M) and the Modified Mixture Rule (M.M.R) in Predicting ΔH_m of Acetic Acid Non- electrolyte Aqueous Solution

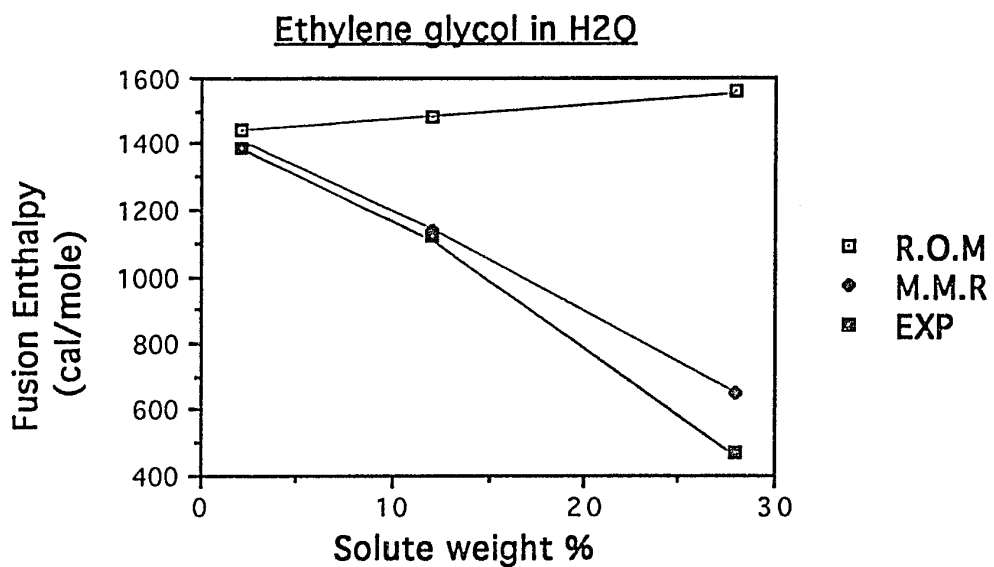


Figure 16c . Comparison of the Rule of Mixtures (R.O.M) and the Modified Mixture Rule (M.M.R) in Predicting ΔH_m of Ethylene Glycol Non- electrolyte Aqueous Solution

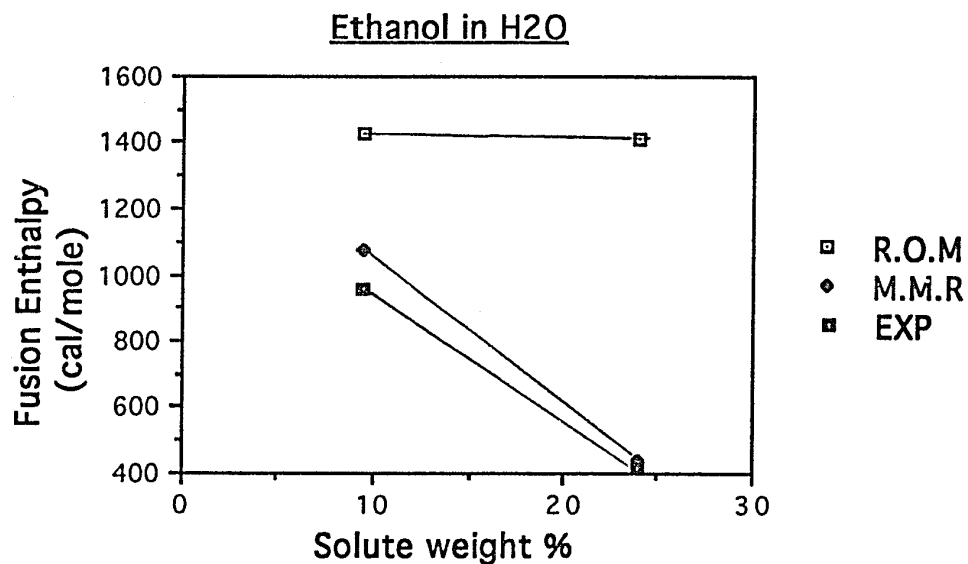


Figure 16d . Comparison of the Rule of Mixtures (R.O.M) and the Modified Mixture Rule (M.M.R) in Predicting ΔH_m of Ethanol Non- electrolyte Aqueous Solution

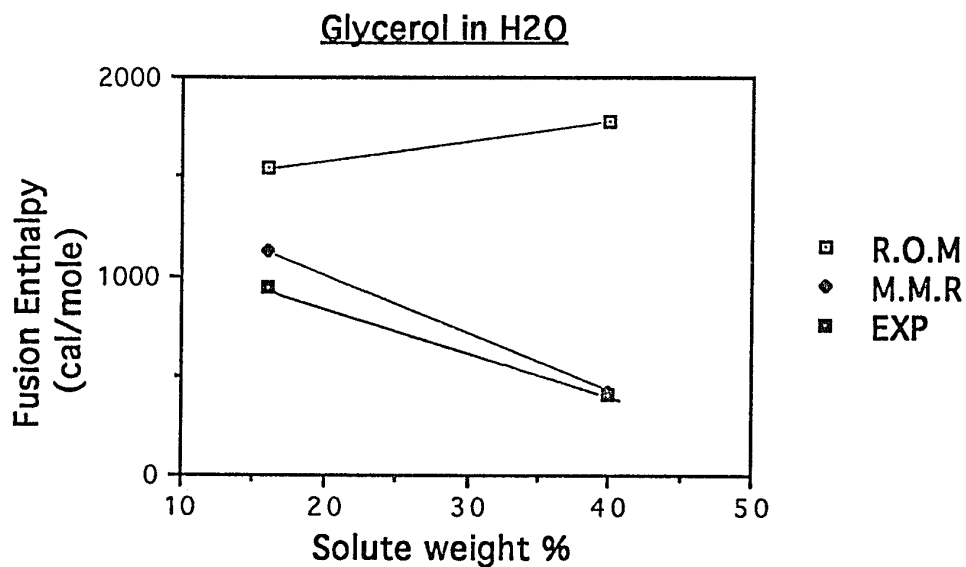


Figure 16e . Comparison of the Rule of Mixtures (R.O.M) and the Modified Mixture Rule (M.M.R) in Predicting ΔH_m of Glycerol Non- electrolyte Aqueous Solution

As can be seen from Figures 15 and 16, the Rule of Mixtures becomes more unreliable as the concentration increases. Modifying the Rule of Mixtures by introducing another parameter, the hydration energy, yields more accurate predictions for fusion enthalpies of concentrated solutions. This supports the assumption that the solute-water interaction plays a significant role in determining the fusion enthalpy.

As can be seen from Table 17, the Modified Mixture Rule is reliable for most aqueous solutions except formic acid at a concentration of 32%. The fusion enthalpy of formic acid is overestimated by 58.1% according to the Modified Mixture Rule. This might be explained by the following equation for formic acid ionization:



Formic acid gives off a proton (H^+) when added to water, resulting in additional hydrogen bonds being broken besides those due to hydration.

It is also possible that the value of the hydrogen bond energy in aqueous solutions may be different from that in pure water and this might account for the residual inaccuracy of this model. Figure 17 shows the possible configurations of H_2O molecules.⁽²⁸⁾ For pure water, the H_2O molecules are arranged in their normal configuration. These molecules are arranged in a bent configuration in the presence of a solute. According to Conway the hydrogen bond energy in water depends both on the angle of the $\text{O-H}\dots\text{O}$ bond and the O-O bond distance.⁽²⁸⁾ The angle of the $\text{O-H}\dots\text{O}$ bond deviates from 180° (normal case in pure water) when a solute (ions) is added. Lennard-Jones and Pople proposed that the hydrogen bond energy decreases slowly with deviation of the $\text{O-H}\dots\text{O}$ bond angle from 180° .⁽²⁹⁾ The hydrogen bond

STRETCHED and BENT H-BOND CONFIGURATIONS

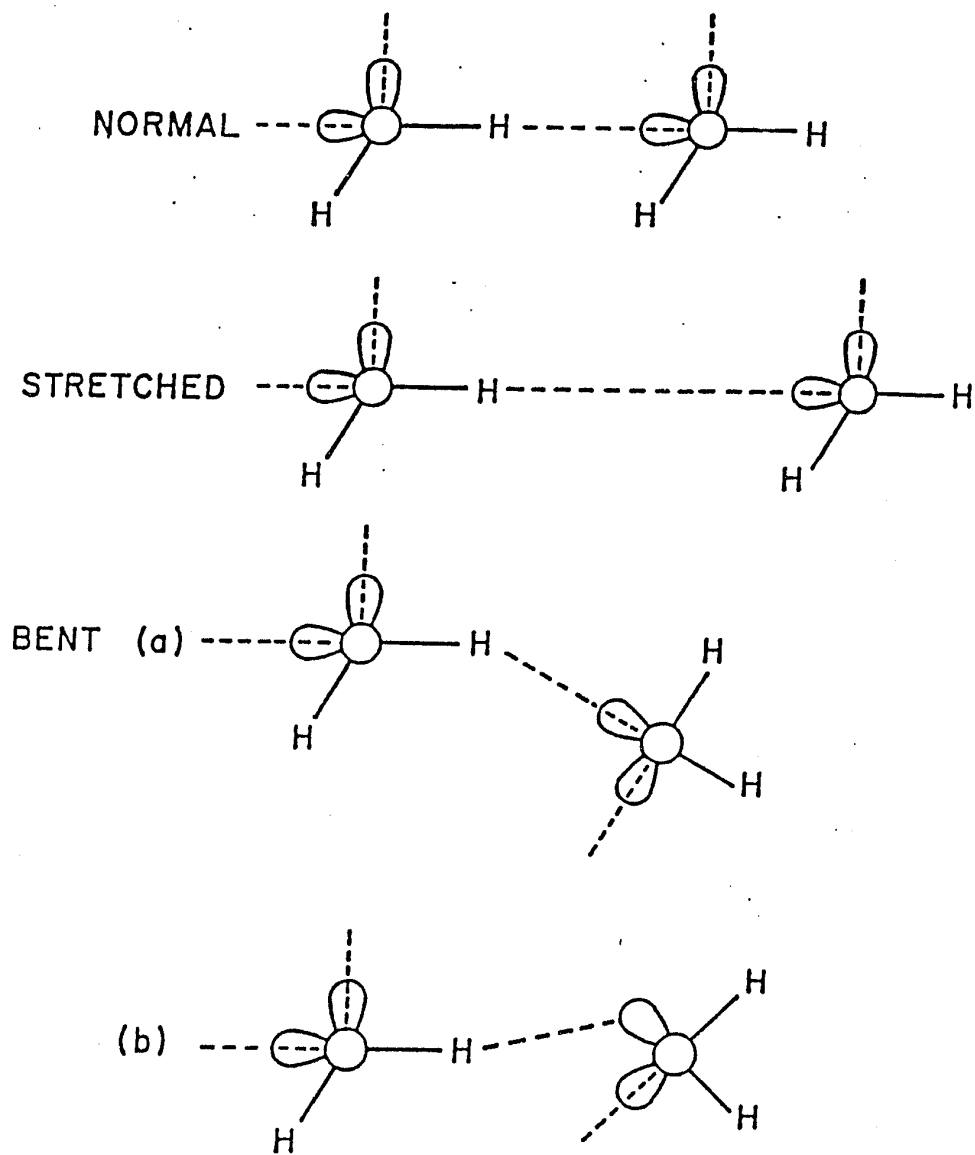


Figure 17 . Bent and Stretched H-Bond Configuration in Water (after Ref. 28)

energy in the solution might be slightly lower than that in pure water (3.0 kcal/mol). This may affect the accuracy of the Modified Mixture Rule in predicting the value of fusion enthalpy for aqueous solutions.

The validity of this model for predicting fusion enthalpies of aqueous solutions at much higher concentrations could not be determined due to the lack of published data for hydration numbers in highly concentrated solutions. According to Robinson, the hydration numbers are applicable only for those solutions in which the ratio of the number of moles of the hydrated water to that of the total water is less than one-fourth.⁽³⁰⁾ When more than one-quarter of the total water molecules are bonded to ions, the hydration numbers will begin to decrease owing to the effects of competition between neighboring cations.⁽³⁰⁾ Different solutes have different degrees of hydration when added to water and therefore lead to different maximum allowable concentrations when applying the Modified Mixture Rule. To find the applicable range of the Modified Mixture Rule, the maximum allowable concentrations for the ten solutions investigated in this project were calculated and are shown in Table 18. The values of the hydration number of the solute in water are in the second column of Table 18. The third column corresponds to the maximum concentration at which 1/4 of the water molecules are hydrated. The detailed calculation is shown in Appendix L.

As seen from Table 18, solutes with higher hydration numbers generally have smaller maximum allowable concentrations for application of the Modified Mixture Rule.

Table 18. The Maximum Allowable Concentrations of the Solutions in the Application of the Modified Mixture Rule

Solute Material	Hydration number	Maximum concentration
Formic acid	1.99 ⁽²⁶⁾	24.3%
Acetic acid	2.90 ⁽²⁶⁾	22.3%
Ethylene glycol	3.01 ⁽²⁶⁾	22.3%
Ethanol	2.94 ⁽²⁶⁾	17.9%
Glycerol	3.95 ⁽²⁶⁾	24.5%
Magnesium chloride	13.7 ⁽²⁵⁾	8.8%
Lithium bromide	7.6 ⁽²⁵⁾	13.7%
Lithium chloride	7.1 ⁽²⁵⁾	7.7%
Calcium chloride	12.0 ⁽²⁵⁾	11.4%
Sodium chloride	3.5 ⁽²⁵⁾	18.8%

5.5 Identification of FHS Materials by the Model

Experiments showed that the Modified Mixture Rule is reliable. Therefore this model will help identify future FHS materials of the aqueous solution type.

According to Equation 22, future FHS materials of the aqueous solution type should have a value of ΔH_a that is greater than ΔH_{H_2O} , and the value of h should be very small, or as close to zero as possible.

Solutes with a fusion enthalpy higher than water were first identified from the literature and are listed in Table 19. The second and third column contain the values of the fusion enthalpy obtained from CRC Handbook of Chemistry and Physics⁽⁶⁾ and Lange's Handbook of Chemistry⁽⁷⁾ respectively. The values of hydration numbers are in the fourth column.

The solutes, $MgCl_2$ and $NaCl$, have reported values of fusion enthalpy, ΔH_a , higher than that of water. Experimental results, as can be seen from Figure 15a and 15e, show that both $MgCl_2$ and $NaCl$ aqueous solutions are not suitable FHS materials because their measured fusion enthalpies are lower than water. This is probably due to the hydration energy which negatively affects the magnitude of the fusion enthalpy. $NiCl_2$ aqueous solution is also unlikely to have a higher fusion enthalpy than water based on this model, because its hydration number is high.

The solutes, KF and NaF , also have a fusion enthalpy higher than water. However, their hydration numbers were not reported. If their hydration numbers are so low that the hydration energy can be ignored, then the fusion enthalpy of the solution, $\Delta H_m(aq)$, will be dominated by the term

Table 19. Solutes with a Fusion Enthalpy Higher than Water

Solute	ΔH_m (cal/mol) from CRC handbook ⁽⁶⁾	ΔH_m (cal/mol) from Lange's handbook ⁽⁷⁾	Hydration number ⁽²⁵⁾
MgCl ₂	8100	10300	13.7
KF	6500	6500	-
NaCl	7220	6730	3.5
NiCl ₂	18470	18470	13.0
NaF	7000	7970	-

- Not reported in the literature

" $X_a\Delta H_a$ ", according to Equation 22. In this situation, the fusion enthalpy, $\Delta H_{m(aq)}$, is expected to increase when more solute is added to water. Actual results show that as the solute concentration increases, the freezing point decreases due to eutectic behavior. The freezing point may decrease below the lower bound (-13°C) of the operating temperature of the FHS when a certain concentration of the solute " X_a " is reached and this may limit the maximum value of the term " $X_a\Delta H_a$ " or the fusion enthalpy $\Delta H_{m(aq)}$.

CHAPTER 6

Verification of Candidate FHS Materials

One of the main purposes of this project was to experimentally verify the preliminary results of candidate FHS materials as determined by Selvaduray and Lomax. The results are presented in this chapter and summarized in Table 20. The third column contains the calculated values of the total cooling capacity, based on the experimental data reported in Section 4.2. The detailed calculations are contained in Appendix M. The cooling capacity was not measured for those candidate materials whose melting points were found to lie outside the desired operating range of -13°C to 5°C . The fourth column contains the values of the total cooling capacity reported by Selvaduray and Lomax for purposes of comparison. Since Selvaduray and Lomax reported their cooling capacity values in units of "cal/g" because total weight of the PLSS is a parameter of concern, the cooling capacities in Table 20 are presented using the unit of "cal/g," rather than "cal/mole," as has been done throughout the rest of this thesis.

As can be seen from Table 20, potassium dichromate at a concentration of 2.5% is the only material which has a melting temperature within -13°C to 5°C and the measured cooling capacity greater than water. The increase in cooling capacity, however, is only 2.2 percent greater than water. The cooling capacity of potassium dichromate at a concentration higher than 2.5% cannot be predicted from the Modified Mixture Rule, due to the lack of the reported hydration number for potassium dichromate.

Table 20. Verification of Candidate FHS Materials

FHS candidate	Melting Point (°C)	Cooling Capacity (cal/g)	
		Measured	Reported
Water	0.087	92.60	90.97
Benzene,hexafluoro	5.34	-	1280.07
Heptanoic acid	-10.14	35.78	1119.59
Cyclohexanol,4-methyl(cis)	-3.96	24.99	874.47
Benzene,1,4-difluoro	-22.79	-	717.29
Cyclohexanone,2-methyl	-14.14	-	613.34
Cinnamionitrile	5.08	-	593.50
Cyclooctatetraene	-8.21	29.65	593.50
4-Methoxybenzaldehyde	-1.89	34.25	469.34
Indene	-6.15	22.58	234.64
Cyclohexane,1,2-dibromo	-4.98	15.33	160.35
Biphenyl,2-methyl	-0.48	22.40	153.35
1,2-dihydronaphthalene	-10.05	25.39	138.26
Piperidene	-18.46	-	97.99
Sodium chloride (7%)	-20.6 (T _{tr,1})	-	94.31
	-10.2 (T _{tr,2})		
Potassium chloride(9%)	-8.55	83.30	93.53
Sodium bromide (11%)	-29.94 (T _{tr,1})	-	93.09
	-9.68 (T _{tr,2})		
Lithium chloride(4%)	-7.96	65.26	92.95
Potassium chromate(18%)	-10.96 (T _{tr,1})	83.22	92.87
	-8.7 (T _{tr,2})		
Potassium bromide(13%)	-12.15 (T _{tr,1})	82.50	92.73
	-11.04 (T _{tr,2})		

- Not obtained because the heat capacity was not measured

T_{tr,1} Eutectic temperature.

T_{tr,2} Liquidus temperature

Table 20. Verification of Candidate FHS Materials (continued)

FHS candidate	Melting Point (°C)	Cooling Capacity (cal/g)	
		Measured	Reported
Sodium nitrate(10%)	-16.35 ($T_{tr,1}$) -8.5 ($T_{tr,2}$)	-	92.50
Potassium iodide(16%)	-20.82 ($T_{tr,1}$) -8.95 ($T_{tr,2}$)	-	92.46
Cesium chloride(19%)	-22.66 ($T_{tr,1}$) -10.75 ($T_{tr,2}$)	-	92.43
Sodium hydroxide(4.5%)	-7.27	53.76	92.34
Silver nitrate(16%)	-8.68 ($T_{tr,1}$) -7.72 ($T_{tr,2}$)	82.91	91.90
Potassium nitrate(10%)	-2.41	90.64	91.82
Potassium sulfate(5%)	-0.81	89.37	91.82
Potassium hydroxide(6%)	-7.26	59.97	91.28
Potassium dichromate(2.5%)	-0.02	94.65	91.26
Formic acid(10%)	-7.53	70.12	92.64
Acetic acid(13%)	-8.54	72.33	92.24
Ethylene glycol(12%)	-5.52	75.05	92.17
Ethanol(9.5%)	-6.72	66.54	91.35
Glycerol(16%)	-7.95	60.90	92.51

- Not obtained because the heat capacity was not measured

$T_{tr,1}$ Eutectic temperature

$T_{tr,2}$ Liquidus temperature

CHAPTER 7

CONCLUSION

The results presented in the previous chapters have led to several conclusions, including verification of candidate FHS materials and evaluation of models for predicting fusion enthalpies of both organic compounds and aqueous solutions. These models will help identify future FHS materials for space suit applications.

From experimental verification of melting points and cooling capacities of candidate FHS materials, potassium dichromate at a concentration of 2.5%, meets both the first criterion ($-13^{\circ}\text{C} < T_m < 5^{\circ}\text{C}$), and the second ($\Delta H_{\text{tot}} > \Delta H_{\text{tot}}(\text{H}_2\text{O})$). To determine if potassium dichromate (2.5%) is suitable for space suit applications, other criteria as mentioned in Section 1.5 need to be further employed in evaluating this material in the future. Ten of the candidate FHS materials, as identified with an "x" in Table 13, did not display a solid-liquid transition between -50°C to 30°C , based on differential scanning calorimetry. These ten materials need to be further investigated to verify their melting points. The rest of the candidate FHS materials are not suitable for space suit applications because they do not meet the first and second criteria.

The existing models for predicting the fusion enthalpy were evaluated against experimental data. The model proposed by Chickos for predicting the fusion enthalpies of 13 organic compounds was found to have an average percent deviation of 26.3% from the experimentally measured values. The accuracy of this model for predicting the fusion enthalpies of organic

compounds can possibly be improved by using a larger database. This will be possible by including more experimental data of fusion enthalpy that may become available in the future.

The Rule of Mixtures and Horvath's model for predicting fusion enthalpies of aqueous solutions had an average percent deviation of 75.9% and 142.9%, respectively, from the experimentally measured values. The experiments revealed that the present models for predicting fusion enthalpies of aqueous solutions are not reliable. For this reason a new model, termed the "Modified Mixture Rule," was developed and evaluated.

This Modified Mixture Rule was employed for predicting the fusion enthalpies of 33 aqueous solutions. It had an average percent deviation of 12.5% when compared to experimentally measured values. The results show that the Modified Mixture Rule is far more accurate than the presently available two models (the Rule of Mixtures and Horvath's model) for predicting the fusion enthalpies of aqueous solutions. In the future, the accuracy of the Modified Mixture Rule may be further improved by considering more factors besides hydration. This may result in more accurate fusion enthalpy prediction modeling.

The Modified Mixture Rule requires the values of the hydration numbers in predicting the fusion enthalpy. The lack of reported values of hydration numbers for many solutes limits the application of the Modified Mixture Rule. As predicted from the Modified Mixture Rule, those aqueous solutions with a solute which has a low hydration number and a high value of enthalpy of fusion might be future candidate FHS materials.

References

1. Smolders, P., Living in Space, Tab/Aero, (1986), p. 71.
2. Stine, H. G., Handbook for Space Colonists, Holt, Rinehart and Winston, New York, (1985), p. 72.
3. Selvadury, G., and Lomax, C., "Fusible Heat Sink Materials: Evaluation of Alternate Candidates", ICES-92, Seattle, WA (July, 1992).
4. Moureu, H., and Dode, M., "Chaleurs de formation de l'oxyde d'ethylene, de l'ethanediol et de quelques homologues", Societe Chimique de France Bulletin, (1937), pp. 637-647.
5. Pickard and Kenyon, "Investigation on the Rotato Power of Chemical Constituents, Part I: The Rotation of the Simplest Secondary Alcohols of the Fatty Series", J. Chem. Soc. , Vol. 99, No. 45, (1911).
6. Weast, R. C., Ed., CRC Handbook of Chemistry and Physics, 70th Edition, CRC Press Inc, (1990), Section B, p. B-224.
7. Dean, J. A., Ed., Lange's Handbook of Chemistry, 13th Edition, McGraw Hill, (1985), Section 9, p. 9-107.
8. Darken, G., Physical Chemistry of Metals, McGraw-Hill, New York, (1953), p. 124.
9. Pauling, L., The Nature of the Chemical Bond, 3rd Edition, Cornell University, (1960), p. 465.
10. Eisenberg, D., and Kauzmann, W., The Structure and Properties of Water, Oxford University Press, (1969), p. 139.
11. Procopiu, S., "Relation entre la chateur de fusion et la temperature absolue de fusion des metaux monoatomiques", Comptes Rendus hebdomadaires des Seances de l'Academie des Sciences, Vol. 223, (1946), p. 503.

12. Walden, P., "Über Die Schmelzwärme, Spezifische Kohäsion Und Molekulargröße Bei Der Schmelztemperatur", Zeitschrift für Elektrochemie, Vol. 14, (1908), p. 713.
13. Partington, J. R., An Advanced Treatise for Physical Chemistry, Vol. 3. Longmans, London, (1952), p. 551.
14. Schierz, E. R., "The nature of the spatial configuration of organic molecules as the determining factor for the magnitude of molar heat of fusion.", American Chemical Abstract, Vol. 31, (1937), p. 2504.
15. Austin, J. E., "The relation between the molecular heat of fusion and the absolute temperature of fusion of monatomic metals and of chemical compounds", American Chemical Abstract, Vol. 42, (1948), p. 2169.
16. Chickos, J. S., "Estimating Entropies and Enthalpies of Fusion of Organic Compounds", J.Org.Chem., Vol. 56, No. 3, (1991), p. 927.
17. Chickos, J. S., "Estimating Entropies and Enthalpies of Fusion of Hydrocarbons", J.Org.Chem., Vol. 55, No. 12, (1990), p. 3833.
18. Horvath, A. L., Handbook of Aqueous Electrolyte Solutions, Ellis Horwood Limited, (1985), p. 44.
19. Acree, W. E. Jr., "Thermodynamic properties of organic compounds: enthalpy of fusion and melting point temperature compilation", Thermochemica Acta, Vol. 189, No. 1, (1991), p. 37.
20. Weast, R. C., Ed., CRC Handbook of Chemistry and Physics, 70th Edition, CRC Press Inc., (1990), Section C, p. C-196.
21. Bockris, J. O., and Reddy, K. N., Modern Electrochemistry, Vol. 1, Plenum Press, New York, (1973), p. 47.
22. Samoilov, O. Y., Structure of Aqueous Electrolyte Solutions and the Hydration of Ions, Consultants Bureau, New York, (1965), p. 75.

23. Bockris, J. O., and Reddy, K. N., Modern Electrochemistry, Vol. 1, Plenum Press, New York, (1973), p. 79.
24. Samoilov, O. Y., Structure of Aqueous Electrolyte Solutions and the Hydration of Ions, Consultants Bureau, New York, (1965), p. 81.
25. Robinson, R. A., Electrolyte Solutions, 2nd Edition, Academic Press Inc., New York, (1959), p. 246.
26. Weast, R. C., Ed., CRC Handbook of Chemistry and Physics, 70th Edition, CRC Press Inc., (1990), Section D, p. D-221.
27. Nemethy, G., and Scheraga, H. A., "Structure of Water and Hydrophobic Bonding in Proteins. IV : The Thermodynamic Properties of Liquid Deuterium Oxide", J. Chem. Phys., Vol. 41, (1964), p. 680.
28. Conway, B. E., "Electrolyte Solutions: Solvation and Structural Aspects", Annual Reviews of Physical Chemistry, Vol. 17, No. 3, (1966), p. 490.
29. Lennard-Jones, J., and Pople, J. A., "Molecular association in liquids I: Molecular association due to lone-pair electrons.", Proc. Roy. Soc., Vol. 205, p. 155.
30. Robinson, R. A., Electrolyte Solutions, 2nd Edition, Academic Press Inc., New York, (1959), p. 248.

Appendix A: Derivation of Horvath's Model

In Equilibrium, the chemical potential of a liquid is equal to the solid.

$$\mu_{\text{liquid}}(T, P, x_1) = \mu_{\text{solid}}(T, P) \quad [1]$$

where x_1 : molar fraction of solvent

$$\begin{aligned} \mu_{\text{liquid}}(T, P, x_1) &= \mu^*_{\text{liquid}} + RT \ln a_1 \\ &= \mu^*_{\text{liquid}} + RT \ln x_1 \text{ (for ideal solution)} \end{aligned} \quad [2]$$

where μ^*_{liquid} : chemical potential of pure liquid.

Combining Equation [1] and [2] yields

$$\begin{aligned} \mu^*_{\text{liquid}} + RT \ln x_1 &= \mu_{\text{solid}}(T, P) \\ \ln x_1 &= -(\mu^*_{\text{liquid}} - \mu_{\text{solid}}(T, P)) / RT \\ \ln x_1 &= -(\Delta G_m) / RT \end{aligned}$$

Differentiation with respect to T yields

$$d \ln x_1 / dT = -1/R * [\partial(\Delta G_m / T) / \partial T] \quad [3]$$

Applying the Gibbs-Helmholtz Equation, below, to Equation 3:

$$\begin{aligned} [\partial(\Delta G_m / T) / \partial T] &= -\Delta H_m / T^2 \\ d \ln x_1 / dT &= \Delta H_m / RT^2 \end{aligned} \quad [4]$$

Integrating Equation 4, from $x_1 = 1$ (pure solvent) to $x_1 = x_1$, result in:

$$\ln x_1 = \Delta H_m / R * (1/T^0_m - 1/T_m) \quad [5]$$

where T^0_m : melting point of pure solvent.

T_m : melting point of the solution.

$$\ln(1 - x_2) = \Delta H_m / R * (1/T^0_m - 1/T_m) \quad [6]$$

where x_2 : molar fraction of the solute

Appendix A: Derivation of Horvath's Model (continued)

In dilute solutions, $x_2 \rightarrow 0$, therefore:

$$\ln(1 - x_2) = -x_2 - \frac{1}{2} x_2^2 - \frac{1}{3} x_2^3 - \dots = -x_2 \quad [7]$$

Combining Equations 6 & 7, yields

$$-x_2 = \Delta H_m / R * (1/T_m^0 - 1/T_m) \quad [8]$$

Assuming there are N_1 mole solvent and N_2 mole solute,

$$-N_2 / (N_1 + N_2) = \Delta H_m / R * (1/T_m^0 - 1/T_m)$$

Approximately, $-N_2 / (N_1 + N_2) = -N_2 / N_1$, for the dilute case. Therefore,

$$-N_2 / N_1 = \Delta H_m / R * (1/T_m^0 - 1/T_m) \quad [9]$$

After arrangement, Equation 9 can be rewritten as Equation 10.

$$T_m = T_m^0 / [1 + (R * T_m^0 * N_2 / (\Delta H_m * N_1))] \quad [10]$$

Appendix B: Values of ΔH_m of Solutes from Published Sources^(6,19)

Materials	Fusion enthalpy (cal/mol)
Water	1436 ⁽⁶⁾
Magnesium chloride	8100 ⁽⁶⁾
Lithium bromide	2900 ⁽⁶⁾
Lithium chloride	3200 ⁽⁶⁾
Calcium chloride	6100 ⁽⁶⁾
Sodium chloride	7220 ⁽⁶⁾
Potassium chloride	6410 ⁽⁶⁾
Sodium bromide	6140 ⁽⁶⁾
Potassium chromate	6920 ⁽⁶⁾
Potassium bromide	5000 ⁽⁶⁾
Sodium nitrate	3760 ⁽⁶⁾
Potassium iodide	4100 ⁽⁶⁾
Cesium chloride	3600 ⁽⁶⁾
Sodium hydroxide	2000 ⁽⁶⁾
Silver nitrate	2755 ⁽⁶⁾
Potassium nitrate	2840 ⁽⁶⁾
Potassium sulfate	8100 ⁽⁶⁾
Potassium hydroxide	1980 ⁽⁶⁾
Potassium dichromate	8770 ⁽⁶⁾
Formic acid	3040 ^(6,19)
Acetic acid	2757 ^(6,19)
Ethylene glycol	2685 ^(6,19)
Ethanol	1200 ^(6,19)
Glycerol	4416 ^(6,19)

Appendix C: Heating Rate v.s. Weight of Sample

As stated earlier, the DSC curve is "peak-like" due to delay of heat transfer. From this point of view, a heavier sample may need a slower heating rate to complete the phase transition.

To investigate how the sample weight affects the maximum allowable heating rate, different amounts of water was used. The results are shown below. In Table C1 the weight of water is approximately 30 mg, in Table C2 the weight of water is approximately 7 mg, and in Table C3 the weight of water is approximately 4 mg. Comparing the three tables below, the maximum allowable heating rates are 5 °C/min for the 30 mg sample, 40°C/min for the 7 mg sample, and 70°C/min for the 4mg sample.

Table C1 : (Weight ~ 30 mg)

Weight of Water (mg)	Heating rate (°C/min)	Fusion enthalpy (cal/mol)
38.8	0.5	1538
27.0	1.0	1557
38.0	2.0	1553
26.3	5.0	1554
37.0	10.0	1162

Appendix C: Heating Rate v.s. Weight of Sample (continued)

Table C2: (weight ~ 7 mg)

Weight of Water (mg)	Heating rate (°C/min)	Fusion enthalpy (cal/mol)
7.8	10	1428
7.1	20	1459
6.9	25	1487
7.5	30	1458
6.9	40	1488
7.3	50	1246

Table C3 : (weight ~ 4 mg)

Weight of Water (mg)	Heating rate (°C/min)	Fusion enthalpy (cal/mol)
4.4	10	1463
4.2	30	1471
4.5	50	1431
3.9	70	1478
4.2	90	1225

Appendix D: Sample Calculations of Fusion Enthalpies from the Differential Scanning Calorimeter

The formula for determining the fusion enthalpy of water from the DSC is given by Equation 18.

$$\Delta H_m = [(R * A) / (W * S)] * K' \quad [18]$$

Before determining ΔH_m , the value of K' should be obtained first. K' is the instrument constant, determined after calibration with indium (In).

Equation 19 below is the formula for determining K' .

$$K' = (\Delta H_{m(\text{ref})}) / [(R * A) / (W * S)] \quad [19]$$

where $\Delta H_{m(\text{ref})}$ of indium is 6.80 cal/g (from Perkin-Elmer Catalogue), the values of R,A,W, and S below, were determined experimentally.

$$K' = (6.80) / [(1 * 1.848) / (8.1 * 0.0332)] = 0.99$$

After the value of K' was obtained, the value of the fusion enthalpy of water was then determined by Equation 18.

$$\Delta H_m = [(R * A) / (W * S)] * K' \quad [18]$$

The values of R,A,W, and S below, were determined experimentally.

$$\begin{aligned} \Delta H_m &= [(5 * 3.718) / (17.2 * 0.01327)] * 0.99 = 80.6 \text{ cal/g} \\ &= 1451 \text{ cal/mol} \end{aligned}$$

Appendix E: Calculations of the Accuracy of the DSC-4

(1) Based on calibration runs with indium

$$\Delta H_{\text{m (ref)}} = 6.80 \text{ cal/g (from Perkin-Elmer Catalogue)}$$

$$= 780.8 \text{ cal/mol}$$

$$\Delta H_{\text{m (exp)}} = 6.87 \text{ cal/g (from DSC-4)}$$

$$= 789.0 \text{ cal/mol}$$

$$\text{Accuracy} = | (\Delta H_{\text{m (ref)}} - \Delta H_{\text{m (exp)}}) | \div (\Delta H_{\text{m (ref)}}) = 1.05 \%$$

(2) Based on calibration runs with water

$$\Delta H_{\text{m (ref)}} = 1436 \text{ cal/mol (from Ref. 6 and 7)}$$

$$\Delta H_{\text{m (exp)}} = 1451 \text{ cal/mol (from DSC-4)}$$

$$\text{Accuracy} = | (\Delta H_{\text{m (ref)}} - \Delta H_{\text{m (exp)}}) | \div (\Delta H_{\text{m (ref)}}) = 1.04 \%$$

Appendix F: Calculations of Fusion Enthalpy from Chickos's Model

1. Benzene, hexafluoro (C₆F₆)

$$\begin{aligned}\Delta S_m &= \sum (n_i) (C_i) (G_i) + \sum (n_j) (C_j) (G_j) + \sum (n_k) (C_k) (G_k) \\ &= 0 + (6 \cdot 1.0 \cdot (-1.02)) + (6 \cdot 1.0 \cdot 3.11) \\ &= 12.54 \text{ e.u.}\end{aligned}$$

$$T_m = 5.34^\circ\text{C (from DSC-4)}$$

$$\Delta H_m = \Delta S_m \cdot T_m = 3490 \text{ kcal/mol} = 18.76 \text{ cal/g}$$

2. Heptanoic acid (CH₃(CH₂)₅CO₂H)

$$\begin{aligned}\Delta S_m &= \sum (n_i) (C_i) (G_i) + \sum (n_j) (C_j) (G_j) + \sum (n_k) (C_k) (G_k) \\ &= (1 \cdot 1.0 \cdot 4.38 + 4 \cdot 1.0 \cdot 2.25) + (1 \cdot 1.0 \cdot 2.25) + (1 \cdot 1.0 \cdot 3.56) \\ &= 19.19 \text{ e.u.}\end{aligned}$$

$$T_m = -10.14^\circ\text{C (from DSC-4)}$$

$$\Delta H_m = \Delta S_m \cdot T_m = 5044 \text{ kcal/mol} = 38.74 \text{ cal/g}$$

3. Cyclohexanol, 4-methyl (4-CH₃C₆H₁₀OH)

$$\begin{aligned}\Delta S_m &= [8.41 + 1.025 (n-3)] + \sum (n_i) (C_i) (G_i) + \sum (n_j) (C_j) (G_j) \\ &\quad + \sum (n_k) (C_k) (G_k) \\ &= [8.41 + 1.025 (6-3)] + [1 \cdot 1.0 \cdot (-3.82) + 1 \cdot 1.0 \cdot 4.38] \\ &\quad + [1 \cdot 0.76 \cdot (-3.82)] + [1 \cdot 1.0 \cdot 0.27] \\ &= 9.4118 \text{ e.u.}\end{aligned}$$

$$T_m = -3.96^\circ\text{C (from DSC-4)}$$

$$\Delta H_m = \Delta S_m \cdot T_m = 2532 \text{ kcal/mol} = 22.17 \text{ cal/g}$$

**Appendix F: Calculations of Fusion Enthalpy from Chickos's Model
(continued)**

4. Benzene, 1,4-difluoro (C₆H₄F₂)

$$\begin{aligned}\Delta S_m &= \sum (n_i) (C_i) (G_i) + \sum (n_j) (C_j) (G_j) + \sum (n_k) (C_k) (G_k) \\ &= [4*1.0*1.54] + [2*1.0*(-1.02)] + [2*1.0*3.11] \\ &= 10.34 \text{ e.u.}\end{aligned}$$

$$T_m = -22.79^\circ\text{C (from DSC-4)}$$

$$\Delta H_m = \Delta S_m * T_m = 2587 \text{ kcal/mol} = 22.67 \text{ cal/g}$$

5. Cyclohexanone ,2-methyl (2-CH₃(C₆H₉O))

$$\begin{aligned}\Delta S_m &= [8.41 + 1.025 (n-3)] + \sum (n_i) (C_i) (G_i) + \sum (n_j) (C_j) (G_j) \\ &\quad + \sum (n_k) (C_k) (G_k) \\ &= [8.41 + 1.025 (6-3)] + [1*1.0*(-3.82) + 1*1.0*4.38] + [1*0.86*(-2.8)] \\ &\quad + [1*1.0*(-0.45)] \\ &= 9.187 \text{ e.u.}\end{aligned}$$

$$T_m = -14.14^\circ\text{C (from DSC-4)}$$

$$\Delta H_m = \Delta S_m * T_m = 2378 \text{ kcal/mol} = 21.20 \text{ cal/g}$$

6. Cinnamionitrile (C₆H₅CH=CHCN)

$$\begin{aligned}\Delta S_m &= \sum (n_i) (C_i) (G_i) + \sum (n_j) (C_j) (G_j) + \sum (n_k) (C_k) (G_k) \\ &= [5*1.0*1.54 + 1*1.0*(-1.02) + 1*1.0*1.16] + [1*3.23*1.16] \\ &\quad + [1*1.0*2.30] \\ &= 13.8868 \text{ e.u.}\end{aligned}$$

$$T_m = 5.08^\circ\text{C (from DSC-4)}$$

$$\Delta H_m = \Delta S_m * T_m = 3862 \text{ kcal/mol} = 29.89 \text{ cal/g}$$

**Appendix F: Calculations of Fusion Enthalpy from Chickos's Model
(continued)**

7. Cyclooctatetraene (C₈H₈)

$$\begin{aligned}\Delta S_m &= [8.41 + 1.025 (n-3)] + \sum (n_i) (C_i) (G_i) \\ &= [8.41 + 1.025 (8-3)] + [8 * 1.0 * (-1.04)] \\ &= 5.215 \text{ e.u.}\end{aligned}$$

$$T_m = -8.21^\circ\text{C (from DSC-4)}$$

$$\Delta H_m = \Delta S_m * T_m = 1381 \text{ kcal/mol} = 13.26 \text{ cal/g}$$

8. 4-methoxybenzaldehyde (CH₃OC₆H₄CHO)

$$\begin{aligned}\Delta S_m &= \sum (n_i) (C_i) (G_i) + \sum (n_j) (C_j) (G_j) + \sum (n_k) (C_k) (G_k) \\ &= [4 * 1.0 * 1.54] + [2 * 1.0 * (-1.02) + 1 * 1.0 * 4.38] \\ &\quad + [1 * 1.0 * 4.70 + 1 * 1.0 * 0.26] \\ &= 13.46 \text{ e.u.}\end{aligned}$$

$$T_m = -1.89^\circ\text{C (from DSC-4)}$$

$$\Delta H_m = \Delta S_m * T_m = 3649 \text{ kcal/mol} = 26.83 \text{ cal/g}$$

9. Indene (C₉H₈)

$$\begin{aligned}\Delta S_m &= [8.41 + 1.025 (n-3)] + \sum (n_i) (C_i) (G_i) \\ &= [8.41 + 1.025 (5-3)] \\ &\quad + [4 * 1.0 * 1.54 + 2 * 1.0 * (-2.8) + 2 * 1.0 * (-1.04)] \\ &= 8.94 \text{ e.u.}\end{aligned}$$

$$T_m = -6.15^\circ\text{C (from DSC-4)}$$

$$\Delta H_m = \Delta S_m * T_m = 2386 \text{ kcal/mol} = 20.57 \text{ cal/g}$$

**Appendix F: Calculations of Fusion Enthalpy from Chickos's Model
(continued)**

10. Cyclohexane, 1,2-dibromo (1,2-Br₂C₆H₁₀)

$$\begin{aligned}\Delta S_m &= [8.41 + 1.025 (n-3)] + \sum (n_i) (C_i) (G_i) + \sum (n_j) (C_j) (G_j) \\ &\quad + \sum (n_k) (C_k) (G_k) \\ &= [8.41 + 1.025 (6-3)] + 0 + [2*0.76*(-3.82)] + [2*1.0*4.29] \\ &= 14.2586 \text{ e.u.}\end{aligned}$$

$$T_m = -4.98^\circ\text{C} \text{ (from DSC-4)}$$

$$\Delta H_m = \Delta S_m * T_m = 3822 \text{ kcal/mol} = 15.79 \text{ cal/g}$$

11. Biphenyl, 2-methyl (2-CH₃C₆H₄C₆H₅)

$$\begin{aligned}\Delta S_m &= \sum (n_i) (C_i) (G_i) \\ &= [9*1.0*1.54 + 2*1.0*(-1.02) + 1*1.0*(-2.47) + 1*1.0*4.38] \\ &= 13.73 \text{ e.u.}\end{aligned}$$

$$T_m = -0.48^\circ\text{C} \text{ (from DSC-4)}$$

$$\Delta H_m = \Delta S_m * T_m = 3742 \text{ kcal/mol} = 22.24 \text{ cal/g}$$

12. Naphthalene, 1,2-dihydro (C₁₀H₁₀)

$$\begin{aligned}\Delta S_m &= [8.41 + 1.025 (n-3)] + \sum (n_i) (C_i) (G_i) \\ &= [8.41 + 1.025 (6-3)] \\ &\quad + [4*1.0*1.54 + 1*1.0*(-1.02) + 1*1.0*(-2.47) + 2*1.0*(-1.04)] \\ &= 12.075 \text{ e.u.}\end{aligned}$$

$$T_m = -10.05^\circ\text{C} \text{ (from DSC-4)}$$

$$\Delta H_m = \Delta S_m * T_m = 3175 \text{ kcal/mol} = 24.39 \text{ cal/g}$$

**Appendix F: Calculations of Fusion Enthalpy from Chickos's Model
(continued)**

13. Piperidine (C₅H₁₀NH)

$$\begin{aligned}\Delta S_m &= [8.41 + 1.025 (n-3)] + \sum (nk) (Ck) (Gk) \\ &= [8.41 + 1.025 (6-3)] + [1*1.0*0.44] \\ &= 11.925 \text{ e.u.}\end{aligned}$$

$$T_m = -18.46^\circ\text{C (from DSC-4)}$$

$$\Delta H_m = \Delta S_m * T_m = 3035 \text{ kcal/mol} = 35.64 \text{ cal/g}$$

Appendix G: Sample Calculations of Fusion Enthalpies from the Rule of Mixtures

Assume the total weight for the solution is 100 grams for all the following solutions.

(1) MgCl₂ (1%) :

for MgCl₂ (wt: 95.21, ΔH_a =8100 cal/mol)

for Water (wt: 18, ΔH_{H₂O})=1436 cal/mol)

Moles of Solute = 0.0105, Moles of Water= 5.5, Total moles = 5.5105

$$\begin{aligned}\Delta H_{m(aq)} &= [X_a \Delta H_a + X_{H_2O} \Delta H_{H_2O}] \\ &= [(0.0105/5.5105) * (8100) + (5.5/5.5105) * (1436)] \\ &= 1449 \text{ cal/mol}\end{aligned}$$

(2) MgCl₂ (5%) :

Moles of Solute = 0.0525, Moles of Water= 5.278, Total moles = 5.330

$$\begin{aligned}\Delta H_{m(aq)} &= [X_a \Delta H_a + X_{H_2O} \Delta H_{H_2O}] \\ &= [(0.0525/5.330) * (8100) + (5.278/5.330) * (1436)] \\ &= 1502 \text{ cal/mol}\end{aligned}$$

(3) MgCl₂ (10%) :

Moles of Solute = 0.105, Moles of Water= 5, Total moles = 5.105

$$\begin{aligned}\Delta H_{m(aq)} &= [X_a \Delta H_a + X_{H_2O} \Delta H_{H_2O}] \\ &= [(0.105/5.105) * (8100) + (5/5.105) * (1436)] \\ &= 1573 \text{ cal/mol}\end{aligned}$$

(4) MgCl₂ (15%) :

Moles of Solute = 0.158, Moles of Water= 4.722, Total moles = 4.880

$$\begin{aligned}\Delta H_{m(aq)} &= [X_a \Delta H_a + X_{H_2O} \Delta H_{H_2O}] \\ &= [(0.158/4.880) * (8100) + (4.722/4.880) * (1436)] = 1651 \text{ cal/mol}\end{aligned}$$

Appendix H: Sample Calculations of Fusion Enthalpies from Horvath's Model

Assume the total weight for the solution is 100 grams.

(1) MgCl_2 (1%) :

for MgCl_2 (wt: 95.21), for Water (wt: 18)

($\text{MgCl}_2 \rightarrow \text{Mg}^{+2} + 2 \text{Cl}^-$) 1 mole of MgCl_2 dissociates to 3 mole of ions,

therefore $N_2 = (1/95.21) * 3 = 0.03151$

$N_1 = (99/18) = 5.5$

$T_m = - 0.13 \text{ }^\circ\text{C} = 272.87 \text{ }^\circ\text{K}$ (from experiment)

$$\begin{aligned}\Delta H_m &= R * T_m^0 * (N_2 / N_1) * [T_m / (T_m^0 - T_m)] \\ &= 1.987 * 273 * (0.03151/5.5) * (272.87/0.13) = 6524 \text{ cal/mol}\end{aligned}$$

(2) MgCl_2 (5%) :

$N_2 = (5/95.21) * 3 = 0.15755$ $N_1 = (95/18) = 5.2778$

$T_m = - 6.53 \text{ }^\circ\text{C} = 266.47 \text{ }^\circ\text{K}$ (from experiment)

$$\begin{aligned}\Delta H_m &= R * T_m^0 * (N_2 / N_1) * [T_m / (T_m^0 - T_m)] \\ &= 1.987 * 273 * (0.15755/5.2778) * (266.47/6.53) = 661 \text{ cal/mol}\end{aligned}$$

(3) MgCl_2 (10%) :

$N_2 = (10/95.21) * 3 = 0.3151$ $N_1 = (90/18) = 5$

$T_m = - 14.43 \text{ }^\circ\text{C} = 258.57 \text{ }^\circ\text{K}$ (from experiment)

$$\begin{aligned}\Delta H_m &= R * T_m^0 * (N_2 / N_1) * [T_m / (T_m^0 - T_m)] \\ &= 1.987 * 273 * (0.3151/5) * (258.57/14.43) = 613 \text{ cal/mol}\end{aligned}$$

(4) MgCl_2 (15%) :

$N_2 = (15/95.21) * 3 = 0.4726$ $N_1 = (95/18) = 4.7222$

$T_m = - 24.94 \text{ }^\circ\text{C} = 248.06 \text{ }^\circ\text{K}$ (from experiment)

$$\begin{aligned}\Delta H_m &= R * T_m^0 * (N_2 / N_1) * [T_m / (T_m^0 - T_m)] \\ &= 1.987 * 273 * (0.4726/4.7222) * (248.06/24.94) = 540 \text{ cal/mol}\end{aligned}$$

Appendix I: Hydration Numbers of Electrolytes⁽²⁵⁾

Material	Hydration number ⁽²⁵⁾
MgCl ₂	13.7
LiBr	7.6
LiCl	7.1
CaCl ₂	12.0
NaCl	3.5
NaBr	4.2
KCl	1.9
KBr	2.1
KI	2.5
NiCl ₂	13.0

Appendix J: Hydration Numbers of Non-electrolytes

Table J (J1~ J5) in the next five pages are the calculated hydration numbers of 5 non-electrolytes. The first column is the weight percent of solute. The second column is the molar concentration of solution (M). The third column (Co-Cw) means the amount of water displaced by an anhydrous solute in a unit of (g/l). The fourth column is the calculated hydration numbers. According to the CRC Handbook, the value of " $(Co-Cw) / (18.015 * M)$ " is defined as the mole number of water displaced by one mole solute and this value is equivalent to the primary hydration number.

Second Column (M) (unit: g-mol/l) : (after Ref. 26)

Third Column (Co-Cw) (unit: g/l) : (after Ref. 26)

Fourth Column: Hydration number (Calculated)

$$= (Co-Cw) / (18.015 * M) \text{ (unit: mol water/mol solute)}$$

Table J (1): Hydration Number of Formic Acid

Solute wt%	Molarity (M) ⁽²⁶⁾ (g-mol/l)	$C_0 - C_w$ ⁽²⁶⁾ (g/l)	Hydration number
0.5	0.109	3.8	1.94
1.0	0.217	7.7	1.97
2.0	0.436	15.3	1.95
3.0	0.655	23.1	1.96
4.0	0.876	30.8	1.95
5.0	1.097	38.6	1.95
10.0	2.221	78.1	1.95
12.0	2.678	94.2	1.95
14.0	3.139	110.5	1.95
16.0	3.605	127.1	1.96
18.0	4.074	143.9	1.96
20.0	4.548	160.9	1.96
24.0	5.507	195.5	1.97
28.0	6.481	231.1	1.98
32.0	7.471	267.5	1.99

Table J (2): Hydration Number of Acetic Acid

Solute wt%	Molarity (M) ⁽²⁶⁾ (g-mol/l)	C ₀ - C _w ⁽²⁶⁾ (g/l)	Hydration number
1.0	0.166	8.6	2.88
2.0	0.333	17.2	2.87
3.0	0.501	25.9	2.87
4.0	0.669	34.5	2.86
5.0	0.837	43.3	2.87
6.0	1.006	52.0	2.87
7.0	1.175	60.8	2.87
8.0	1.345	69.6	2.87
9.0	1.515	78.5	2.88
10.0	1.685	87.4	2.88
11.0	1.856	96.3	2.88
12.0	2.028	105.3	2.88
13.0	2.200	114.3	2.88
14.0	2.372	123.3	2.89
15.0	2.545	132.4	2.89
20.0	3.414	178.2	2.90

Table J (3): Hydration Number of Ethylene Glycol

Solute wt%	Molarity (M) ⁽²⁶⁾ (g-mol/l)	$C_0 - C_w$ ⁽²⁶⁾ (g/l)	Hydration number
1.0	0.161	8.8	3.03
2.0	0.322	17.6	3.03
4.0	0.646	35.2	3.02
6.0	0.972	52.9	3.02
8.0	1.299	70.6	3.02
10.0	1.629	88.5	3.02
12.0	1.959	106.4	3.01
16.0	2.626	142.5	3.01
20.0	3.300	178.9	3.01
28.0	4.669	253.0	3.01

Table J (4): Hydration Number of Ethanol

Solute wt%	Molarity (M) ⁽²⁶⁾ (g-mol/l)	C ₀ - C _w ⁽²⁶⁾ (g/l)	Hydration number
1.0	0.216	11.8	3.03
2.0	0.432	23.6	3.03
4.0	0.860	46.9	3.03
6.0	1.286	69.7	3.01
8.0	1.710	92.3	3.00
9.5	2.026	109.0	2.99
10.0	2.131	114.5	2.98
12.0	2.550	136.6	2.97
16.0	3.382	180.2	2.96
20.0	4.205	223.3	2.95
24.0	5.018	266.2	2.94

Table J (5): Hydration Number of Glycerol

Solute wt%	Molarity (M) ⁽²⁶⁾ (g-mol/l)	$C_0 - C_w$ ⁽²⁶⁾ (g/l)	Hydration number
1.0	0.109	7.7	3.92
2.0	0.218	15.5	3.95
4.0	0.438	31.2	3.95
6.0	0.659	46.9	3.95
8.0	0.883	62.9	3.95
10.0	1.109	78.9	3.95
16.0	1.800	128.0	3.95
24.0	2.752	195.6	3.95
32.0	3.742	265.9	3.94
40.0	4.771	339.2	3.95

Appendix K: Sample Calculations of Fusion Enthalpies from the Modified Mixture Rule

Assume the total weight for the solution is 100 grams.

(1) MgCl₂ (1%) :

for MgCl₂ (wt: 95.21, h=13.7, ΔH_a =8100 cal/mol)

for Water (wt: 18, ΔH_{H₂O}=1436 cal/mol)

Moles of Solute = 0.0105, Moles of Water= 5.5, Total moles = 5.5105

$$\begin{aligned} \Delta H_{m(aq)} &= [X_a \Delta H_a + X_{H_2O} \Delta H_{H_2O}] - (X_a) * (h) * (\text{H bond energy in water}) = \\ &= [(0.0105/5.5105) * (8100) + (5.5/5.5105) * (1436)] - (0.0105/5.5105) * (13.7) * \\ &(3000) = 1370 \text{ cal/mol} \end{aligned}$$

(2) MgCl₂ (5%) :

Moles of Solute = 0.0525, Moles of Water= 5.278, Total moles = 5.330

$$\begin{aligned} \Delta H_{m(aq)} &= [X_a \Delta H_a + X_{H_2O} \Delta H_{H_2O}] - (X_a) * (h) * (\text{H bond energy in water}) \\ &= [(0.0525/5.330) * (8100) + (5.278/5.330) * (1436)] - (0.0525/5.330) * (13.7) * \\ &(3000) = 1097 \text{ cal/mol} \end{aligned}$$

(3) MgCl₂ (10%) :

Moles of Solute = 0.105, Moles of Water= 5, Total moles = 5.105

$$\begin{aligned} \Delta H_{m(aq)} &= [X_a \Delta H_a + X_{H_2O} \Delta H_{H_2O}] - (X_a) * (h) * (\text{H bond energy in water}) \\ &= [(0.105/5.105) * (8100) + (5/5.105) * (1436)] - (0.105/5.105) * (13.7) * (3000) \\ &= 727 \text{ cal/mol} \end{aligned}$$

(4) MgCl₂ (15%) :

Moles of Solute = 0.158, Moles of Water= 4.722, Total moles = 4.880

$$\begin{aligned} \Delta H_{m(aq)} &= [X_a \Delta H_a + X_{H_2O} \Delta H_{H_2O}] - (X_a) * (h) * (\text{H bond energy in water}) \\ &= [(0.158/4.880) * (8100) + (4.722/4.880) * (1436)] - (0.158/4.880) * (13.7) * \\ &(3000) = 324 \text{ cal/mol} \end{aligned}$$

Appendix L: Calculations of Maximum Concentration in the Modified Mixture Rule

Assume the total weight of the following solutions is 100 grams, including m gram of the solute and (100-m) grams of water.

1) Formic acid : (wt=46.03, hydration number=1.99)

$$(m/46.03) * (1.99) / [(100-m)/18] = 25 \% \implies m = 24.3 \%$$

2) Acetic acid : (wt=60.05, hydration number=2.90)

$$(m/60.05) * (2.90) / [(100-m)/18] = 25 \% \implies m = 22.3 \%$$

3) Ethylene glycol : (wt=62.07, hydration number=3.01)

$$(m/62.07) * (3.01) / [(100-m)/18] = 25 \% \implies m = 22.3 \%$$

4) Ethanol : (wt=46.07, hydration number=2.94)

$$(m/46.07) * (2.94) / [(100-m)/18] = 25 \% \implies m = 17.9 \%$$

5) Glycerol : (wt=92.09, hydration number=3.95)

$$(m/92.09) * (3.95) / [(100-m)/18] = 25 \% \implies m = 24.5 \%$$

6) Magnesium chloride : (wt=95.21, hydration number=13.7)

$$(m/95.21) * (13.7) / [(100-m)/18] = 25 \% \implies m = 8.8 \%$$

7) Lithium bromide : (wt=86.85, hydration number=7.6)

$$(m/86.85) * (7.6) / [(100-m)/18] = 25 \% \implies m = 13.7 \%$$

8) Lithium chloride : (wt=42.39, hydration number=7.1)

$$(m/42.39) * (7.1) / [(100-m)/18] = 25 \% \implies m = 7.7 \%$$

9) Calcium chloride : (wt=111, hydration number=12.0)

$$(m/111) * (12.0) / [(100-m)/18] = 25 \% \implies m = 11.4 \%$$

10) Sodium chloride : (wt=58.44, hydration number=3.5)

$$(m/58.44) * (3.5) / [(100-m)/18] = 25 \% \implies m = 18.8 \%$$

Appendix M: Calculations of Cooling Capacities

The calculations contained in this appendix have been performed in a cal/g basis in order to permit easy comparison with the results obtained by Selvaduray and Lomax. The fusion enthalpy and heat capacity data on a cal/g basis are presented in Table M1.

- 1) Water
$$\Delta H_{\text{tot}} = \int_{T_{s,i}}^{T_m} c_{p,s} dT + \Delta H_m + \int_{T_m}^{T_{l,f}} c_{p,l} dT$$
$$= 0.52 * (0.087 - (-13)) + 80.6 + 1.06 * (5 - 0.087) = 92.6 \text{ (cal/g)}$$
- 2) Heptanoic acid
$$\Delta H_{\text{tot}} = 0.581 * (-10.14 - (-13)) + 28.26 + 0.387 * (5 - (-10.14)) = 35.78 \text{ (cal/g)}$$
- 3) Cyclohexanol, 4-methyl,cis
$$\Delta H_{\text{tot}} = 0.30 * (-3.96 - (-13)) + 18.16 + 0.46 * (5 - (-3.96)) = 24.99 \text{ (cal/g)}$$
- 4) Cyclooctatetraene
$$\Delta H_{\text{tot}} = 0.31 * (-8.21 - (-13)) + 23.28 + 0.37 * (5 - (-8.21)) = 29.65 \text{ (cal/g)}$$
- 5) 4-methoxybenzaldehyde
$$\Delta H_{\text{tot}} = 0.345 * (-1.89 - (-13)) + 27.81 + 0.379 * (5 - (-1.89)) = 34.25 \text{ (cal/g)}$$
- 6) Indene
$$\Delta H_{\text{tot}} = 0.36 * (-6.15 - (-13)) + 15.10 + 0.45 * (5 - (-6.15)) = 22.58 \text{ (cal/g)}$$
- 7) Cyclohexane,1,2-dibromo
$$\Delta H_{\text{tot}} = 0.164 * (-4.98 - (-13)) + 11.97 + 0.205 * (5 - (-4.98)) = 15.33 \text{ (cal/g)}$$
- 8) Biphenyl,2-methyl
$$\Delta H_{\text{tot}} = 0.25 * (-0.48 - (-13)) + 17.03 + 0.41 * (5 - (-0.48)) = 22.40 \text{ (cal/g)}$$
- 9) Naphthalene,1,2-dihydro
$$\Delta H_{\text{tot}} = 0.315 * (-10.05 - (-13)) + 18.82 + 0.375 * (5 - (-10.05)) = 25.39 \text{ (cal/g)}$$

Appendix M: Calculations of Cooling Capacities (continued)

10) Lithium chloride (4%)

$$\Delta H_{\text{tot}} = 0.65 * (-7.96 - (-13)) + 50.20 + 0.91 * (5 - (-7.96)) = 65.26 \text{ (cal/g)}$$

11) Potassium chloride (9%)

$$\Delta H_{\text{tot}} = 0.43 * (-8.55 - (-13)) + 71.09 + 0.76 * (5 - (-8.55)) = 83.30 \text{ (cal/g)}$$

12) Potassium chromate (18%)

$$\Delta H_{\text{tot}} = 0.31 * (-8.7 - (-13)) + 70.25 + 0.85 * (5 - (-8.7)) = 83.22 \text{ (cal/g)}$$

13) Potassium bromide (13%)

$$\Delta H_{\text{tot}} = 0.39 * (-11.04 - (-13)) + 67.3 + 0.9 * (5 - (-11.04)) = 82.50 \text{ (cal/g)}$$

14) Sodium hydroxide (4.5%)

$$\Delta H_{\text{tot}} = 0.6 * (-7.27 - (-13)) + 39.9 + 0.85 * (5 - (-7.27)) = 53.76 \text{ (cal/g)}$$

15) Silver nitrate (16%)

$$\Delta H_{\text{tot}} = 0.34 * (-7.72 - (-13)) + 70.05 + 0.87 * (5 - (-7.72)) = 82.91 \text{ (cal/g)}$$

16) Potassium nitrate (10%)

$$\Delta H_{\text{tot}} = 0.33 * (-2.41 - (-13)) + 80.7 + 0.87 * (5 - (-2.41)) = 90.64 \text{ (cal/g)}$$

17) Potassium sulfate (5%)

$$\Delta H_{\text{tot}} = 0.40 * (-0.81 - (-13)) + 79.21 + 0.91 * (5 - (-0.81)) = 89.37 \text{ (cal/g)}$$

18) Potassium hydroxide (6%)

$$\Delta H_{\text{tot}} = 0.70 * (-7.26 - (-13)) + 49.09 + 0.56 * (5 - (-7.26)) = 59.97 \text{ (cal/g)}$$

19) Potassium dichromate (2.5%)

$$\Delta H_{\text{tot}} = 0.40 * (-0.02 - (-13)) + 83.94 + 1.10 * (5 - (-0.02)) = 94.65 \text{ (cal/g)}$$

20) Formic acid (10%)

$$\Delta H_{\text{tot}} = 0.58 * (-7.53 - (-13)) + 56.55 + 0.83 * (5 - (-7.53)) = 70.12 \text{ (cal/g)}$$

Appendix M: Calculations of Cooling Capacities (continued)

21) Acetic acid (13%)

$$\Delta H_{\text{tot}} = 0.6 * (-8.54 - (-13)) + 56.12 + 1.0 * (5 - (-8.54)) = 72.33 \text{ (cal/g)}$$

22) Ethylene glycol (12%)

$$\Delta H_{\text{tot}} = 0.74 * (-5.52 - (-13)) + 56.90 + 1.20 * (5 - (-5.52)) = 75.05 \text{ (cal/g)}$$

23) Ethanol (9.5%)

$$\Delta H_{\text{tot}} = 0.78 * (-6.72 - (-13)) + 49.92 + 1.0 * (5 - (-6.72)) = 66.54 \text{ (cal/g)}$$

24) Glycerol (16%)

$$\Delta H_{\text{tot}} = 0.63 * (-7.95 - (-13)) + 45.81 + 0.92 * (5 - (-7.95)) = 60.90 \text{ (cal/g)}$$

Appendix M: Calculations of Cooling Capacities (continued)

Table M1. Fusion Enthalpy and Heat Capacity of FHS Candidates

FHS candidate	ΔH_m (cal/g)	$C_{p,s}$ (cal/g°C)	$C_{p,l}$ (cal/g°C)
Water	80.6	0.52	1.06
Heptanoic acid	28.26	0.581	0.387
Cyclohexanol,4-methyl(cis)	18.16	0.30	0.46
Cyclooctatetraene	23.28	0.31	0.37
4-Methoxybenzaldehyde	27.81	0.345	0.379
Indene	15.10	0.36	0.45
Cyclohexane,1,2-dibromo	11.97	0.164	0.205
Biphenyl,2-methyl	17.03	0.25	0.41
1,2-dihydronaphthalene	18.82	0.315	0.375
Potassium chloride(9%)	71.09	0.43	0.76
Lithium chloride(4%)	50.20	0.65	0.91
Potassium chromate(18%)	70.25	0.31	0.85
Potassium bromide(13%)	67.3	0.39	0.90
Sodium hydroxide(4.5%)	39.9	0.60	0.85
Silver nitrate(16%)	70.05	0.34	0.87
Potassium nitrate(10%)	80.7	0.33	0.87
Potassium sulfate(5%)	79.21	0.40	0.91
Potassium hydroxide(6%)	49.09	0.70	0.56
Potassium dichromate(2.5%)	83.94	0.40	1.10
Formic acid(10%)	56.55	0.58	0.83
Acetic acid(13%)	56.12	0.60	1.0
Ethylene glycol(12%)	56.90	0.74	1.20
Ethanol(9.5%)	49.92	0.78	1.0
Glycerol(16%)	45.81	0.63	0.92